INFORMATION TO USERS

This manuscript has been reproduced from the microfilm master. UMI films the text directly from the original or copy submitted. Thus, some thesis and dissertation copies are in typewriter face, while others may be from any type of computer printer.

The quality of this reproduction is dependent upon the quality of the copy submitted. Broken or indistinct print, colored or poor quality illustrations and photographs, print bleedthrough, substandard margins, and improper alignment can adversely affect reproduction.

In the unlikely event that the author did not send UMI a complete manuscript and there are missing pages, these will be noted. Also, if unauthorized copyright material had to be removed, a note will indicate the deletion.

Oversize materials (e.g., maps, drawings, charts) are reproduced by sectioning the original, beginning at the upper left-hand corner and continuing from left to right in equal sections with small overlaps.

ProQuest Information and Learning
300 North Zeeb Road, Ann Arbor, MI 48106-1346 USA
800-521-0600

The Development of a Non-Born-Oppenheimer Self-Consistent Field Method and Computational Cluster Studies on the Solvation of Cations and Anions

by

Balakrishnan Viswanathan

Submitted in partial fulfilment of the requirements

for the degree of

Doctor of Philosophy

at

Dalhousie University

Halifax, Nova Scotia

July 2005

श्री पितृगुरुचरणकमलेभ्यो नमः।

Salutations to my parents and teachers

TABLE OF CONTENTS

LIST OF TABLES

LIST OF FIGURES

ABSTRACT

The Born-Oppenheimer approximation is one of the cornerstones upon which modern quantum chemistry is founded. The application of this approximation has it made it possible to perform the vast number of computations performed. However, it must be recalled that the BO method is an approximation. It is therefore preferable to have a method that performs well without the need for invoking the above approximation.

This document outlines the development of a novel method for the *ab initio* computation of molecular systems wherein the Born-Oppenheimer approximation is not invoked. A brief overview of previous methods developed to solve this problem will be presented, mentioning reasons why these methods are inadequate. This will be followed by the development of the new method and its physical implications. Some recent results are also presented.

The thermochemistry and geometries of cation and anion complexes with water, ammonia, formaldehyde, and formamide are essential to understand the solvation and desolvation processes occurring in biological systems. However, experimental data are only available for the interaction of Group I metal cations with water. The thermochemistry and geometries of metal cations with the other mentioned ligands are less well characterised. Theoretical methods afford an alternate method to understanding these systems.

This study was designed to generate an optimal B3LYP-based computational scheme for the calculation of metal cation–ligand clusters. The cation cluster geometries converge only at the 6-311+G(3df,3pd) level. Basis set superposition errors (BSSE) are found to vary from ~0.2 to ~5 kcal mol^{-1}, and are significant for all basis sets smaller than 6-311+G(3df,3pd). Geometry convergence and BSSE disappearance occur only at the 6-311+G(3df,3pd) level, and hence this is the ideal method to employ. Unfortunately, it was also discovered that currently available methods are unable to adequately describe the anion-water clusters, mainly due to the residual BSSE even when the largest basis sets are used.

LIST OF ABBREVIATIONS AND SYMBOLS USED

Abbreviations

BO	Born-Oppenheimer
AO	Atomic Orbital
LCAO	Linear Combination of Atomic Orbitals
STO	Slater-type Orbital
GTO	Gaussian-type Orbital
HO	Hydrogenic Orbital
MO	Molecular Orbital
HF	Hartree-Fock
SCF	Self-consistent Field
DFT	Density Functional Theory
BSSE	Basis Set Superposition Error
ENMO	Electron-nucleus Molecular Orbital (method)
PES	Potential Energy Surface

Symbols Used

m, M	Mass
h	Planck's constant
$\hat{H}$	Hamiltonian operator
κ	Perturbation factor
x_k, r, R, $\mathbf{r}$, $\mathbf{R}$, q	Position coordinate
x	Scaling factor for basis functions
U, V	Potential Energy
T	Kinetic Energy
E	Energy
ϕ, χ	Basis function
ψ	Molecular orbital
Ψ	Wavefunction
ρ	Density
F, $\mathbf{F}$	Fock matrix
$\hat{J}$	Coulomb operator
$\hat{K}$	Exchange operator
Z	Charge
$\mathbf{H}$	Hamiltonian (core) matrix
$\mathbf{G}$	Electron-electron interaction matrix
$\mathbf{S}$	Overlap matrix
$\mathbf{C}$	Coefficient matrix
$\mathbf{P}$	Density matrix
μ	Reduced mass
N	Normalisation factor
n	Number of electrons
K	Number of nuclei
s	Spin coordinates
S	Overlap
α, β	Spin states (electron)
$\mathbf{D}$	Slater determinant
NT	Number of terms in ENMO wavefunction expansion
NE	Number of terms in ENMO energy expansion
$\mathbf{J}$	Coulomb matrix for interactions between dissimilar particles

ACKNOWLEDGEMENTS

I am very thankful to Dr. Russell Boyd without whose guidance and encouragement this document would not have been possible. The faith displayed in me has enabled the development of the method outlined in this dissertation and the implementation of the same. The computational implementation of the modified ENMO is due in large part to the patience and perseverance of Dr. Christopher Barden who was also a source of ideas and experience. The discussions held with him have contributed significantly to the conduct of the various facets of this thesis. In the same vein, I am thankful to Dr. Fuqiang Ban and Dr. John Coxon with whom I have had many fruitful conversations. It is also necessary to thank the funding agencies who have supported the conduct of this work, namely NSERC and the Walter C. Sumner Foundation.

CHAPTER I: INTRODUCTION

The present work is a junction of two different streams of thought. This may at first glance seem to be a collection of disparate viewpoints. However, the goal of this section is to demonstrate to the reader how the two viewpoints are no more than two different sets of eyes with which to perceive the world. The two views that this document is concerned with are those of the theorist and the applied chemist. The two, though seemingly opposites, in fact draw sustenance from each other. Further, these individuals must interact with the experimentalist to generate a holistic picture. The theorist cannot function in the absence of data, which of course is the realm of the experimentalist. Likewise, the work of the theorist is fruitless unless it is applied, and this is the realm of the computational chemist. Moreover, in the absence of the theorist, how is one to make sense of the reams of experimental data available? Data achieves meaning only when set in the context of a model, as ultimately all extant theories are but models used to understand what ultimately may not be understandable. In the meantime, humankind generates better models than those preceding. How is one to understand a better model? Is a better model one that allows us to fit existing data and predict future data? Or is it one that improves the understanding of fundamental processes? These naturally lead one to speculate on the value of a model that is "fundamentally correct" but lacks predictive power. Could such a model be explained as nothing more than an incomplete model, or an incorrect model? It will not be possible to satisfactorily answer the above questions in this document, however it will be possible to discern the motivation for the work presented from the preceding discussion.

As mentioned briefly, two sets of eyes are being used in this document, that of the theorist and that of the applied chemist. The initial section and bulk of this document deals with the world as seen by the theorist. The discussion begins with an overview of the quantum chemical background as developed under the *aegis* of the Born-Oppenheimer approximation. The implications and applications of the same are also explored. It would not be out of place to claim that practically all of computational quantum chemistry falls under the ambit of the applications of the Born-Oppenheimer approximation. As with any other approximation, this approximation also has a range of applicability. The discussion of these issues is the domain of Chapter 2.

If there exist situations where a certain approximation ceases to be valid, it is but natural for there to be attempts to circumvent the approximation. There may also be efforts to do away with it and generate a new freestanding model. Some of the previous attempts at transcending the Born-Oppenheimer approximation are dealt with in Chapter 3. Chapter 4 also deals with the development of a new method that has the same goal in mind. A contrast between the various approaches is provided in these sections.

At this point, the document takes a detour, with the eyes of the theorist merging with the eyes of the applied chemist. In Chapter 5, the application of the model developed in the previous chapter is outlined, along with the benefits and difficulties that this entails. The needs and wishes of the theorist must be balanced with the real

limitations under which the applied chemist works. This chapter brings out the differences in requirements between the theorist and the computational chemist.

The next chapter is completely in the realm of the computational chemist. The focus herein is on the study of clusters as an analogue for the study of solvated systems. Are clusters a good approximation to the solvated system? There have been some arguments that this may be a valid approximation. Moreover, if the previous assumption is valid, can sense be made of the number of calculations that have been performed? There is a need to reconcile the various studies, as they so often are contradictory in their pronouncements. This is dealt with in Chapter 6.

It is obvious and recognised that no single study can purport to be a complete stand-alone work. Just as the current study is a continuation of lines of thought developed previously by others, so also this may lead to other streams of thought. Some possible future directions are explored in Chapter 7.

CHAPTER II: THE BORN-OPPENHEIMER APPROXIMATION

The Schrödinger equation, when first introduced, was solved for the simplest systems (such as the particle in a constrained potential), and this approach was later extended to include atomic systems. The only atomic system for which an exact solution is possible is the hydrogen (and hydrogen-like) atom system. Other systems were then solved by either applying the variational theorem or by means of perturbation theory. The variational solution of molecular systems would then have been prohibitively time-consuming, this being in the era before digital computers. It was therefore necessary to devise a scheme by which such computations could be made tractable and timely. In 1927, M. Born and R. Oppenheimer [1,2] published their proposal, which is now known as the Born-Oppenheimer approximation, for a method to solve the difficulties mentioned above. They took advantage of the fact that nuclei are at least 1830 times more massive than the electron to suggest that the nuclei be considered stationary and the electrons are then treated as though they move in the static electric field of the nuclei. It has been suggested that this approximation is valid, as it can be understood as the electrons adjusting quickly to any change in nuclear positions, such that at any instant of time the electrons only "see" a fixed nuclear framework.[3] This approximation effectively transformed the nuclei into classical particles, as the positions (and hence momenta) of the nuclei were known exactly.

In addition, the computation of electronic spectra requires a high degree of accuracy in the computation of electron density distributions.[4] Inaccuracy has been found to affect both the frequencies and intensities of the transitions.[4] Using a fixed-nuclei model necessarily compromises the accuracy of the density distributions, especially for systems containing light nuclei, as the electrons no longer feel the correct effect of the non-stationary nuclei.

For the reasons presented above, it is necessary to be able to solve the Schrödinger equation without requiring to "fix" the nuclei. Before this can be done, one must understand the Born-Oppenheimer approximation and this will be explored in the following section.

2.1 Born-Oppenheimer Approximation

The Born-Oppenheimer approximation is a technique that implicitly assumes the separability of nuclear and electronic motion in a bound system. The method treats electronic and nuclear motion independently, the only interaction between the two realms being through the electrostatic potential term. The following is a brief summary of the landmark work by M. Born and R. Oppenheimer.[1,2]

In this section, following the notation of Born and Oppenheimer, electronic quantities are presented in lowercase while nuclear quantities are in uppercase. A factor

κ is defined as $\left(\frac{m}{M}\right)^{\frac{1}{4}}$ where m is the mass of an electron and M is a mean value of the nuclear masses (M_l). The nuclear masses are then expressed in terms of the mean as $M_l = \mu_l M$, where μ_l is a pure number. The authors proceed to define the electronic and nuclear kinetic energies in terms of the operators

$$\hat{T}_E = -\frac{h^2}{8\pi^2 m}\sum_k \frac{\partial^2}{\partial x_k^2} \tag{2.1a}$$

$$\hat{T}_K = -\kappa^4 \frac{h^2}{8\pi^2 m}\sum_k \mu_l \frac{\partial^2}{\partial x_k^2} \tag{2.1b}$$

The potential energy U is defined as $U(x,X)$. The total Hamiltonian $\hat{H}$ of the system is then

$$\hat{H} = \hat{H}_0 + \kappa^4 \hat{H}_1 \tag{2.2}$$

where $\hat{H}_0$ and $\hat{H}_1$ are defined as $\hat{H}_0 = \hat{T}_E + \hat{U}$ and $\hat{T}_K = \kappa^4 \hat{H}_1$. It can be seen here that the authors have implicitly separated the nuclear and electronic motions by expanding the kinetic energy term as a sum of single-particle terms. The electrons and nuclei in this model interact with each other only through the electrostatic potential term.

The term κ is treated as a perturbation to the Hamiltonian, wavefunction, and the energy; and the terms are expanded as a series in κ. Collection of terms in κ gives rise to a series of equations. Hence, nuclear motion is treated as a perturbation expanded about a 'mean' (fixed) position, the amplitude of which decreases with κ. The zero order equation is the motion of electrons in a fixed nuclear field. The first-order equation must necessarily vanish, as the bound molecule is required to be at a stationary point. Solution

of the second-order equation yields the vibrational motion of the nuclei in the potential field of the electrons. It is noteworthy that this electronic potential field is generated around a rigidly fixed nuclear potential field. Solving the fourth-order equation yields rotation of the coordinate system (effectively molecular rotation). The higher order equations (though not solved by the authors) yield results to the various couplings between translation, rotation, and electronic motion.

2.2 Applications of the BO Approximation

Invoking the Born-Oppenheimer approximation was necessary to perform quantum chemical calculations on molecular systems, prior to which it was only possible to compute atomic systems. In addition, it became possible to investigate the properties of a system in different 'geometric configurations' (explained in section 2.2). This had resulted in a wide range of studies, which can be broadly categorised as being electronic structure determinations, or energy surface determinations. In the former approach, the interest is in the 'electron configuration' in the system at a fixed nuclear configuration. The quantities of interest can then be computed from this result. In the energy surface approach, the classical behaviour of the nuclei is taken advantage of to compute the energies at various nuclear configurations and estimate dynamic behaviour of the system. In this approach, it is not necessary for the electrons to be treated quantum mechanically, and certain classical mechanical applications have been developed treating the entire atom as an indivisible (classical) particle.

2.2.1: Electronic Structure Methods

Application of the Born-Oppenheimer approximation has made it possible to carry out quantum chemical calculations on molecular systems, whereas until this point, it was only possible to compute atomic systems. This breakthrough stimulated the field to grow in mainly two directions. These are the wavefunction method and the density functional method.

2.2.1.1: Wavefunction Methods

The wavefunction approach captures the wave nature of electrons by use of a wavefunction. The wavefunction of a system, in principle, determines all that is to be known regarding the system. This is in contrast to the density functional methods, which approach the properties of the system as being dependent on the electron density. In practice, the exact wavefunction is only obtained for very simple systems, such as a single particle in a potential. For example, one talks of a particle in a box, a particle on a ring, etc. Similarly, the hydrogen atom (and hydrogen-like atom) is the case of a single particle in a field created by the nucleus. In the atomic system, the coordinates can always be manipulated such that the nucleus is at the origin, thus reducing the situation to a central-field problem. However, there is no exact solution for the interacting three-body problem, and approximation methods must be employed to calculate any system larger than the hydrogen atom.[5]

2.2.1.1.1: Hartree-Fock Method

The Hartree-Fock method derives from the early work of D.R. Hartree [6] and V. Fock [7] on atomic systems. Hartree's results were later modified by Slater [8] correcting to include the anti-symmetrisation of the electronic wavefunction. The method was developed to solve for the "best" wavefunction variationally. The "best" wavefunction is defined as that which gives the lowest energy, and it should be noted that this might not be the optimal wavefunction for other properties.[5]

The total wavefunction is given by [9]

$$\Psi = \frac{1}{\sqrt{N}} \det\left|\phi_1(1)\alpha(1)...\phi_n\beta(2n)\right| \qquad (2.3)$$

in the case of a closed-shell atom. A closed-shell system is defined as one in which there is an even number of electrons $(2n)$ occupying n spatial wavefunctions with each electron having either α or β spin. This is compared to the total wavefunction defined by Hartree [6] as being a Hartree product, where the index runs over all electrons.

$$\Psi = \prod_{i}^{2n} \phi_i \qquad (2.4)$$

The single-particle wavefunction is then defined as being the product of a spatial function ϕ and a spin function. The spatial orbitals are chosen to be orthonormal, or

$$\langle \phi_i | \phi_j \rangle = \delta_{ij} \qquad (2.5)$$

where δ_{ij} is the Kronecker delta. This restriction simplifies the algebraic computations required by allowing one to neglect overlap integrals (which have been uniformly set to

zero). The total energy of a system having a wavefunction of the above form can be shown [5] to be

$$E = 2\sum_{i=1}^{2n} \varepsilon_i^{(0)} + \sum_{i,j}^{2n} (2J_{ij} - K_{ij}) \qquad (2.6)$$

The wavefunction is to be optimised so that the energy of the wavefunction is the lowest possible. In other words, the best possible wavefunction is to be constructed so that the energy is a minimum. This is most commonly done by the method of Lagrangian multipliers. The functional

$$F[E] = 2\sum_{i=1}^{2n} \varepsilon_i^{(0)} + \sum_{i,j}^{2n} (2J_{ij} - K_{ij}) - 2\sum_{i,j}^{2n} \lambda_{ij} \left(\langle \phi_i | \phi_j \rangle - \delta_{ij} \right) \qquad (2.7)$$

is constructed where λ_{ij} are the Lagrangian multipliers. It is then required to find the conditions to be satisfied by the orbitals in order that $F[E]$ is a minimum. Hence, it is necessary that $\delta F[E] = 0$ for arbitrarily small variations $\delta\phi_i$ of the optimised orbitals. The Coulomb and exchange operators can be defined as follows

$$J_i(\mu)\phi_j(\mu) = \langle \phi_i(\nu) | \frac{1}{r_{\mu\nu}} | \phi_i(\nu) \rangle \phi_j(\mu) \qquad (2.8a)$$

$$K_i(\mu)\phi_j(\mu) = \langle \phi_i(\nu) | \frac{1}{r_{\mu\nu}} | \phi_j(\nu) \rangle \phi_i(\mu) \qquad (2.8b)$$

It is to be noted that the exchange operator exchanges electrons μ and ν between the spatial orbitals ϕ_i and ϕ_j. Using the above definitions for the Coulomb and exchange operators, the component terms of the energy expression can be written as

$$J_{ij} = \langle \phi_i(\mu) | J_j(\mu) | \phi_i(\mu) \rangle = \langle \phi_j(\nu) | J_i(\nu) | \phi_j(\nu) \rangle \qquad (2.9a)$$

$$K_{ij} = \langle \phi_i(\mu) | K_j(\mu) | \phi_i(\mu) \rangle = \langle \phi_j(\nu) | K_i(\nu) | \phi_j(\nu) \rangle \qquad (2.9b)$$

The Coulomb operator is the operator for the potential due to the electron distribution $|\phi_i|^2$. Such operators represent the effective potentials for an electron moving in the repulsive field of other electrons. The exchange operator has no classical analogue as it arises from the non-classical anti-symmetry principle.

The first-order variation in $F[E]$ is given by

$$\begin{aligned}
\delta F[E] &= 2\sum_{i}^{2n}\left(\langle\delta\phi_i|h_\mu|\phi_i\rangle + \langle\phi_i|h_\mu|\delta\phi_i\rangle\right) \\
&+ \sum_{i,j}^{2n}\left(\langle\delta\phi_i|2J_j - K_j|\phi_i\rangle + \langle\phi_i|2J_j - K_j|\delta\phi_i\rangle\right) \\
&+ \sum_{i,j}^{2n}\left(\langle\delta\phi_j|2J_i - K_i|\phi_j\rangle + \langle\phi_j|2J_i - K_i|\delta\phi_j\rangle\right) \\
&- 2\sum_{i,j}^{2n}\left(\lambda_{ij}\langle\delta\phi_i|\phi_j\rangle + \lambda_{ij}\langle\phi_i|\delta\phi_j\rangle\right)
\end{aligned} \tag{2.10}$$

where h_μ is the mono-electronic part of the atomic Hamiltonian operator. It can be seen that the second and third terms in the equation above are symmetric and can hence be collapsed into one term and the equation can be rewritten as

$$\begin{aligned}
\delta F[E] &= 2\sum_{i}^{2n}\left[\langle\delta\phi_i|h_\mu + \sum_{j}^{2n}\left(2J_j - K_j\right)|\phi_i\rangle\right] \\
&+ 2\sum_{i}^{2n}\left[\langle\phi_i|h_\mu + \sum_{j}^{2n}\left(2J_j - K_j\right)|\delta\phi_i\rangle\right] \\
&- 2\sum_{i,j}^{2n}\left(\lambda_{ij}\langle\delta\phi_i|\phi_j\rangle + \lambda_{ij}\langle\phi_i|\delta\phi_j\rangle\right)
\end{aligned} \tag{2.11}$$

Recognising that the first two terms are adjoints of each other due to the hermitian nature of the operators, and that $\langle \phi_j | \delta\phi_i \rangle$ and $\langle \delta\phi_i | \phi_j \rangle$ are mutual adjoints, this reduces to

$$\begin{aligned} \delta F[E] = 2\sum_{i}^{2n}\left[\langle \delta\phi_i | h_\mu + \sum_{j}^{2n}(2J_j - K_j)|\phi_i\rangle - \sum_{j}^{2n}\lambda_{ij}\langle \delta\phi_i | \phi_j \rangle \right] \\ + 2\sum_{i}^{2n}\left[\langle \delta\phi_i | h_\mu + \sum_{j}^{2n}(2J_j - K_j)|\phi_i\rangle^* - \sum_{j}^{2n}\lambda_{ij}\langle \delta\phi_i | \phi_j \rangle^* \right] \end{aligned} \tag{2.12}$$

The vanishing $\delta F[E]$ is now satisfied by the conditions

$$\left[h_\mu + \sum_{j}^{2n}(2J_j - K_j) \right]\phi_i = \sum_{j}^{2n}\phi_j\lambda_{ij} \tag{2.13a}$$

$$\left[h_\mu + \sum_{j}^{2n}(2J_j - K_j) \right]\phi_i^* = \sum_{j}^{2n}\phi_j^*\lambda_{ji} \tag{2.13b}$$

Subtracting the complex conjugate of the second equation from the first leads to

$$\sum_{j}^{2n}\phi_j(\lambda_{ij} - \lambda_{ji}^*) = 0 \tag{2.14}$$

Since the orbitals are linearly independent, it is then required that

$$\lambda_{ij} = \lambda_{ji}^* \tag{2.15}$$

Hence, the Lagrangian multipliers form a Hermitian matrix. Consequently, equation 2.13a and equation 2.13b are equivalent, being complex conjugates of each other. Equations 2.13a and 2.13b are known as the Hartree-Fock equations. The Hartree-Fock equations can also be written as

$$\hat{F}\Phi = \Phi\lambda \tag{2.16}$$

where the Fock operator $\hat{F}$ is defined as

$$\hat{F} = h_\mu + \sum_j^{2n} \left(2J_j - K_j\right) \tag{2.17}$$

It can be seen that the Fock operator is a one-electron operator. The operator h_μ yields the kinetic energy of a single electron, while $\sum_j^{2n}(2J_j - K_j)$ represents the average potential experienced by an electron due to the other electrons in the system. Diagonalisation of the λ matrix by means of a unitary transformation yields the solution

$$\hat{F}\phi_i = \varepsilon_i \phi_i \tag{2.18}$$

where the $\{\varepsilon_i\}$ are interpreted as being the energies of the orbitals $\{\phi_i\}$. It has been shown [10] that the negative of the Hartree-Fock orbital energy corresponds to the energy of ionisation of an electron from that orbital (Koopmans' Theorem).

2.2.1.1.2: Roothaan-Hall Method

The above method was further extended to the study of molecules by Roothaan and Hall.[11,12] The Roothaan method is made possible by applying the Born-Oppenheimer approximation.[1,2] The Born-Oppenheimer approximation takes into account the fact that nuclei are at least 1830 times as massive as electrons. Hence, the velocities and ranges of motion are expected to be much reduced as compared to similar quantities for the electrons. It is assumed that the motions of nuclei, being much slower, can be decoupled from the motions of the electrons. This is formalised by holding the nuclei fixed and allowing the electrons to move in the field of the fixed nuclei. This can be understood by

saying that the electrons move much faster than the nuclei and that the electrons adapt instantaneously to any small change in the positions of the nuclei.

In Roothaan's treatment, the one-electron molecular wavefunctions are expanded as a series of atomic wavefunctions. This approach is known as the linear combination of atomic orbitals (LCAO) approach. Under the LCAO approximation, the one-electron wavefunctions are given by

$$\psi_i = \sum_{\lambda} C_{\lambda i}\phi_{\lambda} \tag{2.19}$$

where the ϕ_{λ} correspond to the λ^{th} atomic wavefunction and the $C_{\lambda i}$ are the coefficients that determine the contribution of each atomic wavefunction to the total wavefunction. This can be expressed in matrix notation as

$$\psi = \Phi\ \mathbf{C} \tag{2.20}$$

The molecular wavefunction is formed as a Slater determinant [9] of the one-electron wavefunctions (with N being an arbitrary normalization constant).

$$\Psi = \frac{1}{\sqrt{N}}\det\left|\psi_1(1)\alpha(1)...\psi_n\beta(2n)\right| \tag{2.21}$$

In a derivation analogous to that of the Hartree-Fock method, it was shown [11] that the following system of equations (known as the Roothaan-Hall Equations) is satisfied

$$\mathbf{FC} = \mathbf{SC}\varepsilon \tag{2.22a}$$

which can also be written as

$$\hat{F}c_i = \varepsilon_i S c_i \tag{2.22b}$$

where ε_i is the i^{th} eigenvalue and $\hat{F}$ is the Fock operator given as before, by

$$\hat{F} = h_\mu + \sum_j^N (2J_j - K_j) \tag{2.23}$$

The operator h_μ is the single-electron Hamiltonian, while J_j and K_j are the Coulomb and exchange operators, respectively. The summation is carried out over the N electrons. The matrix $\mathbf{S}$ is defined as the overlap matrix whose elements are the overlap integrals

$$S_{pq} = \int \overline{\chi}_p \chi_q d\tau \tag{2.24}$$

The orthonormalisation criterion constrains $\mathbf{S}$ to be a diagonal matrix with diagonal elements having a value of unity. Hence, $\mathbf{S}$ is the identity operator.

The Coulomb and exchange operators can be defined as [5]

$$J_i(\mu)\phi_j(\mu) = \langle \phi_i(\nu) | \frac{1}{r_{\mu\nu}} | \phi_i(\nu) \rangle \phi_j(\mu) \tag{2.25a}$$

$$K_i(\mu)\phi_j(\mu) = \langle \phi_i(\nu) | \frac{1}{r_{\mu\nu}} | \phi_j(\nu) \rangle \phi_i(\mu) \tag{2.25b}$$

As can be seen from equation 2.25, the operators J_j and K_j depend on the orbitals, which are in turn generated by these operators. Hence, the Hartree-Fock equations cannot be solved directly as a true eigenvalue equation. These equations are then solved by the self-consistent field (SCF) method. In this method, a trial set of orbitals is generated, from which a new set of wavefunctions are obtained as solution to the equations. This process is repeated until the trial set of wavefunctions is identical (within a certain tolerance) with the resultant wavefunction set. Due to the variational

theorem, the total energy obtained is always an upper bound to the true energy of the system.

It is illustrative to compare the Hartree-Fock and Roothaan-Hall equations.

$$\hat{F}\Phi = \Phi\lambda \tag{2.18}$$

$$\mathbf{FC} = \mathbf{SC}\varepsilon \tag{2.22a}$$

It can be seen that the two equations are fundamentally equivalent. Hence, it can be easily understood why the Roothaan-Hall method is also referred to as the Hartree-Fock method, as it is a generalisation of the earlier method for use in systems more extended than the atomic system. In the remainder of this document, the Hartree-Fock method will be the name used to describe both the Hartree-Fock-Slater and Roothaan-Hall approaches. The difference in application can be understood from the context as the former refers to atomic systems and the latter to more extended systems.

From equations 2.4 and 2.19 (or 2.20) it can be seen that the total wavefunction is constructed in terms of various functions that have been left undefined. It is then required that there be some method by which suitable functions can be found. The LCAO approach assumes that the functions are of atomic nature, whereas the atomic model leaves the question unanswered. In practice, the same sets of basis functions are used for both models, as they only have one requirement - the orthonormality of the basis functions. The basis functions are typically approximations to the hydrogenic wavefunctions for the atom in question. Currently there are two types of basis sets in use. The Slater type orbitals (STO) have the form

$$\chi_{\zeta,n,l,m}(r,\theta,\varphi) = NY_{l,m}(\theta,\varphi)r^{n-1}e^{-\zeta r} \qquad (2.25)$$

where n, l, and m refer to the principal, azimuthal, and magnetic quantum numbers, respectively. It can be seen that these functions have no radial nodes, in contrast with the hydrogenic wavefunctions (HOs), which these functions are designed to approximate. However, it can be seen that these functions have a similar behaviour to that of the HOs at increasing distance from the nucleus. Due to their increased ease of use *vis-à-vis* the STOs, Gaussian type orbitals (GTO) have been introduced to fit the profile of the STOs, and are of the form

$$\chi_{\zeta,n,l,m}(r,\theta,\varphi) = NY_{l,m}(\theta,\varphi)r^{2n-2-l}e^{-\zeta r^2} \qquad (2.26)$$

It can be seen that in addition to the lack of radial nodes, GTOs also show incorrect long-range behaviour. However, the time savings offered by the use of GTOs allow one to approximate STOs by ever-larger numbers of GTOs while still reducing the computational effort.[13]

The Hartree-Fock method does not properly account for the Coulombic interactions between electrons. Electron pairs with parallel spins are kept apart by the anti-symmetry principle, more so than electrons of anti-parallel spin. To account for this effect, electrons cannot be allowed to move in an average field of the others, as is the case with the Hartree-Fock method. This modification is referred to as electron correlation and can be understood as the electrons making complex motions in order to maintain the greatest possible separation from all other electrons, while still being attracted by the nuclei. The correlation energy is then defined as the difference between the exact energy and the Hartree-Fock energy. It is to be noted that the exact energy is not the

experimental energy. Since the Hartree-Fock Hamiltonian is non-relativistic, a comparison with experimental energies would include relativistic effects as well. Hence, the Hartree-Fock energy is to be compared to the exact non-relativistic energy, the difference between which yields the non-relativistic correlation energy.[5,13]

Methods have been developed to recoup much of the correlation energy, such as the Møller-Plesset, configuration interaction, and coupled-cluster schemes. These schemes are collectively known as post-Hartree-Fock methods. The Møller-Plesset method is a perturbative method used to solve for the correlation as a perturbation to the Hartree-Fock Hamiltonian.[5] The configuration interaction (CI) method approaches the question of electron correlation by taking it to be approximated by the sum of various excited state configurations. It can be recalled that the Hartree-Fock wavefunction is expressed as a Slater determinant. The CI wavefunction is hence represented as a linear combination of Slater determinants. It is for this reason that CI is referred to as a multi-determinant method. Both of the above mentioned methods are very computationally expensive and need extended expansions before meaningful results are obtained. Due to the computational expense required, these methods are impractical for all but the smallest systems. A more detailed description of these schemes is beyond the scope of this document and can be found elsewhere.[5,13-15]

2.2.1.2: Density Functional Approach

Density functional theory (DFT) is an approach built on the premise that the electron density completely determines the energy and properties of the system under

study. This implies a one-to-one correspondence between the electron density and the ground state energy.[13] Compared to the wavefunction method, wherein the energy is determined by a system of $3N$ (or $4N$, if spin is included) coordinates, the DFT approach is only dependent on three (or four) dimensions, and is independent of the number of electrons.[4] This approach is rationalised since it can be shown that [4]

i. $\int \rho(\bar{r}_1) d\bar{r}_1 = N$, or the electron density integrates to the number of electrons

ii. $\rho(\bar{r})$ has maxima (that are cusps) at the positions of the nuclei, and that

iii. $\lim_{r_A \to 0} \left[\frac{\partial}{\partial r} + 2Z_A \right] \rho(\bar{r}) = 0$, or the density at the nucleus contains information regarding the nuclear charge.

Hence, it can be seen that the electron density has the characteristics required to set up a system-specific Hamiltonian and is plausible that the density suffices for a complete description of molecular properties. Hence, it can be argued that the proponents of density functional theory are justified in their approach to the task of solving the molecular Schrödinger equation. In terms of implementation, it can be shown that the Hamiltonian operator can, analogous to the wavefunction method, be separated into kinetic, Coulomb, and exchange terms.[4,13]

Density functional theory (DFT) has been in use in some form from the 1920s and dates back to the early work by Thomas, Fermi, Dirac, and Wigner.[16] The theory developed by Thomas and Fermi is a true density-functional theory as it expresses all

contributions to the total energy, kinetic as well as electrostatic, in terms of the electron density. The original formulation of Thomas and Fermi is a quantum statistical model of electrons taking into account only the kinetic energy, while treating the nucleus-electron and electron-electron interactions classically. Furthermore, the electron density is treated similar to the uniform (homogeneous) electron gas. The kinetic energy term derived is

$$T_{TF}[\rho(\bar{r})] = \frac{3}{10}\left(3\pi^2\right)^{\frac{2}{3}} \int \rho^{\frac{5}{3}}(\bar{r}) d\bar{r} \tag{2.27}$$

Combined with the classical expressions for the nucleus-electron and electron-electron interactions, this yields the Thomas-Fermi expression for the energy of an atom

$$E_{TF}[\rho(\bar{r})] = \frac{3}{10}\left(3\pi^2\right)^{\frac{2}{3}} \int \rho^{\frac{5}{3}}(\bar{r}) d\bar{r} - Z\int \frac{\rho(\bar{r})}{r} d\bar{r} + \frac{1}{2}\iint \frac{\rho(\bar{r}_1)\rho(\bar{r}_2)}{r_{12}} d\bar{r}_1 d\bar{r}_2 \tag{2.28}$$

As the inter-electron interactions were treated classically, the Hamiltonian necessarily does not contain the electron exchange term (as can be seen above), which would be required by the anti-symmetry principle. Inclusion of the exchange term derived by Dirac

$$K_D[\rho] = -\frac{3}{4}\left(\frac{3}{\pi}\right)^{\frac{1}{3}} \int \rho^{\frac{4}{3}}(\bar{r}) d\bar{r} \tag{2.29}$$

constitutes the Thomas-Fermi-Dirac (TFD) method.

The main importance of the TF (or TFD) method lies not in its accuracy. In fact, the TF and TFD methods were unable to predict bonding. Utilisation of these methods could not predict the existence of molecules![13] This result was due to the incorrect form

of the kinetic energy term, which was derived using the assumption of the uniform electron gas.[4,13] It is obvious from above sections that a molecular system contains regions of vastly different electron densities. Hence, the assumption of uniform electron density in a molecular system would lead to incorrect results. The true importance of the theory developed by Thomas and Fermi is that it is a true density-functional theory as it expresses all contributions to the total energy, kinetic as well as electrostatic, in terms of the electron density.

The Hartree-Fock-Slater (X_α) method was one of the first DFT-based schemes to be used on multi-atomic electronic systems. This method has its origins in the work of Slater, [17] who in 1951 proposed an improvement to the non-local exchange contribution under Hartree-Fock theory wherein the exchange-correlation potential is represented by a function that is proportional to the $1/3$ power of the electron density. The exchange contribution arising from the anti-symmetry of the wavefunction can be expressed as the interaction between the charge density of spin σ and the Fermi hole of the same spin.

$$E_X = \frac{1}{2}\iint \frac{\rho(\vec{r}_1)h_X(\vec{r}_1;\vec{r}_2)}{r_{12}} d\vec{r}_1 d\vec{r}_2 \qquad (2.30)$$

Hence, if a reasonable approximation to the Fermi hole could be developed, the exchange contribution could be calculated with sufficient ease. To this end, Slater assumed that the exchange hole is spherically symmetric and centred on the electron at $\vec{r}_1$. It is further assumed that within the sphere the exchange hole density is constant, being negative the value of $\rho(\vec{r}_1)$, whereas it is zero outside the sphere. The Wigner-Seitz

radius [18,19] is calculated as follows based on the fact that one Fermi hole contains exactly one elementary charge.

$$r_S = \left(\frac{3}{4\pi}\right)^{1/3} \rho(\bar{r}_1)^{-1/3} \tag{2.31}$$

It can be shown from standard electrostatics that the potential of a charged sphere of radius r_S is given by $\frac{1}{r_S} = \rho(\bar{r}_1)^{1/3}$. Hence, the exchange functional is given by

$$E_X[\rho] \cong C_X \int \rho(\bar{r}_1)^{4/3} d\bar{r}_1 \tag{2.32}$$

where C_X is a numerical constant. In order to improve the quality of the approximation, an adjustable parameter α was included in the pre-factor C_X, thus resulting in the Hartree-Fock-Slater X_α method. The exchange functional in the X_α method is thus given by

$$E_{X\alpha}[\rho] = -\frac{9}{8}\left(\frac{3}{\pi}\right)^{1/3} \alpha \int \rho(\bar{r}_1)^{4/3} d\bar{r}_1 \tag{2.33}$$

Typical values for α ranged from 2/3 to unity. It can be seen that the Slater X_α exchange functional is identical to the Dirac exchange functional (equation 2.29) when $\alpha = \frac{2}{3}$, though the two were derived differently.

Both the Thomas-Fermi and X_α methods were at the time of their inceptions considered as useful models based on the foundation that the energy of an electronic system could be expressed in terms of its density. A formal proof of this notion came when Hohenberg and Kohn [20] showed that the ground-state energy of an electronic

system is uniquely defined by its density, although the exact dependence is unknown. For an N-particle system interacting with a given inter-particle interaction, the Hamiltonian and thus the ground state wavefunction (and energy) are completely determined by specification of the external field $\phi(r)$. In other words, the ground state energy is a functional of $\phi(r)$. They showed that there is a one-to-one correspondence between the external field $\phi(r)$ and the single-particle density $\rho(r)$ and that it is then possible to write the total ground state energy as a functional of $\rho(r)$,

$$E[\rho]=E_0[\rho]+\int dr\phi(r)\rho(r) \qquad (2.31)$$

where $E_0[\rho]$ is a functional that is independent of the external potential $\phi(r)$. Hohenberg and Kohn also proved a second theorem, which showed that for any trial density $\rho(r)$ that satisfies $\int\rho(r)dr=N$,

$$E[\rho]\geq E_g \qquad (2.32)$$

where E_g is the true ground state energy, the equality being valid only when $\rho(r)$ is the true ground-state single-particle density. The Hohenberg-Kohn theorems apply specifically to the ground state and hence are strictly valid only at zero absolute temperature.[21]

Kohn and Sham [22] derived a set of one electron equations from which in principle, one could obtain the exact electron density and hence the total energy. The total energy of an N electron system can be written without approximations as

$$E_{el} = -\frac{1}{2}\sum_i \int \phi_i(r_i)\nabla_i^2\phi_i(r_i)dr_i + \sum_A \frac{Z_A}{|R_A - r_1|}\rho(r_1)dr_1 + \frac{1}{2}\int \frac{\rho(r_1)\rho(r_2)}{|r_1 - r_2|}dr_1 dr_2 + E_{XC} \tag{2.33}$$

The first term in the above equation corresponds to the kinetic energy of N non-interacting electrons with the same density $\rho(r_1) = \sum_i^{occ} \phi_i^*(r_1)\phi_i(r_1)$ as the actual system of interacting electrons. The second term accounts for the attraction between electrons and nuclei, and the third term for the Coulomb repulsion between the two charge distributions $\rho(r_1)$ and $\rho(r_2)$. The last term contains the exchange-correlation energy E_{XC}. The one-electron orbitals of equation (2.33) are solutions to the set of one-electron Kohn-Sham equations

$$\left[-\frac{1}{2}\nabla_1^2 + \frac{Z_A}{|R_A - r_1|} + \int \frac{dr_2\rho(r_2)}{|r_1 - r_2|} + V_{XC}\right]\phi_i(r_1) = \hat{h}_{KS}\phi_i(r_1) = \varepsilon_i\phi_i(r_1) \tag{2.34}$$

where the exchange-correlation potential V_{XC} is given as the functional derivative of E_{XC} with respect to the density

$$V_{XC} = \frac{\delta E_{XC}[\rho]}{\delta\rho} \tag{2.35}$$

It is to be emphasised that the E_{XC} is different from the traditional quantum chemical definition of the exchange-correlation energy as being the sum of the Hartree-Fock exchange energy and the correlation energy, the latter being traditionally defined as the difference between the exact and Hartree-Fock energies. The traditional definition has the operational advantage that the reference Hartree-Fock energy does not contain

unknown quantities and can be calculated to virtually arbitrary accuracy. This is definitely not the case for the Kohn-Sham system, E_{XC} and its functional derivative V_{XC} being known only approximately. Obtaining them exactly is equivalent to a full solution of the many-electron problem. [16,21]

It may be noted that the Kohn-Sham equations closely resemble the Hartree-Fock equations. Hence, the methods of calculation are computationally similar, both in methodology and in time consumed. The computation is however performed with electron correlation included in the description. A major point of contention is the exact form of the exchange-correlation functional. Since Hohenberg and Kohn state that an exact form for the Hamiltonian cannot be known *a priori*, the form of the exchange-correlation functional also cannot be known exactly. This has led to a myriad of functionals that seem to be suitable for specific applications.

Density functional theory has seen many advances since the early days when it was first proposed by Thomas and Fermi in 1927. The Thomas-Fermi method was a true density functional method in that the kinetic and potential energy terms were completely evaluated using the electron density as the only variable. Unfortunately, this model was not very successful, as it could not predict energies accurately, nor did it permit bonding. This was in spite of including the exchange term derived by Dirac, to correct for the anti-symmetric nature of electrons, a property that had been ignored in the original formulation. The source of the error was determined to lie in the kinetic energy term. This was due to the fact that the kinetic energy functional was derived applying the

approximation of the uniform electron gas, whereas atomic and molecular systems exhibit widely varying electron densities. Hence, one of the basic assumptions applied was untenable. However, the basic premise that the electron density can be used as the principal variable for calculation of atomic properties is still valid, as proved by Hohenberg and Kohn.[20] It is therefore conceivable that the Thomas-Fermi method could be made useful, if an appropriate functional based on the inhomogeneous electron gas could be developed. Such a technique, would in general, be of great computational importance, especially for larger systems where the scaling afforded by currently used correlated methods would prove prohibitive.

The Slater X_α method was an approach developed to correct for the non-local exchange in the Hartree-Fock method. It so happens that the resulting formulation depends on the local electron density (which was related to the local hole density). As a result, this method is recognised as one of the earlier density functional methods, and acquired popularity as a computational tool among physicists.[4]

The Hohenberg-Kohn theorems [20] offered the first formal proof that the electron density can be used as the principal variable to compute molecular properties. This was done by proving that the electron density and system energy share a one-to-one correspondence, and that the calculated energy was an upper bound to the true energy. However, the theorems were only applicable to the ground state, and hence are strictly applicable only at zero absolute temperature.

Kohn and Sham [22] later derived a method where the electron density was divided into a number of 'orbitals'. These Kohn-Sham orbitals, though sharing the name of their Hartree-Fock counterparts, are different. This is due to the fact that Koopmans' Theorem is not valid in the case of Kohn-Sham orbitals and their energies, thereby losing the physical significance of the Hartree-Fock orbitals. Koopmans' Theorem would be valid if the exact exchange-correlation functional were employed.[13] However, the exact form of the exchange-correlation functional is not known and various approximation schemes have been developed over the years. It may be that the common assumption of separable exchange and correlation functional contributions may not be accurate.[4,13] This would preclude a solution of the exact exchange-correlation functional. As the difference between the Hartree-Fock and Kohn-Sham equations lies in the exchange-correlation potential, the Kohn-Sham formalism has the possibility of providing the exact solution to the Schrödinger equation. This is due to the fact that the Hartree-Fock energy differs from the exact solution by the correlation energy, which is recovered under the Kohn-Sham scheme. Hence, derivation of the exact exchange-correlation functional would result in a computationally tractable method to obtain the exact solution under the set of approximations employed.

2.2.1.3: Implementation of Structure Methods

Implementation schemes for the Hartree-Fock (including Roothaan-Hall) and Kohn-Sham density functional methods are very similar. The only difference lies in the mode of generation of the Fock matrix. Hence, as an illustration, the implementation of the Hartree-Fock (HF) method is outlined below.[23] This leads to a template based on

which the implementation of the modified ENMO method (Section 4.3.4) can be easily understood.

As mentioned earlier, the HF method is a self-consistent field method. It is therefore useful to separate the constant and flexible terms of the operator to simplify the computations. The Fock matrix $\mathbf{F}$ is separated into the core $\mathbf{H}$ matrix and the variable $\mathbf{G}$ matrix.

$$\mathbf{F} = \mathbf{H} + \mathbf{G} \tag{2.36}$$

The core matrix $\mathbf{H}$ contains terms that are invariant during the course of the SCF computation as its contents are constant for a fixed nuclear configuration. The terms contained are the one-electron kinetic energy and nuclear attraction terms expressed in terms of the basis $\{\phi\}$.

$$H_{\mu\nu} = \int d\mathbf{r}_1 \phi_\mu^*(1)\left(-\frac{1}{2}\nabla_1^2 - \sum_A \frac{Z_A}{|\mathbf{r}_1 - \mathbf{R}_A|}\right)\phi_\nu(1) \tag{2.37}$$

As the $\mathbf{H}$ matrix is a one-electron matrix (containing kinetic energy and nuclear-electronic interaction information), it does not contain any information relating to the spin and is retained as is. Hence, the $\mathbf{H}$ matrix is invariant between the spin restricted and unrestricted cases.

The terms of the $\mathbf{G}$ matrix contain information regarding the electron repulsions including the Coulomb and exchange interactions. The elements of the $\mathbf{G}$ matrix are initialised to 0 before the first iteration. The first iteration yields a guess density matrix

$\mathbf{P}$. Under the unrestricted (Pople-Nesbet) formalism, the electronic density is expressed in terms of the α and β densities. [24]

$$P_{\mu\nu}^{\alpha} = \sum_{a}^{N^{\alpha}} C_{\mu a}^{\alpha} (C_{\nu a}^{\alpha})^{*} \tag{2.38}$$

The relation for $\mathbf{P}^{\beta}$ can be obtained in an analogous fashion and hence only the α results are shown in this section. Under the unrestricted formalism, two other density matrices are defined, the total density matrix

$$\mathbf{P}^{T} = \mathbf{P}^{\alpha} + \mathbf{P}^{\beta} \tag{2.39a}$$

and the spin density matrix

$$\mathbf{P}^{S} = \mathbf{P}^{\alpha} - \mathbf{P}^{\beta} \tag{2.39b}$$

The spin density matrix, though of chemical interest is not used in the implementation of the method. The terms of the $\mathbf{G}$ matrix are then obtained in terms of the $\mathbf{P}$ matrix. As the $\mathbf{G}$ matrix deals exclusively with inter-electron interactions, the unrestricted method requires $\mathbf{G}^{\alpha}$ and $\mathbf{G}^{\beta}$ matrices to be generated. The terms of the $\mathbf{G}^{\alpha}$ matrix are given by

$$G_{\mu\nu}^{\alpha} = \sum_{\lambda}\sum_{\sigma}\left(P_{\lambda\sigma}^{T}(\mu\nu|\lambda\sigma) - P_{\lambda\sigma}^{\alpha}(\mu\lambda|\sigma\nu)\right) \tag{2.40}$$

As can be seen from the above, the α and β electrons interact with each other through the $\mathbf{G}$ matrix. In fact, it is to be noted that the interaction between electrons of differing spin is only through the Coulomb term in the expression. The differing spin makes the particles distinguishable (magnetically) and hence there is no exchange interaction between the electrons of differing (opposite) spin.

The Pople-Nesbet equations [24] are then solved to yield the eigenvalues (energies) and eigenvectors (coefficient matrix).

$$\mathbf{F}^{\alpha}\mathbf{C}^{\alpha} = \mathbf{S}\mathbf{C}^{\alpha}\varepsilon^{\alpha} \tag{2.41a}$$

$$\mathbf{F}^{\beta}\mathbf{C}^{\beta} = \mathbf{S}\mathbf{C}^{\beta}\varepsilon^{\beta} \tag{2.41b}$$

The $\mathbf{S}$ matrix in the above equations contains the overlaps between the various basis functions used, and hence is invariant between the two equations. In fact, the $\mathbf{S}$ matrix only need be calculated once at each nuclear orientation. The coefficient matrices $\mathbf{C}$ obtained above are used to generate new $\mathbf{P}$, $\mathbf{G}$, and $\mathbf{F}$ matrices. Recursion through this procedure until the energy of the system

$$E_0 = \frac{1}{2}\sum_{\mu}\sum_{\nu}\left[P^{T}_{\nu\mu}H_{\mu\nu} + P^{\alpha}_{\nu\mu}F^{\alpha}_{\mu\nu} + P^{\beta}_{\nu\mu}F^{\beta}_{\mu\nu}\right] \tag{2.42}$$

is minimised and stable (within a set tolerance) is performed to attain the optimal solution of the system. An alternate convergence criterion may be considered to be the convergence of the density matrices $\mathbf{P}$. This automatically leads to an optimised energy as the energy depends only on the density matrices as variables (since the $\mathbf{F}$ matrix also only depends on $\mathbf{P}$).

2.2.2: Property Hyper-surfaces

The major advantage to the Born-Oppenheimer approach is that it permits the calculation of property hyper-surfaces for molecules and larger systems. A property hyper-surface is defined as being the variation in the property of interest as a function of the positions of the nuclei. As there are three degrees of freedom for each nucleus, the hyper-surface exists in $3N+1$ dimensions, with N being the number of nuclei in the system. The hyper-surfaces are constructed by calculating the value of the property in question at various configurations of the nuclei. The most commonly calculated surfaces are the potential energy (PES) and free energy surfaces (FES). The PES refers to the

dependence of the sum of electronic energy and nuclear repulsion energy on the variation of nuclear positions.[15] The equilibrium geometry is then defined as the position on the PES at which the molecule is at an absolute minimum. Of course, there may be several minima on the PES (depending on the size of the system), leading to several possible conformations. The minima on the PES necessarily correspond to equilibrium structures since the ground state is required to be a stationary point, i.e. the total energy is required to be a minimum with respect to all degrees of freedom. One also observes saddle points, points at which the property is at a maximum in one or more dimensions. A first-order saddle point in the potential energy (or the free energy) hyper-surface corresponds to a transition state. Reaction rates can then be calculated in accordance with transition state theory [25,26] or RRKM theory, [27-33] as the case warrants. Harmonic vibrational frequencies of a molecule are obtained from the curvature of its PES. Use of the quantum simple harmonic oscillator model leads to a zero-point vibrational energy that is higher than the equilibrium energy. This, in effect, causes the "fixed" nuclei to be delocalised within a small region of space, confined to a region near the bottom of the potential well, correcting for the uncertainty in position implied by the Heisenberg principle. Unfortunately, this delocalisation does not affect the energy distribution, since the potential surface is calculated based on the fixed point-charge model for the nuclei.

2.3 Implications of the BO Approximation

The BO approximation mentions that the nuclear and electronic wavefunctions are separable. Hence, the implication is that the electronic delocalisation is decoupled from that of the nuclei. The nuclei can then be taken to be stationary point charges and the

electrons are then assumed to move in the mean field generated by the nuclei. Separating the nuclear and electronic wavefunctions leads to a few results of fundamental importance. Primarily, treating the nuclei as classical point charges implies that the electronic states are identical for all isotopomers of a given molecule. This also leads to the result that gradients and force constants must be independent of isotopic substitution. As a result, optimised geometries are also required to be identical. For example, for a diatomic molecule with two isotopomers, if one were to define $\rho = \sqrt{\frac{\mu_1}{\mu_2}}$ where the 1 and 2 refer to two isotopomers, the following relationships are necessarily true:

$$\frac{\omega_e^2}{\omega_e^1} = \rho \qquad (2.43a)$$

$$\frac{B_v^2}{B_v^1} = \rho^2 \qquad (2.43b)$$

$$\frac{D_v^2}{D_v^1} = \rho^4 \qquad (2.43c)$$

where ω, B, and D refer to the vibrational frequency, rotational constant, and first order centrifugal distortion respectively.

Due to this requirement, computational packages typically do not invoke isotopes unless vibrational frequencies are to be calculated, in which case the mass of the atom is used explicitly.

2.4 Inadequacies of the Born-Oppenheimer Approximation

As noted earlier, the Born-Oppenheimer approximation assumes that the nuclear and electronic motions are completely decoupled and that they can hence be separated. This assumption leads to the situation where nuclear motion occurs in a potential field of

electrons, which themselves are calculated with respect to a fixed nuclear framework! This is definitely true of how vibrations and rotations are obtained from the Born-Oppenheimer expansion and is obviously an inconsistent situation.

The purpose of this study is to explore ways in which the separability approximation can be removed. Removal of the separability approximation would allow the accurate calculation of the electron density distribution in a molecule. The inability to compute the density distribution accurately currently precludes the ability to compute electronic spectra to high accuracy, for example using time-dependent methods.[4] This is further illustrated by the fact that Born-Oppenheimer calculations are unable to reproduce the difference in electronic excitation energies that have been observed in small molecules.[34] In addition, there are systems for which the "fixed nuclei" model yields inadequate results, such as the cooperative electron-proton transfer (CEPT) reactions observed in biological systems.[35]

CHAPTER III: PREVIOUS ATTEMPTS TO RESOLVE BORN-OPPENHEIMER INADEQUACIES

The need for a comprehensive method to account for the inadequacies of the Born-Oppenheimer approximation has been discussed in the previous chapter. An accurate method that is able to take effects of non-Born-Oppenheimer behaviour into account is highly desirable. In fact, it has been suggested that in some cases, the effect of the omission may exceed the relativistic corrections.[36] It is hence not surprising to notice that attempts have been made to fill the void. However, due to the theoretical complexities and lack of powerful computational techniques, the proposed methods have not been very successful. These methods could not be implemented either due to the difficulty in formulating a general method, or due to the difficulty in employing these methods. Previous studies on transcending the Born-Oppenheimer approximation have traditionally taken two approaches (a) treating nuclear motion as a perturbation, or (b) solving the molecular wavefunction for electrons and nuclei in a self-consistent manner. The current study is of the second type and will be explained in detail in the following chapter.

3.1: Born-Oppenheimer Diagonal Correction (BODC)

The BODC method of Handy and Schaefer [36] draws on work by Sellers and Pulay, [37] and is inspired in part by the method adopted by Kolos and Wolniewicz. [38,39] The latter method was derived primarily for use on diatomic systems, whereas the former method is

in a sense a modification for use in any size of system. Though the two methods are not entirely intertwined in the sense of the goals and approach, their similarity of motivation and approach allows them to be treated together. It is to be noted, however, that the paths of the two methods are divergent. Under the adiabatic approximation, the molecular wavefunction can be approximated as the product of electronic and nuclear wavefunctions.

$$\Psi = \psi_e \psi_n \tag{3.1}$$

In the given method, the molecular wavefunction is expanded as

$$\Psi(r,R) = \sum_n \psi_n^n(R)\psi_n^e(r,R) \tag{3.2}$$

The Kolos-Wolniewicz method [39] then yields a set of n equations to be solved, which are of the form

$$\left\{-\frac{\hbar^2}{2\mu}\nabla_R^2 + U_n(R) + C_{nn} - E\right\}\psi_n^n = -\sum_{n'\neq n} C_{n'n}\psi_{n'}^n(R) \tag{3.3}$$

The $U_n(R)$ are the solutions of the eigen-equation

$$H_0\psi_n^n(r,R) = U_n(R)\psi_n^n(r,R) \tag{3.4}$$

where H_0 is the Hamiltonian for the system under the clamped-nuclei assumption. The total Hamiltonian for a diatomic molecule containing nuclei A and B is given by separating the BO Hamiltonian and the correction term.

$$H = H_0 + H' \tag{3.5a}$$

The BO term of the Hamiltonian is given by

$$H_0 = -\frac{1}{2}\sum_i \nabla_i^2 + V \tag{3.5b}$$

and the correction term is given by

$$H' = -\frac{m}{2\mu}\nabla_{\mathrm{R}}^2 - \frac{m}{8\mu}\left(\sum_j \nabla_{\mathrm{r}}\right)^2 - \frac{m}{2\mu_a}\nabla_{\mathrm{R}}\sum_j \nabla_{\mathrm{r}_j} \qquad (3.5c)$$

where as before, the upper-case quantities refer to those pertaining to the nuclei and lower-case quantities are electronic quantities. The position vectors are centre-of mass transformed vectors given by

$$\mathbf{R} = \mathbf{R}_A - \mathbf{R}_B \qquad (3.6a)$$

$$\mathbf{r}_i = r_i - \frac{1}{2}(\mathbf{R}_A + \mathbf{R}_B) \qquad (3.6b)$$

The quantities μ (reduced mass) and μ_a (increased mass) are obtained when a centre-of-mass transformation is made, and are defined below

$$\mu = \frac{M_A M_B}{M_A + M_B} \qquad (3.7a)$$

$$\mu_a = \frac{M_A M_B}{M_A - M_B} \qquad (3.7b)$$

In the specific implementation of Kolos and Wolniewicz, the equations are derived for the two-electron diatomic molecule. The Hamiltonian is separated into four segments, for simplicity's sake. The three individual terms in H' are then the terms H_1 through H_3. The wavefunction is expanded as

$$\Psi = \frac{1}{2\pi}\sum_{i,n} c_{i,n} g_i(\xi_1, \eta_1, \xi_2, \eta_2, \phi) h_n(R) \qquad (3.8)$$

In the above equation, the electronic functions g are defined in terms of the electron positions in elliptic coordinates. Since the model is designed for a diatomic molecule, the only nuclear degree of freedom available in the molecule is the vibrational degree of

freedom, and hence the nuclear wavefunction terms are members of a series of vibrations. The nuclear component to the total molecular wavefunction is given by

$$h_n(R) = R^{-3} \exp\left[-\frac{\beta^2}{2}|R - R_e|^2\right] H_n(\beta|R - R_e|) \qquad (3.9)$$

where β and R_e are variational parameters and H_n is the n^{th} Hermite polynomial. The above expression is the standard solution for the simple harmonic oscillator.[40] By means of increasing the number of terms in the expansion for electronic and nuclear terms, one can theoretically obtain ever-improving results; especially since the curvature and equilibrium separation are variational parameters. This is also true since the Hamiltonian is designed to include inter-particle (kinetic) correlation terms as well. However, since the method has only been developed for the case of the two-electron diatomic, it is not of general utility and cannot be used on any system larger than the hydrogen molecule.

In the implementation of Handy and co-workers, [36] the BODC for a system whose electronic energy is

$$E_e = 2\sum_i f_i h_{ii} + \sum_{i,j}\left[\alpha_{ij}(ii|jj) + \beta_{ij}(ij|ij)\right] \qquad (3.10)$$

where f_i, α_{ij}, and β_{ij} are fixed parameters, can be expressed as

$$\left\langle \psi_e \left| -\frac{1}{2}\sum_I \frac{1}{M_I}\nabla_I^2 \psi_e \right\rangle = -\sum_I \frac{1}{2M_I}\left[2\sum_i f_i\left(\phi_i|\nabla_I^2\phi_i\right) + \sum_{i,j}\beta_{ij}\left(\phi_i\nabla_I\phi_j\right)\cdot\left(\phi_j\nabla_I\phi_i\right)\right] \qquad (3.11)$$

Hence, the BODC provides a perturbative correction to the energy of the system by means of a coupling of the electronic state to the kinetic energy of the nuclei. This follows directly from the suggestion that the BODC can be given by $\sum_I \frac{1}{2M_I}\langle \nabla_I \psi_e | \nabla_I \psi_e \rangle$. [37] The above equation is solved in an analogous fashion to the analysis of curvature at a point on the potential energy surface.[36] It can be seen that since the BODC method treats nuclear delocalisation as a perturbation, a regular BO computation is carried out and the correction is added in. The implication of this, no doubt, is that while the delocalisation of nuclei is included in the energy of the system, this has no bearing on the electron density distribution. Furthermore, though there is a difference in the energies of isotopomers, one can only deduce a variation in the molecular geometries by plotting the potential energy surfaces for the isotopomers.

3.2: Pseudo-atomic (Planetary) Model

The planetary model was developed independently by Pettitt, [41,42] and Adamowicz and co-workers.[43-56] In this model, one heavy atom is placed at the origin and the other particles (nuclei and electrons) are permitted to occupy the space around this central nucleus. As a matter of practice, the heaviest nucleus is placed at the origin. This model was initially derived for a system of protons (^1H nuclei) in a molecule containing one heavy atom.[41] The other branch of development of this model due to Adamowicz and co-workers was implemented primarily in the study of diatomic molecules. Recently, an extension to triatomic systems has been reported.[57] The Hamiltonian applicable to this model is given by

$$\hat{H} = -\frac{1}{2}\left(\sum_{i}^{n}\frac{1}{m_i}\nabla_i^2 + \sum_{i\neq j}^{n}\frac{1}{M_1}\nabla_i{}'\nabla_j\right) + \sum_{i=1}^{n}\frac{q_0 q_i}{r_i} + \sum_{i<j}^{n}\frac{q_i q_j}{r_{ij}} \quad (3.12)$$

In the above equation, the heavy particle at the centre of the coordinate system is not present, and the masses of the particles are denoted by upper case M. The reduced mass between a given particle and the fixed particle is denoted by lower case m. Hence, the system of $n+1$ particles has been reduced to a system of n pseudo-particles with one particle fixed, wherein the masses are now replaced by reduced masses. The second term in the expression leads to the non-superposition of the fixed particle with any of the pseudo-particles and can be interpreted as a form of kinetic correlation with the fixed particle. The last two terms in the expression relate to the Coulombic interaction between the various particles and a) the fixed particle, and b) each other. This is similar to the result obtained when a centre-of mass transformation is carried out on a system of $n+1$ quantum particles.[58] In fact, the above equation corresponds to the result obtained for a system where one particle is situated at the centre of mass. Hence, this equation is most suited for atomic poly-electronic systems, as the nucleus in a poly-electronic atom is bound to be situated at the centre of mass to a good approximation. For systems where there is no particle at the centre of mass, this equation is not strictly true; the difference being that in the case of a centre-of-mass transformation, the $\sum_{i\neq j}^{n}\frac{1}{M_1}\nabla_i{}'\nabla_j$ term would be replaced by $\frac{-1}{2M_{tot}}\sum_{i\neq j}^{n}\nabla_i\cdot\nabla_j$. As an atomic model is invoked for the study of molecules, the molecular wavefunction is expanded as a set of pseudo-atomic basis functions centred on the fixed nucleus. The wavefunction is expanded as a set of explicitly correlated

Gaussian basis functions and the energy is minimised by invoking the variational principle.

As is fairly obvious from the preceding section, the molecule is treated as a pseudo-atom in which the nucleus is replaced by the fixed heavy particle. The remaining particles in the system are then considered to be moving in the mean field of the fixed nucleus and all other particles. The implications of the model are many and far-reaching. For one, the concept of a molecular geometry is lost, as the molecule now has spherical symmetry. Due to this spherical symmetry, the net molecular dipole moment is necessarily zero. Similarly, the molecule would only have an isotropic polarisability and no anisotropic polarisability due to the isotropic nature of the results from this model.

One possible interpretation of these results is that the model only considers the time averaged particle distributions as 'viewed' from the fixed nucleus. Hence, the distributions over all time are necessarily spherical. All possible orientations and nuclear configurations of a molecule in a given state as viewed from one atom would lead to a spherical probability distribution for each of the other particles. This implies that the results obtained include all rotational modes as well as the expected zero-point vibrational information expected. In the case of a diatomic, the inter-nuclear separation and its uncertainty can be directly obtained from the distribution. Obviously, this method is best suited for diatomic molecules and is expected to be of greatest import in asymmetric diatomic molecules where the mass ratio of the two nuclei is large. Under such circumstances, the centre of mass transformation will favour the fixing of the heavy

nucleus, and results would be similar to those obtained from any other scheme in centre of mass coordinates.

3.3: Electron-Nuclear MO (ENMO) Approach

3.3.1: Development and Theory

The approach was pioneered by Thomas [59-66] and involves placing the electrons in an anti-symmetrised electronic wavefunction and the nuclei in an anti-symmetrised (or symmetrised in the case of bosons) nuclear wavefunction. This has been further developed and now forms the basis of the ENMO (electrons and nuclei molecular orbital) method. [67] The wavefunction for an N-electron and M-nuclear system in this method is defined as

$$\Psi \equiv \Psi(r_1, r_2, ..., r_N, R_1, R_2, ..., R_M)$$
$$= \frac{1}{\sqrt{N!M!}} \begin{vmatrix} \varphi_1(r_1) & \varphi_2(r_1) & ... & \varphi_N(r_1) \\ \varphi_1(r_2) & \varphi_2(r_2) & ... & \varphi_N(r_1) \\ ... & ... & ... & ... \\ \varphi_1(r_N) & \varphi_2(r_N) & ... & \varphi_N(r_N) \end{vmatrix} \times \begin{vmatrix} \Phi_1(R_1) & \Phi_2(R_1) & ... & \Phi_M(R_1) \\ \Phi_1(R_2) & \Phi_2(R_2) & ... & \Phi_M(R_1) \\ ... & ... & ... & ... \\ \Phi_1(R_M) & \Phi_2(R_M) & ... & \Phi_M(R_M) \end{vmatrix} \tag{3.13}$$

This is equivalent to writing the molecular wavefunction in the form

$$\Psi = \psi^e \psi^n \tag{3.1}$$

It is suggested that the total wavefunction for a $K = N + M$ particle system be given by

$$\Psi(r_1, r_2, ..., r_K) = \frac{1}{\sqrt{N!M!}} \begin{vmatrix} \varphi_1(r_1) & \varphi_2(r_1) & ... & \varphi_K(r_1) \\ \varphi_1(r_2) & \varphi_2(r_2) & ... & \varphi_K(r_1) \\ ... & ... & ... & ... \\ \varphi_1(r_K) & \varphi_2(r_K) & ... & \varphi_K(r_K) \end{vmatrix} \tag{3.14}$$

where the (off-diagonal) terms $\varphi_1(r_L),\varphi_2(r_L),...\varphi_N(r_L)=0$ when $L\in(N+1,K)$ and $\varphi_L(r_{N+1}),\varphi_L(r_{N+2}),...\varphi_L(r_K)=0$ when $L\in(1,N)$. The basis functions used for the nuclei have their exponents scaled so as to reproduce the relative localisation of the nuclear position *vis-à-vis* the electron delocalisation. Taking α_e to be the exponent for the electronic basis function, the exponent for the nuclear basis function α_n is given by scaling relative to the mass ratio

$$\alpha_n = \alpha_e\left(\frac{m_n}{m_e}\right)^x \tag{3.15}$$

Bochevarov *et al.* [67] use a value of unity for x. Re-computing from the values of the optimised exponents obtained by Tachikawa *et al.*, [68] one obtains a value of x ranging from $1/2$ to $1/3$.

The Hamiltonian operator is given by

$$\hat{H} = \hat{T}^e + \hat{T}^n + \hat{V}^{ee} + \hat{V}^{en} + \hat{V}^{nn} \tag{3.16}$$

The terms in the above equation have their usual meanings and forms.

The variation of the energy $E = \dfrac{\langle\Psi|\hat{H}|\Psi\rangle}{\langle\Psi|\Psi\rangle}$ yields a set of integro-differential equations that can be solved using the Pople-Nesbet equations of the form

$$F^{e\alpha}C^{e\alpha} = S^eC^{e\alpha}\varepsilon^{e\alpha} \tag{3.17a}$$

$$F^{e\beta}C^{e\beta} = S^eC^{e\beta}\varepsilon^{e\beta} \tag{3.17b}$$

$$F^{n\alpha}C^{n\alpha} = S^nC^{n\alpha}\varepsilon^{n\alpha} \tag{3.17c}$$

$$F^{n\beta}C^{n\beta} = S^nC^{n\beta}\varepsilon^{n\beta} \tag{3.17d}$$

where the Fock matrices are analogous to the α-electron case given below

$$F_{ij}^{e\alpha} = T_{ij}^{e\alpha} + \sum_{k}^{N^{e\alpha}} \left[\left(i_\alpha^e j_\alpha^e \middle| k_\alpha^e k_\alpha^e \right) - \left(i_\alpha^e k_\alpha^e \middle| j_\alpha^e k_\alpha^e \right) \right] + \sum_{k}^{N^{e\beta}} \left(i_\alpha^e k_\alpha^e \middle| j_\alpha^e k_\alpha^e \right) - \sum_{k}^{N^{n\alpha}} \left(i_\alpha^e j_\alpha^e \middle| k_\alpha^n k_\alpha^n \right) - \sum_{k}^{N^{n\beta}} \left(i_\alpha^e j_\alpha^e \middle| k_\beta^n k_\beta^n \right) \tag{3.18}$$

3.3.2: Shortcomings of ENMO Method

As noted in the previous section, the ENMO molecular wavefunction can be represented as

$$\Psi = \psi^e \psi^n \tag{3.1}$$

Hence, the wavefunction is separable into electronic and nuclear components. Thus, the ENMO method can be taken to be a zero-order correction to the Born-Oppenheimer (BO) approximation. This is since the nuclei and electrons are not completely interacting, however, the nuclei are no longer fixed in space. The separability of the wavefunction into electronic and nuclear components is the crux of the BO approximation.[1,2] Hence, the ENMO wavefunction only provides a delocalisation correction to the nuclei. The extended single-determinant formalism suggested [67] is also unacceptable for similar reasons. The block-diagonal form of the determinant ensures that the final wavefunction is identical in value to the product of the electronic and nuclear determinants. Additionally, the wavefunction is now anti-symmetric with respect to interchange of distinguishable particles (electron and nuclear particle). This is an unphysical situation, as the wavefunction is required to be symmetric with respect to interchange of distinguishable particles (though they may both be fermions).

CHAPTER IV: MODIFIED ENMO METHOD

The previous chapter outlined some methods that have been implemented in an attempt to correct for the (previously ignored) non-Born-Oppenheimer effects. There was also a brief discussion as to why each of the methods was inadequate. Currently, the most promising method is the ENMO method (section 3.3) as it is the most general method and attempts to deal with the electrons and nuclei in a self-consistent manner. However, the ENMO method is incomplete for a number of reasons. Due to the separability of the ENMO wavefunction into electronic and nuclear contributions, the ENMO method can be considered to be a zero-order correction to the Hartree-Fock (Roothaan-Hall) method. This chapter outlines the development of a method that is designed to go beyond the ENMO method and will be referred to herein as the modified ENMO method.

To be a true non-Born-Oppenheimer method, the wavefunction should be non-separable between electronic and nuclear contributions. As has been argued in previous chapters, the nuclei should be treated as quantum particles and hence represented by density distributions (or wavefunctions). In addition, it is required that the wavefunction for the system be anti-symmetric with respect to interchange of identical fermions, and symmetric with respect to interchange of distinguishable particles and bosons. With these basic restrictions, the modified ENMO method is developed. As with the ENMO method, the need for the scaling of nuclear basis functions is taken into account. These basis functions are used to construct single particle MOs by means of the LCAO approximation. The remainder of the chapter deals with the construction of the

wavefunction and the solution of the Schrödinger equation for the system in a self-consistent manner. The actual computational implementation of the method is provided in the following chapter.

4.1: Modification of Basis Set

As is well recognised, the basis sets for the nuclei should be scaled in order to account for the reduced delocalisation of the nuclei *vis-à-vis* the electrons.[67,68] All available basis sets are either of the Slater or of Gaussian type. Hence, scaling of the exponents is the most direct mechanism by which the nuclear basis can be constructed. This is expressed as

$$\alpha_n = \alpha_e \left(\frac{m_n}{m_e} \right)^{1/x} \tag{4.1a}$$

This can also be written as

$$\chi_n = A \left(\frac{\chi_e}{A} \right)^{\left(m/m_e\right)^{1/x}} \tag{4.1b}$$

The simplest solution would be to set $x = 1$ [67] or to obtain the exponents by optimisation. It is curious that in the latter case one obtains a value for x ranging from 2 to 3 [68] for the systems studied. Due to the small number of nuclei for which basis sets have been optimised, it is not known whether this factor is transferable to other systems as well. The demands of kinetic energy equipartition lead to a value of $x = 4$.[2] Due to the widely varying estimates of the value of the scaling factor for the exponent, it is necessary to determine the optimal value that is of general applicability. This is dealt with in greater detail in Chapter 5.

4.2: Construction of Molecular Wavefunction

The spin-unrestricted formalism is preferred in this study for a few reasons. The subset of spin-restricted (in the conventional sense) systems among systems of chemical interest is bound to be relatively small. There is also further uncertainty as to how the spin system of a molecule containing an assemblage of particles of various spins is to be determined. The current thinking separates the spin systems for each set of particles. Hence, the H_2 molecule could exist as a singlet electronically and a singlet in protons (para-hydrogen) or a singlet with respect to electrons and a triplet with respect to protons (ortho-hydrogen). One could argue that the former is singlet hydrogen and the latter is triplet hydrogen. Though this is true for the examples above, this distinction is not unambiguous as similar states are available from excited states wherein electron(s) and nuclei may be in excited states. These would necessarily be different from the excited singlet and triplet states commonly understood. Another reason to use the unrestricted formalism is due to its general applicability.

4.2.1: LCAO Approach

The basis set space consists of all atomic basis functions for that type of particle, along with the corresponding spin indices. Since it is possible for certain nuclei to possess spins other than ±½, the α-β designation is discarded in favour of S^a where a can range from $-s$ to $+s$, s being the spin of the particle in units of $\hbar$. Therefore, for a particle of type k, the basis space is given by

$$\chi^k = \begin{bmatrix} \chi_1^k S^{-s} & \chi_1^k S^{-s+1} & \cdots & \chi_1^k S^{+s} \\ \chi_2^k S^{-s} & \chi_2^k S^{-s+1} & \cdots & \chi_2^k S^{+s} \\ \cdots & \cdots & \cdots & \cdots \\ \chi_n^k S^{-s} & \cdots & \cdots & \chi_n^k S^{+s} \end{bmatrix} \tag{4.2}$$

where n is the number of spatial basis functions available. Hence, the basis space for k is of magnitude $n(2s+1)$. In order to maintain spin-purity in the final single-particle wavefunctions, χ^k is separated into $(2s+1)$ column vectors χ_a^k, which can be written

$$\chi_a^k = \begin{bmatrix} \chi_1^k S^a \\ \chi_2^k S^a \\ \cdots \\ \chi_n^k S^a \end{bmatrix} \tag{4.3}$$

The n single-particle wavefunctions ψ_a^k are given by

$$\psi_a^k = C_a^k \chi_a^k \tag{4.4}$$

where C_a^k is a square matrix of dimension n containing the contribution of each of the components of χ_a^k to each of the n wavefunctions contained in ψ_a^k.

4.2.2: Fermion Wavefunction

The general non-Born Oppenheimer wavefunction attributed to Born and Huang*, is given by Handy *et al.* [36] and others [38] to be

$$\Psi = \sum_i \psi_{ni}(R)\psi_{ei}(r,R) \tag{4.5}$$

The coordinates R and r refer to the nuclear and electronic coordinates. It can be directly seen that the above wavefunction is non-separable into the electronic and nuclear

* Allusion to the said result is not present in M. Born and K. Huang, *Dynamical Theory of Crystal Lattices*, Oxford University Press, New York, 1956.

wavefunctions, this being the major complaint with the Born-Oppenheimer method. The index i runs over a series of unspecified pairs of nuclear and electronic wavefunctions.

The wavefunction is required to be anti-symmetric with respect to interchange of identical fermions, and symmetric with respect to interchange of bosons,[69] wavefunction of non-identical particles is also symmetric with respect to interchange.[70] This leads to a larger number of contributions to the ground state (and excited states) than obtained using the ENMO method. For example, the wavefunction for the H_2 molecule is given by

$$\begin{aligned}\Psi = &[\psi_1(r_1)\psi_2(r_2)\psi_3(r_3)\psi_4(r_4) - \psi_2(r_1)\psi_1(r_2)\psi_3(r_3)\psi_4(r_4) + \psi_2(r_1)\psi_1(r_2)\psi_4(r_3)\psi_3(r_4)\\ &- \psi_1(r_1)\psi_2(r_2)\psi_4(r_3)\psi_3(r_4)] + [\psi_3(r_1)\psi_2(r_2)\psi_1(r_3)\psi_4(r_4) - \psi_2(r_1)\psi_3(r_2)\psi_1(r_3)\psi_4(r_4)\\ &+ \psi_2(r_1)\psi_3(r_2)\psi_4(r_3)\psi_1(r_4) - \psi_3(r_1)\psi_2(r_2)\psi_4(r_3)\psi_1(r_4)] + [\psi_4(r_1)\psi_2(r_2)\psi_3(r_3)\psi_1(r_4)\\ &- \psi_2(r_1)\psi_4(r_2)\psi_3(r_3)\psi_1(r_4) + \psi_2(r_1)\psi_4(r_2)\psi_1(r_3)\psi_3(r_4) - \psi_4(r_1)\psi_2(r_2)\psi_1(r_3)\psi_3(r_4)]\\ &+ [\psi_1(r_1)\psi_3(r_2)\psi_2(r_3)\psi_4(r_4) - \psi_3(r_1)\psi_1(r_2)\psi_2(r_3)\psi_4(r_4) + \psi_3(r_1)\psi_1(r_2)\psi_4(r_3)\psi_2(r_4)\\ &- \psi_1(r_1)\psi_3(r_2)\psi_4(r_3)\psi_2(r_4)] + [\psi_1(r_1)\psi_4(r_2)\psi_3(r_3)\psi_2(r_4) - \psi_4(r_1)\psi_1(r_2)\psi_3(r_3)\psi_2(r_4)\\ &+ \psi_4(r_1)\psi_1(r_2)\psi_2(r_3)\psi_3(r_4) - \psi_1(r_1)\psi_4(r_2)\psi_2(r_3)\psi_3(r_4)] + [\psi_3(r_1)\psi_4(r_2)\psi_1(r_3)\psi_2(r_4)\\ &- \psi_4(r_1)\psi_3(r_2)\psi_1(r_3)\psi_2(r_4) + \psi_4(r_1)\psi_3(r_2)\psi_2(r_3)\psi_1(r_4) - \psi_3(r_1)\psi_4(r_2)\psi_2(r_3)\psi_1(r_4)]\end{aligned} \tag{4.6}$$

where particles 1 and 2 are particles of one type (say electrons) and particles 3 and 4 are of the other type (protons), and the ψs refer to occupied wavefunctions. The above expression can also be written as

$$\begin{aligned}\Psi = &\begin{vmatrix}\psi_1(r_1) & \psi_2(r_1)\\ \psi_1(r_2) & \psi_2(r_2)\end{vmatrix}\begin{vmatrix}\psi_3(r_3) & \psi_4(r_3)\\ \psi_3(r_4) & \psi_4(r_4)\end{vmatrix} + \begin{vmatrix}\psi_3(r_1) & \psi_2(r_1)\\ \psi_3(r_2) & \psi_2(r_2)\end{vmatrix}\begin{vmatrix}\psi_1(r_3) & \psi_4(r_3)\\ \psi_1(r_4) & \psi_4(r_4)\end{vmatrix}\\ &+ \begin{vmatrix}\psi_4(r_1) & \psi_2(r_1)\\ \psi_4(r_2) & \psi_2(r_2)\end{vmatrix}\begin{vmatrix}\psi_3(r_3) & \psi_1(r_3)\\ \psi_3(r_4) & \psi_1(r_4)\end{vmatrix} + \begin{vmatrix}\psi_1(r_1) & \psi_3(r_1)\\ \psi_1(r_2) & \psi_3(r_2)\end{vmatrix}\begin{vmatrix}\psi_2(r_3) & \psi_4(r_3)\\ \psi_2(r_4) & \psi_4(r_4)\end{vmatrix}\\ &+ \begin{vmatrix}\psi_1(r_1) & \psi_4(r_1)\\ \psi_1(r_2) & \psi_4(r_2)\end{vmatrix}\begin{vmatrix}\psi_3(r_3) & \psi_2(r_3)\\ \psi_3(r_4) & \psi_2(r_4)\end{vmatrix} + \begin{vmatrix}\psi_3(r_1) & \psi_4(r_1)\\ \psi_3(r_2) & \psi_4(r_2)\end{vmatrix}\begin{vmatrix}\psi_1(r_3) & \psi_2(r_3)\\ \psi_1(r_4) & \psi_2(r_4)\end{vmatrix}\end{aligned} \tag{4.7}$$

It is trivial to show that this can be extended further for systems containing more types of fermions. It is obvious that the first term above is the ENMO wavefunction. The requirements of exchange symmetry lead to a situation wherein the electrons can occupy nucleus-like orbitals and *vice-versa*. This permits for a better description of the electron density near the mean position of the nucleus – an issue that is currently difficult to deal with adequately. Additionally, permitting nuclei to occupy electronic orbitals lends some flexibility in their positional distributions, thus eliminating the need for polarisation and diffuse functions for the nuclei. The probability of interchange between two particles is a function of the overlap between the wavefunctions housing the two particles.[70] Hence, the various terms in Ψ are scaled by the overlap integrals S_{ij}.

$$\Psi = \frac{1}{\sqrt{N}} \left[\begin{array}{l} \begin{vmatrix} \psi_1(r_1) & \psi_2(r_1) \\ \psi_1(r_2) & \psi_2(r_2) \end{vmatrix} \begin{vmatrix} \psi_3(r_3) & \psi_4(r_3) \\ \psi_3(r_4) & \psi_4(r_4) \end{vmatrix} + S_{13} \begin{vmatrix} \psi_3(r_1) & \psi_2(r_1) \\ \psi_3(r_2) & \psi_2(r_2) \end{vmatrix} \begin{vmatrix} \psi_1(r_3) & \psi_4(r_3) \\ \psi_1(r_4) & \psi_4(r_4) \end{vmatrix} \\ + S_{14} \begin{vmatrix} \psi_4(r_1) & \psi_2(r_1) \\ \psi_4(r_2) & \psi_2(r_2) \end{vmatrix} \begin{vmatrix} \psi_3(r_3) & \psi_1(r_3) \\ \psi_3(r_4) & \psi_1(r_4) \end{vmatrix} + S_{23} \begin{vmatrix} \psi_1(r_1) & \psi_3(r_1) \\ \psi_1(r_2) & \psi_3(r_2) \end{vmatrix} \begin{vmatrix} \psi_2(r_3) & \psi_4(r_3) \\ \psi_2(r_4) & \psi_4(r_4) \end{vmatrix} \\ + S_{24} \begin{vmatrix} \psi_1(r_1) & \psi_4(r_1) \\ \psi_1(r_2) & \psi_4(r_2) \end{vmatrix} \begin{vmatrix} \psi_3(r_3) & \psi_2(r_3) \\ \psi_3(r_4) & \psi_2(r_4) \end{vmatrix} + S_{13}S_{24} \begin{vmatrix} \psi_3(r_1) & \psi_4(r_1) \\ \psi_3(r_2) & \psi_4(r_2) \end{vmatrix} \begin{vmatrix} \psi_1(r_3) & \psi_2(r_3) \\ \psi_1(r_4) & \psi_2(r_4) \end{vmatrix} \end{array} \right] \tag{4.8}$$

The overlap integrals are only computed for the terms containing interchange between different types of particles. In addition, interchange should only be permitted between states in such a way that the interchanged states are both within the permitted range of spins available to each of the particles. In this way, care is taken to ensure that a particle does not occupy a spin orbital beyond the spin range that the particle may occupy. This automatically precludes interchange between fermions and bosons, as the range of

permitted spin states is mutually exclusive between the two classes of particles. Hence, the molecular wavefunction can be written as

$$\Psi = \psi_{fermions}\psi_{bosons} \tag{4.9}$$

The above relation describing the molecular wavefunction can also be written as

$$\Psi = \frac{1}{\sqrt{N}}\sum_{i}\left[S_i\prod_{n=1}^{k}\left|\mathbf{D}_i^n\right|\right] \tag{4.10}$$

where

$$\begin{aligned} S_i &= \left\langle \prod_{n=1}^{k}\left|\mathbf{D}_0^n\right| \middle| \prod_{n=1}^{k}\left|\mathbf{D}_i^n\right| \right\rangle \\ &= \prod_{n=1}^{k}\left\langle \left|\mathbf{D}_0^n\right| \middle| \left|\mathbf{D}_i^n\right| \right\rangle \end{aligned} \tag{4.11}$$

In the above relation, the $\left|\mathbf{D}_i^n\right|$ refer to the determinant of particle type n in the i^{th} term of the expansion. The $\left|\mathbf{D}_0^n\right|$ refers to the first ('reference') term in the expansion. The maximum number of terms in the wavefunction expansion for a system of K particles of k distinguishable types, where there are n_i particles of type i (i is contained in k) is given by

$$NT = \prod_{i=1}^{k-1}\frac{(K-\sum_{p=1}^{i-1}n_p)!}{n_i!(K-\sum_{p=1}^{i}n_p)!} \tag{4.12}$$

This is the maximum number of terms possible and is only accessible when all particles in the system have an absolute spin of ½. In all other cases, there will be a number of terms that go to zero due to the interchange exclusion rule mentioned above. The normalisation factor N for a set of orthonormal wavefunctions is obtained by

$$N = 1 + \sum S_{ij}^2 \tag{4.13}$$

It can be shown that the terms in the wavefunction expansion are not mutually orthogonal. Hence, the normalisation factor N is given in terms of

$$N = \sum_{a=0}^{NT-1} \sum_{b=0}^{NT-1} S_a S_b \tag{4.14}$$

Since the system contains k particle types, each containing n_k particles, the overall normalisation constant becomes

$$N = \left(\prod_{i=1}^{k} n_i! \right) \sum_{a=0}^{NT-1} \sum_{b=0}^{NT-1} S_a S_b \tag{4.15}$$

4.2.3: Extension to Include Bosons

The wavefunction of identical bosonic nuclei, on the other hand, is required to be symmetric with respect to exchange.[71] In a system of four particles containing only bosons, the wavefunction for the system is given in terms of the occupied orbitals as

$$\begin{aligned}
\Psi = & [\psi_1(r_1)\psi_2(r_2)\psi_3(r_3)\psi_4(r_4) + \psi_1(r_1)\psi_2(r_2)\psi_4(r_3)\psi_3(r_4) + \psi_1(r_1)\psi_3(r_2)\psi_2(r_3)\psi_4(r_4) \\
& + \psi_1(r_1)\psi_3(r_2)\psi_4(r_3)\psi_2(r_4) + \psi_1(r_1)\psi_4(r_2)\psi_2(r_3)\psi_3(r_4) + \psi_1(r_1)\psi_4(r_2)\psi_3(r_3)\psi_2(r_4)] \\
& + [\psi_2(r_1)\psi_1(r_2)\psi_3(r_3)\psi_4(r_4) + \psi_2(r_1)\psi_1(r_2)\psi_4(r_3)\psi_3(r_4) + \psi_2(r_1)\psi_3(r_2)\psi_1(r_3)\psi_4(r_4) \\
& + \psi_2(r_1)\psi_3(r_2)\psi_4(r_3)\psi_1(r_4) + \psi_2(r_1)\psi_4(r_2)\psi_1(r_3)\psi_3(r_4) + \psi_2(r_1)\psi_4(r_2)\psi_3(r_3)\psi_1(r_4)] \\
& + [\psi_3(r_1)\psi_1(r_2)\psi_2(r_3)\psi_4(r_4) + \psi_3(r_1)\psi_1(r_2)\psi_4(r_3)\psi_2(r_4) + \psi_3(r_1)\psi_2(r_2)\psi_1(r_3)\psi_4(r_4) \\
& + \psi_3(r_1)\psi_2(r_2)\psi_4(r_3)\psi_1(r_4) + \psi_3(r_1)\psi_4(r_2)\psi_1(r_3)\psi_2(r_4) + \psi_3(r_1)\psi_4(r_2)\psi_2(r_3)\psi_1(r_4)] \\
& + [\psi_4(r_1)\psi_1(r_2)\psi_2(r_3)\psi_3(r_4) + \psi_4(r_1)\psi_1(r_2)\psi_3(r_3)\psi_2(r_4) + \psi_4(r_1)\psi_2(r_2)\psi_1(r_3)\psi_3(r_4) \\
& + \psi_4(r_1)\psi_2(r_2)\psi_3(r_3)\psi_1(r_4) + \psi_4(r_1)\psi_3(r_2)\psi_1(r_3)\psi_2(r_4) + \psi_4(r_1)\psi_3(r_2)\psi_2(r_3)\psi_1(r_4)]
\end{aligned} \tag{4.16}$$

The wavefunction is now symmetric with respect to interchange of identical and distinguishable particles. This general form can be extended to include all possible occupations and rewritten as

$$\Psi = \prod_{i=1}^{4} \sum_{j=1}^{4} \psi_j(r_i) \tag{4.17}$$

Extending to a general N_p-particle system,

$$\Psi = \prod_{i=1}^{N_p} \sum_{j=1}^{N_p} \psi_j(r_i) \tag{4.18}$$

This yields an expansion containing ${N_p}^{N_p}$ terms, not all of which are of chemical interest, including condensation-like terms ($\psi_1(r_1)\psi_1(r_2)\psi_1(r_3)\psi_1(r_4)$). Of the total, there are $N_p!$ terms of chemical interest. In addition, care must be taken to exclude interchange between terms where one particle is to occupy a spin orbital beyond its normal spin range. There are then two approaches to solve the problem of representing the wavefunction in a chemically intuitive manner. The first solution would be to include only the $N_p!$ terms in the wavefunction expansion. This can then be nominally rewritten as

$$\Psi = \begin{vmatrix} \psi_1(r_1) & \psi_2(r_1) & \cdots & \psi_N(r_1) \\ \psi_1(r_2) & \psi_2(r_2) & \cdots & \psi_N(r_2) \\ \cdots & \cdots & \cdots & \cdots \\ \psi_1(r_N) & \psi_2(r_N) & \cdots & \psi_N(r_N) \end{vmatrix}_+ \tag{4.19}$$

It is to be noted that the above is not written as a determinant, as a determinant would violate the symmetry rules required to be obeyed by bosons. During the rest of this document, the $|\ |_+$ symbol refers to a determinantal expansion wherein all terms are positive, also known as a *permanent*. The wavefunction is then the sum of products over all combinations of wavefunctions and particles such that no two particles occupy the same wavefunction simultaneously. The wavefunction is written in the above manner, as

it is then easily analogous to the fermionic case after applying the Hamiltonian. This is due to the fact that all terms in $\langle\Psi|\hat{H}|\Psi\rangle$ are positive (pending evaluation of the integrals) in both cases. Hence, the bosonic contribution to the total wavefunction can be represented as a matrix. This matrix can then be employed directly when solving the Pople-Nesbet equations. This is more conveniently written as a sum of products of quasi-determinants of different particle types. Hence,

$$\Psi = \frac{1}{\sqrt{N}}\left[\begin{array}{l} \begin{vmatrix}\psi_1(r_1) & \psi_2(r_1)\\ \psi_1(r_2) & \psi_2(r_2)\end{vmatrix}_+ \begin{vmatrix}\psi_3(r_3) & \psi_4(r_3)\\ \psi_3(r_4) & \psi_4(r_4)\end{vmatrix}_+ + S_{13}\begin{vmatrix}\psi_3(r_1) & \psi_2(r_1)\\ \psi_3(r_2) & \psi_2(r_2)\end{vmatrix}_+ \begin{vmatrix}\psi_1(r_3) & \psi_4(r_3)\\ \psi_1(r_4) & \psi_4(r_4)\end{vmatrix}_+ \\ + S_{14}\begin{vmatrix}\psi_4(r_1) & \psi_2(r_1)\\ \psi_4(r_2) & \psi_2(r_2)\end{vmatrix}_+ \begin{vmatrix}\psi_3(r_3) & \psi_1(r_3)\\ \psi_3(r_4) & \psi_1(r_4)\end{vmatrix}_+ + S_{23}\begin{vmatrix}\psi_1(r_1) & \psi_3(r_1)\\ \psi_1(r_2) & \psi_3(r_2)\end{vmatrix}_+ \begin{vmatrix}\psi_2(r_3) & \psi_4(r_3)\\ \psi_2(r_4) & \psi_4(r_4)\end{vmatrix}_+ \\ + S_{24}\begin{vmatrix}\psi_1(r_1) & \psi_4(r_1)\\ \psi_1(r_2) & \psi_4(r_2)\end{vmatrix}_+ \begin{vmatrix}\psi_3(r_3) & \psi_2(r_3)\\ \psi_3(r_4) & \psi_2(r_4)\end{vmatrix}_+ + S_{13}S_{24}\begin{vmatrix}\psi_3(r_1) & \psi_4(r_1)\\ \psi_3(r_2) & \psi_4(r_2)\end{vmatrix}_+ \begin{vmatrix}\psi_1(r_3) & \psi_2(r_3)\\ \psi_1(r_4) & \psi_2(r_4)\end{vmatrix}_+ \end{array}\right] \tag{4.20}$$

where the overlap integrals S are as defined earlier.

The more rigorous solution is to build the wavefunction analogous to the fermion case, wherein each term is scaled by the overlap integral to restrict the solutions only to those that are of chemical interest. Hence, the wavefunction becomes

$$\begin{aligned}\Psi_{bosons} &= \prod_{i=1}^{N}\sum_{j=1}^{N}\langle\psi_j(r_i)|\psi_i(r_i)\rangle\psi_j(r_i) \\ &= \prod_{i=1}^{N}\sum_{j=1}^{N}S_{ij}\psi_j(r_i)\end{aligned} \tag{4.21}$$

Due to the similarity in solution and the projected smaller contributions of the extraneous terms in the more rigorous approach, only those terms are included wherein only single-occupancy is permitted. Hence, the total molecular wavefunction is given by

$$\Psi = \frac{1}{\sqrt{N}} \sum_i \left[S_i \prod_{n=1}^{fermions} \left| \mathbf{D}_i^n \right| \right] \sum_j \left[S_j \prod_{n=1}^{bosons} \left| \mathbf{D}_j^n \right|_+ \right] \tag{4.22}$$

The total number of terms in the wavefunction expansion is given by

$$NT = \prod_{i=1}^{k_f - 1} \frac{(K_f - \sum_{p=1}^{i-1} n_p)!}{n_i!(K_f - \sum_{p=1}^{i} n_p)!} \prod_{i=1}^{k_b - 1} \frac{(K_b - \sum_{p=1}^{i-1} n_p)!}{n_i!(K_b - \sum_{p=1}^{i} n_p)!} \tag{4.23}$$

where K_f and K_b refer to the numbers of fermion and boson particles, respectively, k_f and k_b are the numbers of fermionic and bosonic particle types. Since the total wavefunction can be factored into fermionic and bosonic parts, the two parts can be solved separately and independently. In the extreme case of a system in which there are no fermionic nuclei, this leads to a relaxed Born-Oppenheimer implementation analogous to the canonical ENMO method.

A completely coupled wavefunction can be constructed by

$$\Psi = \frac{1}{\sqrt{N}} \sum_i \left[S_i \prod_{n=1}^{fermions} \left| \mathbf{D}_i^n \right| \prod_{n=1}^{bosons} \left| \mathbf{D}_i^n \right|_+ \right] \tag{4.24}$$

wherein the interchange is permitted between particles of both types. In this method, the interchange is only between the spatial parts of the single-particle wavefunctions, and the spin part of the wavefunction is retained on the particle determinant that it originates from. For example, $\psi_a S_a$ and $\psi_b S_b$ would interchange to give $\psi_b S_a$ and $\psi_a S_b$, which are subsequently processed in the determinantal equations. This allows an even-handed treatment between fermion nuclei and boson nuclei, while still allowing them to retain their intrinsic characters. The added advantage is that both systems can be solved in an

identical fashion. In addition, control over the spin state of the molecule can also be exercised, as it is now possible to constrain the spin state of each type of particle. In so doing, the number of determinantal terms increases to

$$NT = \prod_{i=1}^{k-1} \frac{(K - \sum_{p=1}^{i-1} n_p)!}{n_i!(K - \sum_{p=1}^{i} n_p)!} \tag{4.25}$$

where the summation is over all particle types (k) and all particles (K) are included in the combinatorial expansion. It should also be remembered that there are now no zero terms in the expansion as the interchange has been constrained to only the spatial parts of the spin orbitals. The total number of Fock equations to be solved then becomes

$$NE = \left(\prod_{i=1}^{k-1} \frac{(K - \sum_{p=1}^{i-1} n_p)!}{n_i!(K - \sum_{p=1}^{i} n_p)!} \right)^2 \sum_{i=1}^{k} (2|s_i| + 1) \tag{4.26}$$

The term s_i in the above equation refers to the "native" spin of the particle of type i, and absolute values are applied as many particle types have negative spins. This is then an upper bound as there may be systems wherein there are inadequate numbers of particles to justify use of $(2s_i + 1)$ Fock equations.

4.3: Inclusion of Correlation Effects

Several methods have been developed to estimate the correlation contribution to the Hartree-Fock solution. One such method, the density functional approach was outlined in Chapter 2. Other methods collectively form the group of post-Hartree-Fock methods, and these include the perturbative (MP2 and couple cluster) and configuration

interaction methods. These latter methods have been very effective in estimating the correlation energy in a molecule, though at great computational expense. The current method is far more computationally demanding than the Hartree-Fock method, and hence it is desirable to have a method that computes the correlation simultaneously with the energy. Such a situation can be attained by means of employing the density functional approach. Unfortunately, the density functional method suffers from the effects of self-interaction, [13,72,73] and hence cannot be introduced in this method. It is disagreeable to introduce a larger source of error than the effect one is aiming to include (correct for). Hence, the density functional approach is not suitable for implementation in the modified ENMO method. The method that is being included is based on a notion that has existed in the literature for a long time, but was not implemented. This involves computing the kinetic correlation as a sum over terms of the form $\bar{\nabla}_i \cdot \bar{\nabla}_j$.

The kinetic energy term is traditionally given by the operator presented below.

$$\hat{T}_i = -\frac{1}{2m}\nabla_i^2 \tag{4.27}$$

It has been argued that a complete description should include the kinetic energy cross-terms of the form $\bar{\nabla}_i \cdot \bar{\nabla}_j$, [41,42,74,75] and it is suggested that these terms may in fact be understood as a correlation term. [41,42] The kinetic energy term is then written (with μ_{ij} being the reduced mass of particles i and j) as

$$\hat{T} = -\frac{\hbar^2}{4}\sum_{i=1}^{n+N}\sum_{j=1}^{n+N}\frac{1}{\mu_{ij}}\bar{\nabla}_i \cdot \bar{\nabla}_j \tag{4.28}$$

The extra factor of ½ occurs in the above equation since the double summation counts each pair of interactions twice. In the case of the single particle kinetic energy term (∇_i^2), however, the factor of ½ arises from a false "reduced mass".

$$\mu_{ii} = \frac{m_i m_i}{m_i + m_i} = \frac{m_i}{2} \tag{4.29}$$

Though there is no basis for the reduced mass of a single particle, the above notation is retained for mathematical convenience, and is appropriately corrected for.

This is analogous to considering the simultaneous kinetic correlation in terms of the operator $\mathbf{p}_i \cdot \mathbf{p}_j$. The momentum operator is $\mathbf{p} = -i\hbar\bar{\nabla}$. It can be recalled the kinetic energy is given by $T = \frac{p^2}{2m}$. Since there are two particles involved in the off-diagonal terms of the kinetic energy, one can define a scaled momentum $\mathbf{p}_i' = \frac{-i\hbar\bar{\nabla}_i}{\sqrt{m_i}}$. This is analogous to the treatment involved in constructing the mass-weighted Hessian matrix (section 4.4.3). Representing the kinetic energy by $\mathbf{p}_i' \cdot \mathbf{p}_j'$, the kinetic energy operator including kinetic correlation becomes

$$\hat{T} = -\frac{\hbar^2}{2}\sum_{i=1}^{n+N}\sum_{j=1}^{i}\frac{1}{\sqrt{m_i m_j}}\bar{\nabla}_i \cdot \bar{\nabla}_j \tag{4.30}$$

Taking the kinetic energy integral,

$$T = -\frac{1}{4}\sum_{i,j}\frac{1}{\sqrt{m_i m_j}}\left\langle \psi_a(i)\psi_b(j)\middle|\bar{\nabla}_i \cdot \bar{\nabla}_j\middle|\psi_c(i)\psi_d(j)\right\rangle \tag{4.31}$$

one can define a kinetic energy matrix **T** such that

$$T_{ij} = -\frac{1}{4\sqrt{m_i m_j}} \langle \psi_a(i)\psi_b(j) | \bar{\nabla}_i \cdot \bar{\nabla}_j | \psi_c(i)\psi_d(j) \rangle \qquad (4.32)$$

It is evident that **T** is a symmetric square matrix and that $T_{ij} = T_{ji}$. It is also seen that the diagonal terms ($i = j$) collapse to the single particle expressions presented earlier. For $i \neq j$,

$$T_{ij} = -\frac{1}{4\sqrt{m_i m_j}} \langle \psi_a(i) | \bar{\nabla}_i | \psi_b(i) \rangle \langle \psi_a(j) | \bar{\nabla}_j | \psi_b(j) \rangle \qquad (4.33)$$

One can then define

$$T_i = \langle \psi_a(i) | \bar{\nabla}_i | \psi_b(i) \rangle \qquad (4.34)$$

The integral terms in the summation go to zero when $a \neq b$, leading to

$$T_i = \langle \psi_a(i) | \bar{\nabla}_i | \psi_a(i) \rangle \qquad (4.35)$$

Hence, the off-diagonal terms of the kinetic energy matrix become

$$T_{ij} = -\frac{1}{4\sqrt{m_i m_j}} T_i T_j \qquad (4.36a)$$

and the diagonal terms are, as before,

$$T_{ii} = -\frac{1}{2\sqrt{m_i}} \langle \psi_a(i) | \nabla_i^2 | \psi_a(i) \rangle \qquad (4.36b)$$

The total kinetic energy then becomes

$$T = 2\sum_{i<j} T_{ij} + \sum_i T_{ii} \qquad (4.37)$$

The factor of two appears in front of the off-diagonal terms as the summation is carried out over the lower diagonal, taking advantage of the fact that $T_{ij} = T_{ji}$. The kinetic energy

can be expanded in terms of the basis functions making up the one-particle wavefunctions. The terms then become, after simplification,

$$T_i = \sum_{\alpha} C_{a\alpha}^{k(i)^*} C_{a\alpha}^{k(i)} \left\langle \chi_{\alpha}^{k(i)}(i) \middle| \bar{\nabla}_i \middle| \chi_{\alpha}^{k(i)}(i) \right\rangle \tag{4.38a}$$

$$T_{ii} = \frac{1}{2m_i} \sum_{\alpha} C_{a\alpha}^{k(i)^*} C_{a\alpha}^{k(i)} \left\langle \chi_{\alpha}^{k(i)}(i) \middle| \nabla_i^2 \middle| \chi_{\alpha}^{k(i)}(i) \right\rangle \tag{4.38b}$$

This leads directly to the following equations, from the definition of the vector product.

$$T_i = \sum_{\alpha} C_{a\alpha}^{k(i)^2} \left\langle \chi_{\alpha}^{k(i)}(i) \middle| \bar{\nabla}_i \middle| \chi_{\alpha}^{k(i)}(i) \right\rangle \tag{4.39a}$$

$$T_{ii} = \frac{1}{2m_i} \sum_{\alpha} C_{a\alpha}^{k(i)^2} \left\langle \chi_{\alpha}^{k(i)}(i) \middle| \nabla_i^2 \middle| \chi_{\alpha}^{k(i)}(i) \right\rangle \tag{4.39b}$$

From the above, it is possible to define a matrix $\mathbf{T}'$, which contains the $\mathbf{p}_i'$ computed in terms of the basis functions χ. Hence, the total kinetic energy including kinetic correlation can be expressed in terms of the matrix as $\mathbf{T} = \mathbf{PT}'$ for each set of particles (of a homogeneous type).

4.4: Computation of Molecular Properties

The method outlined above, it will be noticed, is only specified for a 'single-point calculation' and the method employed to solve the relevant equations is described. The purpose behind developing any method lies in the extraction of relevant information regarding the properties of the system under study. The primary observable that can be extracted is the energy of the system. This is typically the most important piece of information that is desired. Additionally, it is required in most cases to be able to optimise the structure of a system to a minimum. This is mainly due to the notion that any molecule tends to occupy a minimum (or local minimum) energy orientation, as a

preferred state. Hence, it is necessary for there to be a method by which preferred structures of molecules can be determined. Two such procedures are also outlined in the following sections. Additionally, the curvature at a stationary point has been used to determine the vibrational frequencies of a molecule. The required procedure for the computation of the curvature (and vibrational frequencies) is also presented.

4.4.1: Computation of Energy

The Hamiltonian operator is only slightly modified with respect to the Hartree-Fock Hamiltonian. The Hamiltonian operator is

$$\hat{H} = \sum_n \left(-\frac{1}{2m_n} \nabla_n^2 \right) + \sum_{a<b} \frac{Z_a Z_b}{r_{ab}} \tag{4.40}$$

and includes a summation over all (pairs of) particles. Applying the above Hamiltonian to the molecular wavefunction, the Schrödinger equation becomes

$$\begin{aligned} E &= \langle \Psi | \hat{H} | \Psi \rangle \\ &= \frac{1}{N} \left\langle \sum_i S_i \prod_{n=1}^{k} |\mathbf{D}_i^n| \middle| \hat{H} \middle| \sum_i S_i \prod_{n=1}^{k} |\mathbf{D}_i^n| \right\rangle \\ &= \frac{1}{N} \sum_{a=0}^{NT-1} \sum_{b=0}^{NT-1} S_a S_b \left\langle \prod_{n=1}^{k} |\mathbf{D}_a^n| \middle| \hat{H} \middle| \prod_{n=1}^{k} |\mathbf{D}_b^n| \right\rangle \\ &= \frac{1}{N} \sum_{a=0}^{NT-1} \sum_{b=0}^{NT-1} S_a S_b \left\langle \prod_{c=1}^{k} |\mathbf{D}_a^c| \middle| \sum_i \left(-\frac{\nabla_i^2}{2m_i} + \sum_{j>i} \frac{Z_i Z_j}{r_{ij}} \right) \middle| \prod_{c=1}^{k} |\mathbf{D}_b^c| \right\rangle \\ &= \frac{1}{N} \sum_{a=0}^{NT-1} \sum_{b=0}^{NT-1} S_a S_b E_{ab} \end{aligned} \tag{4.41}$$

The energy of each term is given by E_{ab} and can be partitioned into the kinetic energy and potential contributions.

$$E_{ab} = T_{ab} + V_{ab} \tag{4.42}$$

The kinetic energy and potential energy contributions are given by

$$T_{ab} = \prod_{c=1}^{k} n_c \left(\prod_{d=1}^{n_r} \left(\prod_{e \neq d} \left\langle \psi_e^{c,a} \middle| \psi_e^{c,b} \right\rangle \right) \frac{-1}{2m_d} \left\langle \psi_d^{c,a} \middle| \nabla_d^2 \middle| \psi_d^{c,b} \right\rangle \right) \qquad (4.43a)$$

$$V_{ab} = \sum_{i=1}^{N-1} \sum_{j=i+1}^{N} Z_i Z_j \left(\prod_{c=1}^{k} n_c \right) \left(\prod_{d \neq i,j} \left\langle \psi_d^a \middle| \psi_d^b \right\rangle \right) \left(\left\langle \psi_i^a \psi_j^a \middle| \frac{1}{r_{12}} \middle| \psi_i^b \psi_j^b \right\rangle \right) \qquad (4.43b)$$

Each term in the energy expansion E_{ab} can be minimised independently using the Pople-Nesbet equations. Minimising each term separately would naturally minimise the energy. Hence, the above relation can be solved variationally. The Fock matrix used would be similar in form to that used in the ENMO method, except that the Fock matrix for each term would be different from the others owing to the difference in the orbitals used from one term to the next. In the most general situation, it can be seen that the self-consistent coefficient matrix obtained for each term need not be identical. However, as the differences between the terms arise strictly due to interchange, the coefficient rows corresponding to a given spin orbital necessarily must be identical at the completion of wavefunction optimisation. This can be forced by averaging the corresponding terms from across the various resultant coefficient matrices before further refining through the self-consistent approach. These averaged values can then be used to generate the Fock matrices and overlap integrals for the following iteration, and as an initial guess. This process may be continued until the coefficient matrices do not change to within a set tolerance. Section 4.4.2.1 outlines a method by which one can generalise the SCF procedure to directly yield a molecular geometry.

4.4.2: Geometry Optimisation

In a true non-Born-Oppenheimer method, it is strictly not possible to think in terms of a definite molecular geometry. The concept of a molecular geometry (with known bond lengths and bond angles) suggests that the exact relative positions of the various atoms (nuclei) in the system are known. This would imply invocation of the Born-Oppenheimer approximation. However, the concept of a molecular geometry is something that is of great interest to chemists. It is to be kept in mind that all experimental determinations of the molecular geometries are necessarily time-averages of the various instantaneous orientations of the molecule over the time frame of the experiment. Two different approaches have been outlined below, by which one may determine the mean molecular geometry of the molecule. The first involves computation of the mean positions of the nuclei in the system. The vectorial differences in position will lead to mean inter-nuclear separations and hence mean bond angles can also be calculated. As the experimental determination yields a time-average position, this is analogous to the expectation value of the nuclear positions. The second method seeks to determine the mean geometry by means of a pseudo-PES (pseudo-potential energy surface).

4.4.2.1: Method of Mean Positions

In principle, the optimised wavefunction also yields an optimised geometry for the system. The mean position of any given nucleus is given by

$$\langle r_i \rangle = \frac{\langle \Psi | \hat{r}_i | \Psi \rangle}{\langle \Psi | \Psi \rangle} \qquad (4.44)$$

Since "atom-centred" basis sets are used (in modified form or otherwise), it is necessary for the mean positions of the nuclei to coincide with the origins (centres) of the basis functions. Hence, the basis functions are translated to the new 'positions' of the nuclei as computed above at the beginning of each SCF iteration. This is necessary as otherwise highly deformed wavefunctions may result, especially when input geometries are sufficiently different from the optimal geometry for the given set of basis functions. One of the convergence criteria would then be that the mean positions of the nuclei do not change from one iteration to the next.

As noted above, the mean position of a given nucleus is given by

$$\langle r_i \rangle = \frac{\langle \Psi | \hat{r}_i | \Psi \rangle}{\langle \Psi | \Psi \rangle} \tag{4.44}$$

Since the total wavefunction can be written as $\Psi = \frac{1}{\sqrt{N}} \sum_i \left[S_i \prod_{n=1}^{k} |\mathbf{D}_i^n| \right]$, after factoring in the normalisation condition the above expression then becomes

$$\begin{aligned} \langle r_i \rangle &= \left\langle \sum_a S_a \prod_{n=1}^{k} |\mathbf{D}_a^n| \middle| \hat{r}_i \middle| \sum_a S_a \prod_{n=1}^{k} |\mathbf{D}_a^n| \right\rangle \\ &= \sum_a \sum_b S_a S_b \left\langle \prod_{n=1}^{k} |\mathbf{D}_a^n| \middle| r_i \middle| \prod_{n=1}^{k} |\mathbf{D}_b^n| \right\rangle \end{aligned} \tag{4.45}$$

Integrating over all types of particles other than that of the nucleus of interest,

$$\begin{aligned} \langle r_i \rangle &= \sum_a \sum_b S_a S_b \left\langle |\mathbf{D}_a^n| \middle| r_i \middle| |\mathbf{D}_b^n| \right\rangle \\ &= \sum_a \sum_b S_a S_b \sum_{j,k} \left\langle \psi_j^a(r_i) r_i \psi_k^b(r_i) \right\rangle \end{aligned} \tag{4.46}$$

Expanding the single-particle wavefunctions as $\psi_j = \sum_x C_{xj} \chi_x$,

$$\begin{aligned}\langle r_i \rangle &= \sum_a \sum_b S_a S_b \sum_j \sum_k \left\langle (\sum_x C_{xj}^a \chi_x) r_i (\sum_x C_{xk}^b \chi_x) \right\rangle \\ &= \sum_a \sum_b S_a S_b \sum_j \sum_k \sum_x \sum_y C_{xj}^a C_{xy}^b \langle \chi_x r_i \chi_y \rangle\end{aligned} \tag{4.47}$$

In the case that real functions are used, corrections must be made for double counting. Hence,

$$\langle r_i \rangle = \frac{1}{2} \sum_a \sum_b S_a S_b \sum_j \sum_k \sum_x \sum_y C_{xj}^a C_{yk}^b \langle \chi_x r_i \chi_y \rangle \tag{4.48}$$

When χ_x and χ_y are centred on the same centre, the integral becomes $r_C^{x,y} \delta_{xy}$ where $r_C^{x,y}$ refers to the coordinates of the centre around which χ_x and χ_y are based. Thus, terms involving basis functions on the same centre reduce to the form $C_{xj} C_{xk} r_C^x$. The overlap integrals thus act as weighting terms in the redistribution of the mean nuclear position.

Optimisation of the geometry allows one to converge only to stationary points respective to both electronic and nuclear coordinates simultaneously. Hence, the computation of the geometry by this method could yield either a minimum or a saddle point. Implementation of such a method would enable optimisation only to stationary points, such that the optimised result is a stationary point with respect to electronic and nuclear coordinates. Hence, one can gather that the only possible results would be optimisation to minima and saddle points (as understood in the language of the PES). Identification of the same could be achieved by investigating the curvature at the final geometry (section 4.4.3).

4.4.2.2: Hessian Approach

It is important to remember that the concept of a potential energy surface (PES) is lost upon leaving the realm of the Born-Oppenheimer approximation. However, it is also a concept that carries much meaning in chemistry. It is desirable to retain a method by which the understanding of chemical reactions can be retained while still transcending the BO approximation. Since chemical reactions are in general understood in terms of the motion of molecules across a PES (or FES), some means must be devised whereby the advances made in these fields are not lost or rendered unusable. Hence, the application of this method to the calculation of a PES may be understood as incorporating the effects of non-BO corrections to the PES.

In this approach, the nuclei are translated in accordance with the gradients generated and the curvature as calculated using the Hessian matrix. The gradient vector in Cartesian coordinates at each nuclear position can be calculated by

$$[GRAD] = \begin{bmatrix} \frac{\partial E}{\partial x_1} \\ \frac{\partial E}{\partial y_1} \\ \cdots \\ \frac{\partial E}{\partial z_K} \end{bmatrix} = \begin{bmatrix} \frac{\partial E}{\partial q_1} \\ \frac{\partial E}{\partial q_2} \\ \cdots \\ \frac{\partial E}{\partial q_{3K}} \end{bmatrix} \tag{4.48}$$

This vector is of dimension $1 \times 3K$ and the coordinates span the $3K$ coordinates of the K nuclei. At a stationary point (extremum), the elements of the gradient vector would be uniformly zero. The terms of the gradient matrix can be calculated as

$$[GRAD]=\begin{bmatrix}\frac{\partial E}{\partial q_1}\\ \frac{\partial E}{\partial q_2}\\ \cdots\\ \frac{\partial E}{\partial q_{3K}}\end{bmatrix}=\frac{1}{\langle\Psi|\Psi\rangle}\begin{bmatrix}\frac{\partial\langle\Psi|\hat{H}|\Psi\rangle}{\partial q_1}\\ \frac{\partial\langle\Psi|\hat{H}|\Psi\rangle}{\partial q_2}\\ \cdots\\ \frac{\partial\langle\Psi|\hat{H}|\Psi\rangle}{\partial q_{3K}}\end{bmatrix}=\frac{1}{N}\begin{bmatrix}\frac{\langle\Psi|\hat{H}|\partial\Psi\rangle}{\partial q_1}\\ \frac{\langle\Psi|\hat{H}|\partial\Psi\rangle}{\partial q_2}\\ \cdots\\ \frac{\langle\Psi|\hat{H}|\partial\Psi\rangle}{\partial q_{3K}}\end{bmatrix}=\frac{1}{N}[Gr] \tag{4.49}$$

As the energy is additive in the various terms of the wavefunction, the gradient vector can be separated into its constituents.

$$[Gr]=\sum_{a,b=0}^{NT-1}S_aS_b[Gr_{ab}] \tag{4.50}$$

The elements of $[Gr_{ab}]$ can be separated into

$$Gr_{ab}(q_i)=\sum\left(T_{ab}(q_i)+V_{ab}(q_i)\right) \tag{4.51}$$

where the summation is over all terms in the T and V matrices. The terms of the kinetic energy and potential energy terms are calculated as before, except that $\frac{\partial\psi}{\partial q_i}$ evaluated at q_i is substituted for the wavefunction corresponding to the coordinate q_i. For a system containing n electrons and K nuclei, the T and V matrices are of dimension $(3n+3K)\times(3n+3K)$. In this study, the convention is adopted that the electrons are the first n particles in the system and the nuclei are hence the remaining K particles. Hence, the first $3n$ rows/columns of the T and V matrices correspond to the electrons. Since the differentiation is performed relative to the nuclear coordinates, these terms are largely unchanged relative to the energy calculations. The first derivative of the kinetic energy matrix becomes

$$T_{ab}^{(1)}(q_i)=\begin{pmatrix} \left\langle \psi_1 \left| \frac{\partial^2 \psi_1}{\partial q_1^2} \right\rangle & 0 & & & 0 \\ 0 & \left\langle \psi_1 \left| \frac{\partial^2 \psi_1}{\partial q_2^2} \right\rangle & & & \\ & & \cdots & & \\ & & & \left\langle \psi_i \left| \frac{\partial^3 \psi_i}{\partial q_i^3} \right\rangle & \\ & & & & \cdots \quad 0 \\ 0 & & & & 0 \quad \left\langle \psi_K \left| \frac{\partial^2 \psi_K}{\partial q_{3K}^2} \right\rangle \right. \end{pmatrix} \tag{4.52}$$

In a similar fashion, the first derivative of the potential energy matrix can be calculated as

$$V_{ab}^{(1)}(q_i)=\begin{pmatrix} 0 & \cdots \left\langle \psi_1\psi_2 \left| \frac{1}{q_4-q_1} \right| \psi_1\psi_2 \right\rangle & \cdots & \left\langle \psi_1\psi_i \left| \frac{1}{q_i-q_1} \right| \psi_1\psi_i \right\rangle \\ \cdots & 0 \quad \cdots & & \\ \left\langle \psi_1\psi_2 \left| \frac{1}{q_1-q_4} \right| \psi_1\psi_2 \right\rangle & 0 & & \\ \cdots & & 0 & \cdots \\ \left\langle \psi_1\psi_i \left| \frac{Z_1 Z_i}{q_1-q_i} \right| \frac{\psi_1 \partial \psi_i}{\partial q_i} \right\rangle & & 0 & \left\langle \psi_{3K}\psi_i \left| \frac{Z_{3K} Z_i}{q_{3K}-q_i} \right| \frac{\psi_{3K} \partial \psi_i}{\partial q_i} \right\rangle \\ & & \cdots \left\langle \psi_{3K}\psi_i \left| \frac{1}{q_i-q_{3K}} \right| \psi_{3K}\psi_i \right\rangle & 0 \end{pmatrix} \tag{4.53}$$

The elements of the Hessian matrix are $\frac{\partial^2 E}{\partial r_i \partial r_j}$ where the indices i and j run over only the nuclei. In Cartesian coordinates, the Hessian is expressed as a $3K \times 3K$ matrix of the form

$$K = \begin{pmatrix} \frac{\partial^2 E}{\partial x_1^2} & \frac{\partial^2 E}{\partial x_1 \partial y_1} & \cdots & \frac{\partial^2 E}{\partial x_1 \partial z_n} \\ \frac{\partial^2 E}{\partial y_1 \partial x_1} & \frac{\partial^2 E}{\partial y_1^2} & \cdots & \frac{\partial^2 E}{\partial y_1 \partial z_n} \\ \cdots & \cdots & \cdots & \cdots \\ \frac{\partial^2 E}{\partial z_n \partial x_1} & \frac{\partial^2 E}{\partial z_n \partial y_1} & \cdots & \frac{\partial^2 E}{\partial z_n^2} \end{pmatrix} = \begin{pmatrix} \frac{\partial^2 E}{\partial q_1^2} & \frac{\partial^2 E}{\partial q_1 \partial q_2} & \cdots & \frac{\partial^2 E}{\partial q_1 \partial q_{3k}} \\ \frac{\partial^2 E}{\partial q_2 \partial q_1} & \frac{\partial^2 E}{\partial q_2^2} & \cdots & \frac{\partial^2 E}{\partial q_2 \partial q_{3K}} \\ \cdots & \cdots & \cdots & \cdots \\ \frac{\partial^2 E}{\partial q_{3K} \partial q_1} & \frac{\partial^2 E}{\partial q_{3K} \partial q_2} & \cdots & \frac{\partial^2 E}{\partial q_{3K}^2} \end{pmatrix} \tag{4.54}$$

The Hessian is typically symmetrised [76] by

$$K_{ij} = K_{ji} = \frac{(K_{ij} + K_{ji})}{2} \tag{4.55}$$

The symmetrisation method suggested above is necessary in the case that real functions are used to create the molecular basis. The terms of the molecular Hessian can be obtained by computing the Hessian for each energy term and adding the overlap weighted matrix elements.

$$K^{mol} = \sum_{a,b} S_a S_b K_{ab} \tag{4.56}$$

The elements of K_{ab} can be given by

$$K_{ab} = \begin{pmatrix} \frac{\partial^2 E_{ab}}{\partial q_1^2} & \frac{\partial^2 E_{ab}}{\partial q_1 \partial q_2} & \cdots & \frac{\partial^2 E_{ab}}{\partial q_1 \partial q_{3k}} \\ \frac{\partial^2 E_{ab}}{\partial q_2 \partial q_1} & \frac{\partial^2 E_{ab}}{\partial q_2^2} & \cdots & \frac{\partial^2 E_{ab}}{\partial q_2 \partial q_{3K}} \\ \cdots & \cdots & \cdots & \cdots \\ \frac{\partial^2 E_{ab}}{\partial q_{3K} \partial q_1} & \frac{\partial^2 E_{ab}}{\partial q_{3K} \partial q_2} & \cdots & \frac{\partial^2 E_{ab}}{\partial q_{3K}^2} \end{pmatrix} \tag{4.57}$$

Each element in the above matrix, $K_{ab}(q_i, q_j)$ is given by

$$K_{ab}(q_i,q_j)=\sum\left(T_{ab}(q_i,q_j)+V_{ab}(q_i,q_j)\right) \tag{4.58}$$

The elements of the $T_{ab}(q_i,q_j)$ and $V_{ab}(q_i,q_j)$ matrices are calculated in an analogous fashion to the terms calculated for the gradient matrix and are given by

$$T_{ab}^{(2)}(q_i)=\begin{pmatrix} \left\langle \psi_1 \left| \frac{\partial^2 \psi_1}{\partial q_1^2} \right\rangle & 0 & & & 0 \\ 0 & \left\langle \psi_1 \left| \frac{\partial^2 \psi_1}{\partial q_2^2} \right\rangle & & & \\ & & \cdots & & \\ & & & \left\langle \psi_i \left| \frac{\partial^4 \psi_i}{\partial q_i^4} \right\rangle \right. & \\ & & & \cdots & 0 \\ 0 & & & 0 & \left\langle \psi_K \left| \frac{\partial^2 \psi_K}{\partial q_{3K}^2} \right\rangle \right. \end{pmatrix} \tag{4.59}$$

and the contribution of the gradient to the potential energy is

$$V_{ab}^{(2)}(q_i,q_j)=\begin{pmatrix} 0 & \cdots \left\langle \psi_1\psi_2 \left| \frac{1}{q_1-q_1} \right| \psi_1\psi_2 \right\rangle & \cdots & \left\langle \psi_1\psi_i \left| \frac{1}{q_i-q_1} \right| \psi_1\psi_i \right\rangle & \\ \cdots & 0 \quad \cdots & & & \\ \left\langle \psi_1\psi_2 \left| \frac{1}{q_1-q_4} \right| \psi_1\psi_2 \right\rangle & 0 & \left\langle \psi_1\psi_j \left| \frac{1}{q_j-q_4} \right| \psi_1 \frac{\partial \psi_j}{\partial q_j} \right\rangle & & \\ \cdots & & 0 & & \cdots \\ \left\langle \psi_1\psi_i \left| \frac{Z_1 Z_1}{q_1-q_i} \right| \frac{\psi_1 \partial \psi_i}{\partial q_i} \right\rangle & & \left\langle \psi_1\psi_i \left| \frac{Z_1 Z_1}{q_i-q_i} \right| \frac{\partial \psi_i \partial \psi_i}{\partial q_i \partial q_i} \right\rangle & 0 & \left\langle \psi_{3K}\psi_i \left| \frac{Z_{3K} Z_i}{q_{3K}-q_i} \right| \frac{\psi_{3K} \partial \psi_i}{\partial q_i} \right\rangle \\ & & \cdots & \left\langle \psi_{3K}\psi_i \left| \frac{1}{q_i-q_{3K}} \right| \psi_{3K}\psi_i \right\rangle & 0 \end{pmatrix} \tag{4.60}$$

The displacement vector is then given by

$$[DISP] = \left(K^{mol}\right)^{-1}[GRAD] \tag{4.61}$$

It can be seen that the displacement vector is of dimension $1\times 3K$. Translation of the nuclear positions by the displacement vector leads to the new nuclear positions.

$$[q_i] = [q_i]_{old} + [DISP] \tag{4.62}$$

Successive repetitions until the displacement vector becomes uniformly zero (within a specified tolerance) leads to a geometry that is a stationary point for the energy with respect to change in the mean positions of the nuclei.

4.4.3: Computation of Vibrational Frequencies

Computation of the vibrational frequencies of a molecule involves exploring the curvature of the PES in the neighbourhood of the optimised position (or geometry of interest, if not a stationary point). The set of vibrational frequencies is obtained directly from the values of the curvature in the number of dimensions corresponding to the system being studied.

The vibrational frequencies are computed by means of diagonalising the mass-weighted Hessian matrix. The elements of the Hessian matrix are $\frac{\partial^2 E}{\partial r_i \partial r_j}$ where the indices i and j run over only the nuclei. These terms of the mass-weighted Hessian are $\frac{1}{\sqrt{m_i m_j}}\frac{\partial^2 E}{\partial r_i \partial r_j}$. The Hessian K is calculated as before (Section 4.4.2.2).

$$K = \begin{pmatrix} \frac{\partial^2 E}{\partial x_1^2} & \frac{\partial^2 E}{\partial x_1 \partial y_1} & \cdots & \frac{\partial^2 E}{\partial x_1 \partial z_n} \\ \frac{\partial^2 E}{\partial y_1 \partial x_1} & \frac{\partial^2 E}{\partial y_1^2} & \cdots & \frac{\partial^2 E}{\partial y_1 \partial z_n} \\ \cdots & \cdots & \cdots & \cdots \\ \frac{\partial^2 E}{\partial z_n \partial x_1} & \frac{\partial^2 E}{\partial z_n \partial y_1} & \cdots & \frac{\partial^2 E}{\partial z_n^2} \end{pmatrix} \tag{4.54}$$

The Hessian is then symmetrised [76] by

$$K_{ij} = K_{ji} = \frac{(K_{ij} + K_{ji})}{2} \tag{4.55}$$

The terms of the total molecular Hessian can be obtained by computing the Hessian for each energy term and adding the overlap weighted matrix elements.

$$K^{mol} = \sum_{a,b} S_a S_b K_{ab} \tag{4.56}$$

The mass-weighted Hessian is then computed as explained earlier.

$$\overline{K}_{ij}^{mol} = \frac{1}{\sqrt{m_i m_j}} K_{ij}^{mol} \tag{4.63}$$

The eigenvalues λ_i for the diagonalised mass-weighted Hessian yield the vibrational frequencies ν_i as

$$\nu_i = \frac{\lambda_i^{1/2}}{2\pi} \tag{4.64}$$

4.5: Features of Modified ENMO Method

The modified ENMO method by its construction was required to fit certain conditions. Among these is the requirement that the molecular wavefunction should not be separable into electronic and nuclear contributions. This means that it should not be

possible for the molecular wavefunction to be expressed as $\Psi = \psi_e \psi_n$ or simply as $\Psi = \sum_i \sum_j \psi_e^i \psi_n^j$, since the latter can be rearranged to $\Psi = \left(\sum_i \psi_e^i \right) \left(\sum_j \psi_n^j \right)$. Obviously, this latter representation is only a restatement of the initial approximation. It is therefore necessary that the molecular wavefunction be expressed as a sum of products, where the terms of the series are non-factorable. In the current method, the total molecular wavefunction is given by

$$\Psi = \frac{1}{\sqrt{N}} \sum_i \left[S_i \prod_{n=1}^{fermions} \left| \mathbf{D}_i^n \right| \prod_{n=1}^{bosons} \left\| \mathbf{D}_i^n \right\| \right] \tag{4.24}$$

In the above equation, the summation is over various 'configurations' where the configuration space extends over the molecular orbital space computed under the separability approximation. The available space for a particle includes the 'orbital' space of every type of particle in the system. The probability of particle interchange is governed by the overlap integral of the two occupied functions. This scaling of the overlap makes it impossible to factorise the molecular wavefunction into separable components, thus satisfying the primary requirement of a truly non-Born-Oppenheimer method. However, due to the formation of an electron-nucleus coupled wavefunction, one can strictly no longer consider the system as a collection of occupied MOs. The system is now specified only in terms of a state, described by the wavefunction. Of course, this was always expected for a true *ab initio* method, though recent history has run contrary to such views. It has been customary to think of a molecule in terms of an electronic state (or even assemblage of MOs), assuming that the nuclei offer nothing more than the Coulombic potential background on which the electrons interact.

As is obvious from the implementation described previously in this chapter, the nuclei have been 'placed' in orbitals and hence the nuclei are necessarily delocalised. Since the extent of delocalisation is a factor of the mass of the particle, it can be seen that the deviation from Born-Oppenheimer behaviour is small for the heavier nuclei and larger for the lighter nuclei. This is consistent with expectations, as the basis of the BO approximation is the separability of nuclear and electronic motion due to the large mass differential. This would tend to be a more valid assumption as the nucleus increases in mass.

Another important feature of this method is the introduction of interchange between particles of different types. This leads to an increased region of delocalisation for the nuclei. At the same time, this increases the concentration of the electronic density in the region of the mean positions of the nuclei. It is also noteworthy that no effort is made to correct for the cusp at the nuclear positions. This is because the cusp is an artefact of the Born-Oppenheimer approximation. The cusp originates from the fact that an electron cannot occupy the same position as a nucleus, leading to a singularity. Since the nuclei are no longer required to be clamped in position, there is no necessity to have a singularity (cusp) at the nuclear positions. Since the nuclei are treated as quantum particles, they occupy a region of space that is given by the wavefunction. The electronic wavefunction must satisfy the Hamiltonian operator used in conjunction with the nuclear charge distribution (as described by the nuclear MO). As the nuclei are represented as continuum charge distributions, there cannot exist a cusp in the electronic wavefunction at the mean nuclear position. This is analogous to the result obtained when employing the

finite-nucleus model.[13] However, the tendency for an increased electron density in the vicinity of the nuclear positions is undiminished, and satisfied by the interchange principle built into the model. Hence, the interchange principle serves two purposes. It helps to improve the particle density distributions while at the same time making the wavefunction non-separable (non-factorisable) into separate electronic and nuclear contributions.

In attempting to make the wavefunction non-separable, it may be recalled that the various terms were added after being scaled by the overlap integral involving the particles being interchanged. This leads to a situation where certain terms become less important when they are centred at different positions. Hence, for example, in a fragmentation (dissociation) process, certain terms in the energy expansion (involving interchange of particles in the separating fragments) become less important and vanish as the separation between the fragments increases. This leads to a smooth removal of certain energy terms from the expansion and a smooth profile to the 'PES'. This will lead to the correct dissociation behaviour, as at infinite separation there is no contribution to the energy from terms involving interchange of particles between separated fragments. Hence, the current method retains the size consistency of the Hartree-Fock method (of which it is but an extension).

CHAPTER V: APPLICATION OF MODIFIED ENMO METHOD

The development of the modified ENMO method was outlined in the previous chapter. Pursuant to the development, it is necessary to determine the efficacy of the method. The applicability of a computational method depends on various factors. The primary factor that determines the use of a method deals with its applicability. A method will not be used if it is incapable of quantifying the effect one wishes to study. On the other hand, the method should be capable of adequately quantifying the effect of interest. As is evident, the modified ENMO method is designed to study the effects of nuclear delocalisation in a molecule. The second most important factor to be considered is the accuracy of the method. Thirdly, one is interested in the computational expense associated with the method. A discussion of these factors as they relate to the modified ENMO method is the focus of the present chapter. This discussion necessarily begins with the manner in which the method has been implemented, with particular emphasis on peculiarities relative to extant methods.

5.1: Computational Implementation

The modified ENMO method explained in the previous chapter is implemented by modifying the PSI code base.[77] In order to not bias the results of a calculation, and to avoid symmetry breaking effects (present in the energy terms beyond the zero order), the method has been implemented to run in C_1 symmetry. This is also necessary to avoid the

difficulties involved when separating the various particle types, which are treated as being self-contained systems. This is a relic of the manner in which quantum chemical codes have been implemented to date, as there was never a necessity to consider any more than the electrons in the system. It is also worth remembering that isotopic substitution leads to symmetry-breaking, and currently extant codes are not capable of accepting these differences. Hence, in order to avoid re-writing the entire package, it was deemed prudent to ignore symmetry constraints and perform all calculations without symmetry.

As in any other implementation, the input for the modified program contains a guess geometry for the system of interest. In addition, it is necessary to specify the isotope for each atom in the system. The first step in the analysis involves the placing of the various particles in 'boxes', one for each particle type. For a system with k particle types, the numbering ranges from 0 to $k-1$, with box 0 always containing electrons. The other boxes are labelled as per the order of appearance in the input stream.

For each box, the basis to be used is read in from the input file. The basis functions for the nuclei are generated internally based on the information provided. There are two procedures implemented by which nuclear basis functions can be generated. In the first method, the basis functions for electrons at each centre are scaled (see following section) for the particles in each box. In the second approach, the electronic basis functions for the hydrogen atom are retrieved and scaled to generate the basis functions for a given nucleus. It is also possible to specify a user-defined basis for the nuclei if so desired. In case a nuclear basis is not defined, the hydrogen atom set from the cc-pVTZ

basis is pulled and scaled accordingly. This set was chosen as the default since it is a well-balanced basis of sufficient quality containing $p-$ and $d-$ type polarisation functions for the hydrogen atom. This enables one to attain sufficient flexibility in the optimised density distribution of the nuclei. Of course, care must be taken to ensure that the nuclei are not over-specified relative to the electrons, as ultimately, the bulk of the chemistry depends on how well the electrons are described. Any method that does not treat the electrons adequately is irrelevant, irrespective of how accurately the nuclei are treated.

Once the basis functions are scaled and placed in boxes, the remainder of the problem is one for which a solution is already known: the unrestricted Hartree-Fock method. Prior to solving the UHF wavefunction by means of the Pople-Nesbet equations, it is necessary to generate a list of the various basis functions and their 'origins' (namely, which box they come from). This ensures that the basis functions belonging to a certain box are only optimised within that box. Moreover, the 'inter-box' interactions need to be quantified and hence it is more convenient to generate a comprehensive list of all possible interactions and choose the relevant integrals as and when required. In this manner, one can retain the integrals necessary for the post-ENMO energy terms without resorting to regeneration of the same.

The $\mathbf{H}$ matrix for each box is constructed from the $\mathbf{T}$ matrix for each box. The other contribution to the $\mathbf{H}$ matrix comes from the inter-box Coulombic interactions. For the sake of convenience, these will be referred to as $\mathbf{J}_{ij}$ where the subscripts refer to the

boxes connected by these terms. From the guess functions, the **P** matrices for each box can be generated. The density distribution matrix **D** is generated according to the property $D(i,j) = S(i,j)P(i,j)$, where the **S** matrix is the (previously defined) overlap matrix relevant to the box. This matrix denotes the distribution of particle density as a function of the basis, whereas the **P** matrix signifies the occupation distribution along the same axis. The **H** matrix for a given box i can then be given by

$$\mathbf{H}_i = \mathbf{T}_i + \sum_{j \neq i} \mathbf{D}_j \mathbf{J}_{ij} \tag{5.1}$$

This includes all the interactions except the Coulomb and exchange interactions present within each box. The intra-box Coulomb interactions are introduced *via* the **G** matrix. Solving the Pople-Nesbet equations then optimises the density matrix **P** (by optimising the coefficient matrix). Since the **H** matrix remains unchanged during the optimisation of the coefficient matrix for a box, the **H** matrix needs to be updated based on the new **P** matrices generated. Hence, it can be considered that the convergence of the **H** matrices be a condition of convergence of the system. It is to be remembered that the **T** matrix remains constant for any given geometric configuration. Hence, convergence of the **H** matrix implies convergence of the **P** matrices.

It may be recalled that the computation of energy in the Pople-Nesbet (UHF) method is related to the density distributions ($\mathbf{P}^{\alpha}$ and $\mathbf{P}^{\beta}$ matrices) through the **H** and **F** matrices, where **F** is the sum of the **H** and **G** matrices. The UHF energy is given by

$$E_0 = \frac{1}{2} \sum_{\mu} \sum_{\nu} \left[\mathbf{P}^{T}_{\nu\mu} \mathbf{H}_{\mu\nu} + \mathbf{P}^{\alpha}_{\nu\mu} \mathbf{F}^{\alpha}_{\mu\nu} + \mathbf{P}^{\beta}_{\nu\mu} \mathbf{F}^{\beta}_{\mu\nu} \right] \tag{2.42}$$

In an analogous fashion, the energy of each box can be computed by

$$E^i = \frac{n^i!}{2N_0}\sum_{\mu}\sum_{\nu}\left[\mathbf{P}^{T,i}_{\nu\mu}\left(\frac{\mathbf{H}^i{}_{\mu\nu}+\mathbf{T}^i{}_{\mu\nu}}{2}\right)+\sum_{s}^{spins}\mathbf{P}^{s,i}_{\nu\mu}\mathbf{F}^{s,i}_{\mu\nu}\right] \qquad (5.2)$$

The term $N_0 = \prod_{i=0}^{k}(n^i!)$ is the overall particle normalisation term that enables the energies to be additive, and n^i is the number of particles in a given box i. This is necessary as each box is internally normalised by $n^i!$. It may be recalled that $\mathbf{H} = \mathbf{T} + \mathbf{V}$. In this case, the $\mathbf{V}$ terms relate to the Coulomb interactions involving particles in a given box and all other boxes. The full magnitude of the force is seen by the particle through the $\mathbf{H}$ matrix. However, to include the full magnitude in the energy computation would lead to a double counting (and hence over-estimation) of the Coulomb energy between dissimilar particles. In order to correct for this, the 'single particle' energy is given by $\mathbf{P}(\mathbf{T}+\mathbf{V}/2)$, and it can be trivially shown that this leads to the result shown above. The zero-order energy of the system (term 00), is then

$$E_{00} = \sum_{i=0}^{k} E^i \qquad (5.3)$$

Once the energies are computed for the higher-order correction terms, one can then generate the total energy of the system using

$$E = \frac{\sum_{a,b} E_{ab}}{\sum_{a,b} S_a S_b} \qquad (5.4)$$

The computation of the higher order correction terms is dealt with in greater detail in the following section.

5.1.1: Computation of Terms Beyond 00

The interchange terms (01, 10, etc.) are given in terms of $\langle \psi_i | \hat{O} \psi_j \rangle$. From the LCAO method, each of ψ_i and ψ_j is given in terms of the basis space χ^i or χ^j. In general, the dimension of the basis space will vary from one box to another, so a direct interchange of basis functions (and coefficients) in a determinantal (matrix) form is not practical. It then becomes necessary to express the energy in a modified fashion, taking into account the various interactions separately. It is to be remembered that this analysis is also performed on the optimised density distributions (*via* SCF, section 5.1). In the following, it is to be remembered that the left hand side refers to the occupation in configuration a, and the right hand side refers to the occupation in configuration b. The elements of the kinetic and potential energy matrices are given by

$$T_{ab}(i,i) = \frac{-1}{2m_i} \left\langle \sum_{l=1}^{size\text{-}of\text{-}box\text{-}i\text{-}in\text{-}a} C_{li}\chi_l \middle| \sum_{l=1}^{size\text{-}of\text{-}box\text{-}i\text{-}in\text{-}b} C_{li}\nabla^2\chi_l \right\rangle \qquad (5.5a)$$

$$V_{ab}(i,j) = Z_i Z_j \left\langle \sum_{l=1}^{size\text{-}of\text{-}box\text{-}i\text{-}in\text{-}a} C_{li}\chi_l \middle| \hat{J} - \hat{K}/2 \middle| \sum_{l=1}^{size\text{-}of\text{-}box\text{-}j\text{-}in\text{-}b} C_{lj}\chi_l \right\rangle \qquad (5.5b)$$

where i and j refer to the specific particles in question. The off-diagonal terms in the kinetic energy matrix accruing from the effects of inter-particle correlation are given by

$$T_{ab}(i,j) = \frac{\left\langle \sum_{l=1}^{size\text{-}of\text{-}box\text{-}i\text{-}in\text{-}a} C_{li}\chi_l \middle| \sum_{l=1}^{size\text{-}of\text{-}box\text{-}i\text{-}in\text{-}b} C_{li}\nabla\chi_l \right\rangle \left\langle \sum_{l=1}^{size\text{-}of\text{-}box\text{-}j\text{-}in\text{-}a} C_{lj}\chi_l \middle| \sum_{l=1}^{size\text{-}of\text{-}box\text{-}j\text{-}in\text{-}b} C_{lj}\nabla\chi_l \right\rangle}{2\sqrt{m_i m_j}} \qquad (5.6)$$

Summation over the terms leads to the energy of each term within each box. Since this method is ignorant of the box structure, it is possible to include all inter-particle interactions in one matrix and to then sum the terms. In addition, it can be seen that in general $E_{ab} \neq E_{ba}$. However, the inequality is only observed when complex basis functions are employed. In the case where real basis functions are used (the vast majority of calculations), the total energy can then be given by

$$E = \frac{\sum_{a=0}^{N} S_a^2 E_{aa} + 2\sum_{a=1}^{N}\sum_{b=0}^{a-1} S_a S_b E_{ab}}{\sum_{a=0}^{N} S_a^2 + 2\sum_{a=1}^{N}\sum_{b=0}^{a-1} S_a S_b} \qquad (5.7)$$

Hence, only half as many energy terms need be calculated when real basis functions are used in the computation.

5.1.2: Computational Expense and Scaling

The utilisation of a method is limited by three factors – its applicability, accuracy, and the resources required to perform the computations. Applicability automatically becomes a pre-requisite before the other two factors are even considered. Hence, the limiting conditions for an appropriate method are the accuracy and resource requirement. It is observed that the current method is resource intensive. The fixed resource requirement is not over-bearing, however, the time requirements increase rapidly.

There are two components to the time requirement. The initial component is the time required for SCF convergence. As the SCF convergence is carried out in several 'boxes' independently and serially, the time requirement increases as the number of boxes

and the fourth power of the number of basis functions in each box. This requirement is identical to the time requirement for a Hartree-Fock computation on each box separately. This aspect of the computational expense can also be reduced by parallelising the SCF computations of the boxes. In the current (serial) implementation, the time required for SCF convergence (barring difficult convergence cases) increases as $T^{SCF} \sim \sum_{boxes} N_B^4$ where N_B is the number of basis functions in box B.

By far the largest contribution to the time required for a computation is the post-processing step. This is greatly affected by the number of 'configurations' (in CI terminology) to be included in the computation. The number of configurations increases with the number of particles and the number of boxes in the system. It is, in a sense, a measure of the amount of flexibility in a system. As a rough approximation, the number of configurations is given by kK, and the number of energy terms is given by the square of the number of configurations. Hence, isotopic substitution becomes a factor that affects the computational requirements, as it increases the number of boxes in the system. It has been found that when real basis functions are used, the number of energy terms one need compute is nearly halved, as the off-diagonal terms are identical. Within each energy term, the time expense varies as $\left(\sum_{boxes} N_B\right)^4$, leading to an overall post-processing time that varies as $[kK]^2\left(\sum_{boxes} N_B\right)^4$. For any moderately sized system, this is the limiting step in terms of the computational resources. It is for this reason that it is recommended that the post-processing only be performed on the optimised densities and not during

intermediate steps (though the option currently exists). It is evident that the total number of computations to be performed is severely dependent on the basis set employed, as the computational time increases rapidly with the total number of basis functions as can be seen from Figure 5.1.

Figure 5.1: Time required for SCF optimisation and energy computations on atoms as a function of basis set.

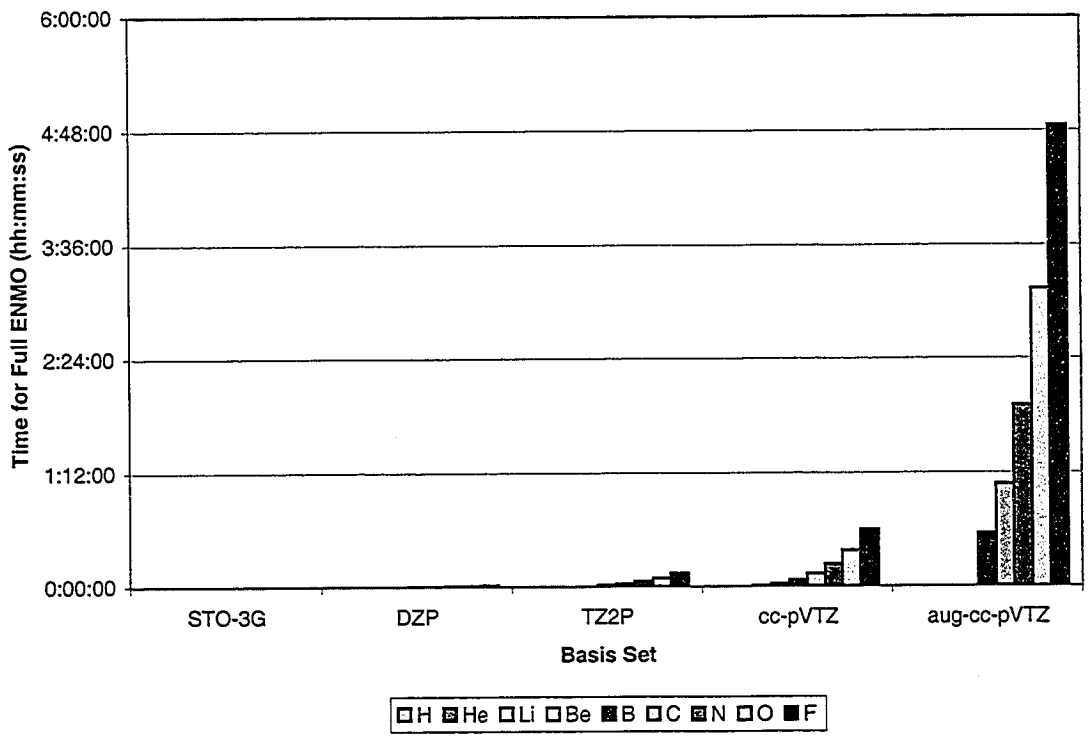

The SCF convergence in all cases was obtained in less than 2 seconds. Since it is known that the effect of delocalisation of the nuclei is small, it is necessary to employ reasonably large basis sets to capture the effect accurately. As can be seen from the above figure, the computational effort increases steeply as the basis space is increased. It is therefore beneficial to use the smallest basis set possible that would provide results of requisite

accuracy. Furthermore, the computational effort can be reduced by parallelising the computation of the total energy. This is possible by 'farming out' the computation of the various energy terms into mini-processes.

5.2: Instability in Wavefunction

The ENMO wavefunction is by its nature very unstable, as the wavefunction depends immensely on the density distributions of the various particle types. It is observed that as the SCF procedure is repeated, the density distributions of the boxes oscillate wildly through the epochs. Part of the problem seems to be a flip between the occupied and virtual MOs, occurring usually in the third epoch. The instability in the wavefunction has been traced to the methodology used in the SCF procedure. A matrix $\mathbf{X}$ is generated from the Fock matrix and the coefficient matrix as $\mathbf{X} = \mathbf{C}^T\mathbf{F}\mathbf{C}$. This matrix is then diagonalised to yield $\mathbf{X}'$. The new coefficient matrix is obtained by left multiplying by $\mathbf{X}'$.[23] It turns out that during the third epoch, $\mathbf{X}'$ becomes anti-diagonal. It has not been possible to determine the cause for this behaviour, and it is expected that it is possible this can be rectified. Since it is noticed that the system usually converges to an excited state when full convergence is permitted, the numbers presented in this study are the results obtained after only one epoch. This is justified under the premise that the Hartree-Fock density is a good density for the system (especially for the electrons), and that the nuclear densities are optimised in the electronic field. Unfortunately, refining the densities further instigates the behaviour outlined above and must be avoided until better convergence techniques are available.

In addition to the above observation, a further observation is that in certain instances the initial guess **C** matrix has an opposite sign to what is normally expected. Under the Hartree-Fock formalism, this does not alter the results. It may be recalled that the Hartree-Fock energy is computed exclusively using the density matrices. The computation of the density matrix removes the information regarding the sign of the coefficient matrix. However, in the modified ENMO method, the computation of energy is strongly dependent on the sign of the **C** matrix. A negative coefficient matrix yields a valid eigenvector to the Hamiltonian. Hence, the state obtained by negating the **C** matrix for any one box yields a mathematically acceptable solution, though this may lead to unphysical solutions (energetically) in many situations. Therefore, there are twice as many "equivalent" solutions as there are particle types in a system, and many of these would lead to spurious results. Unfortunately, a method has not been found to correct for the sign of the coefficient matrix. The anomaly can be easily identified in atomic systems, but is not easy to identify in larger systems.

5.3: Optimisation of Exponent Scaling Factor

Unlike for the pseudo-atom method, the basis space for the nuclei, describing the extent of delocalisation, should necessarily be reduced in geometric extent relative to that of the electrons. This can be rationalised based on the knowledge that the de Broglie wavelength of a particle is inversely related to its mass. The de Broglie wavelength in a sense characterises the extent of uncertainty in the position of the particle, and hence its delocalisation about a mean position. Since nuclei are in general ~2000 times more

massive than electrons, it is reasonable to assume that the delocalisation of a nucleus be ~2000 times smaller than that of an electron.

In modern computational chemical techniques, the delocalisation of the electron is approximated by means of a set of basis functions (typically Gaussian in behaviour but not necessarily so), referred to as a basis set. The basis functions provide a means to approximate the extent of delocalisation of the electrons in a molecule. As most basis functions are of the form $\chi = Y_{l,m} e^{-\alpha r^2}$, the radial delocalisation is completely concentrated in the exponential term. Hence, it is adequate to scale the exponential term to achieve the requisite behaviour for the nuclei. This cannot be attained by scaling the function by a scalar multiplicative factor, as the normalisation procedure would nullify its effects. Hence, it is necessary to modify the radial dependence by modifying the exponential part of the term. This is achieved by scaling the exponent by a factor of $\left(\frac{m}{m_e}\right)^{1/x}$, the value of x left to be determined. The ratio represents the mass of the nucleus in atomic units, as it can be recalled that the mass of an electron in atomic units is unity.

It can be seen that as the value of x is varied, the extent of scaling is strongly affected. As the value of x is reduced, the nucleus becomes more localised, and an increasing value of x leads to an increasingly delocalised nuclear state. At the extreme limits, as x tends to zero, the nuclei are completely localised. This is the Born-Oppenheimer limit and the energy computed at this level is the electronic energy of the

system. As the nuclei are completely localised in this situation, there is very little overlap between the nuclear wavefunctions. This leads to the inter-nuclear repulsion terms being ignored in the 00 energy term, and the classical repulsion needs to be added in *post hoc*, as in traditional calculations. The inter-nuclear repulsion is however recovered by the inclusion of the interchange energy terms. At the other extreme, as $x \rightarrow \infty$ the nuclear scaling tends to unity and hence the nuclear basis functions approach the radial distributions of the electronic basis. Thus, x provides a sliding measure of the extent of delocalisation of the nuclei. At one extreme, the nuclei are indistinguishable in character from electrons; and at the other extreme, the Born-Oppenheimer (classical) limit is attained.

The value of x, though not known directly can be inferred from other sources. It may be recalled that based on the equipartition of kinetic energy, the total wavefunction was expanded in terms of $\left(\frac{m}{m_e}\right)^{1/4}$. [1,2] This yields a suggested value of $x = 4$. Bochevarov *et al.* [67] implemented the ENMO method in which a value of unity is employed for x. This may be due to expedience as no satisfactory explanation is proffered as to why this should be the case. Interestingly, Tachikawa and others [68] obtained a value of $x = 1.2$ for their basis set, when recalculated from the published exponents. In another work, Tachikawa and Osamura obtain values of x between 2.1 and 3.5. [78] A strict comparison is complicated by the fact that the basis functions were optimised in the molecule and not for the free atom. Hence, the reported basis functions vary by the isotopomer, and not the isotope. Though the Tachikawa approach is valuable,

it does not provide a general method to determine the scaling factors. There is also no information as to what the physically expected scaling factor must be, so a completely general means of generating scaling factors is required in order to be of widespread applicability. However, the similarity to the values predicted by Born and Oppenheimer lends credence to the view that the optimised value is dominated by the physically predicted equipartition principle.

The equipartition principle states that the energy contribution of each of the degrees of freedom in a system should be of the same order of magnitude.[79] Depending on the form of the specific potential, the various contributions differ by a simple multiplicative factor.[79] Hence, as a first approximation to the expected scaling factor, one can determine the scaling factor that would yield a nuclear kinetic energy similar in magnitude to the electronic kinetic energy. For simplicity's sake, one can consider a single electronic basis function χ and the scaled nuclear analogue χ'. If one were to consider a Gaussian shape for the basis function $\chi = e^{-\alpha r^2}$, then the nuclear function is $\chi' = e^{-\alpha' r^2}$ where $\alpha' = \left(q^{1/x}\right)\alpha$. One need not consider the angular contribution, as the angular contribution cancels out ($\int Y_{l_1,m_1} Y_{l_2,m_2} d\tau = \delta_{l_1,l_2}\delta_{m_1,m_2}$). For a Gaussian function, it can be shown that $\chi\frac{d^2}{dr^2}\chi = \left(4\alpha^2 r^2 - 2\alpha\right)\chi^2$. Integrating, $\int_0^\infty \chi\frac{d^2}{dr^2}\chi dr = -\frac{1}{2}\sqrt{2\alpha\pi}$. The kinetic energy for a single electron in a single basis function (in atomic units) is given by $T = -\frac{1}{2}\int_0^\infty \chi\frac{d^2}{dr^2}\chi dr$. Similarly, the kinetic energy for a nucleus is

$T' = -\frac{1}{2q}\int_0^\infty \chi' \frac{d^2}{dr^2}\chi' dr$. Hence the results $T = \frac{1}{4}\sqrt{2\alpha\pi}$ and $T' = \frac{1}{4q}\sqrt{2q^{1/x}\alpha\pi}$ are obtained. The ratio of the two yields $T'/T = q^{(1-2x)/2x}$. If the two kinetic energy contributions are required to be of the same order of magnitude, this can only be satisfied if x is in the neighbourhood of $1/2$. Since a highly simplified case is presented here, it is likely that the actual value obtained may be significantly different from that predicted here. It is interesting that an analogous treatment for Slater functions yields an optimal (exact) value of unity for x.

As a part of developing the extended ENMO method, a method that is intended for general use must also prescribe a general method for scaling the basis functions. In other words, one must know the proper scaling factor *a priori* when performing a computation, and it should not be system-specific. The possibility of system-specific scaling can be nullified by evaluating the optimal scaling coefficient on atomic systems. The value obtained can then be utilised in molecular (or larger) computations. In this regard, the basis functions for a series of atoms are scaled by varying factors ranging from $x = 1$ to $x = 4$. The optimal value is that which minimises the energy of the atom. It is expected that the optimal value lies in the above-prescribed range and that it is common to all atoms.

The value of x was optimised by plotting the energy as a function of x for the naturally occurring isotopes of the elements hydrogen through fluorine. The basis sets used in this study are STO-3G, DZP [80], TZ2P [81], cc-pVTZ, and aug-cc-pVTZ. The basis

sets that were employed were so chosen as they encompass a range from the minimal basis to an extended basis, thus facilitating an understanding of the optimal value of x. Due to the computational expense involved, aug-cc-pVTZ could only be employed up to the isotopes of carbon and cc-pVTZ could be applied only as far as the isotopes of nitrogen. The smaller bases were applied to all the atoms in this study.

There were two approaches involved in the optimisation of x. The profile of the 00 term energy (zero-order correction) and the profile of the full ENMO energies were plotted as a function of x for each of the basis sets studied. All atoms have been presented on the same graph for each basis set and the energies have been re-zeroed such that the lowest computed energy is zero. This enables one to see the trends in all the atoms without having to traverse wide ranges of absolute energies. The energies of the 00 term are convergent with respect to increasing x and since this behaviour is duplicated for all the basis sets studied, the results for STO-3G are presented in Figure 5.2. It is to be noted that the larger (heavier) atoms tend to have smaller deviations and less trouble reaching the optimised energy. In most cases, atoms beyond carbon are converged to within a μh when $x > 2$.

Figure 5.2: Convergence of the zero-order Born-Oppenheimer correction for Period I and II atoms computed using the STO-3G basis.

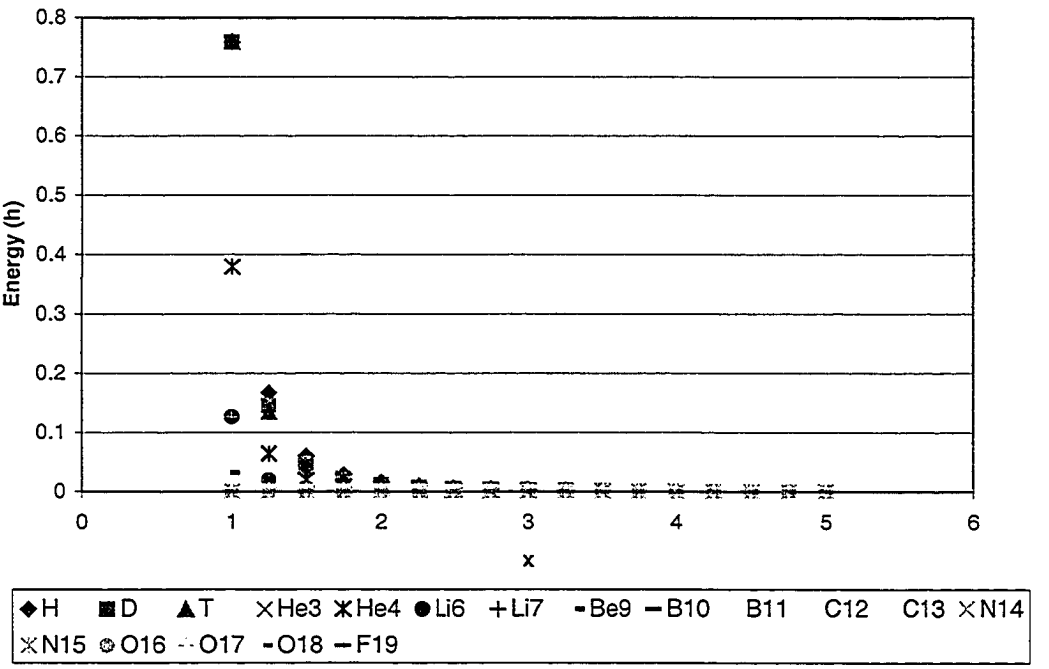

The energy of the 00 term is strongly dependent on the value of x when x is very small. The energy is practically converged (to within a mh) for all atoms when $x \geq 4$ for STO-3G. As the basis set is increased in size, the level at which convergence is attained shifts leftward as seen in Table 5.1 below.

Table 5.1: Convergence level of scaling factor for exponent as a function of basis set.

Basis Set	STO-3G	DZP	TZ2P	cc-pVTZ	aug-cc-pVTZ
x	4	3.25	2.75	2.75	2

Similarly, the full energy was plotted as a function of x for the various atoms. It is found that the value of x corresponding to the minimum atomic energy is element and basis set dependent. Interestingly, the optimal value of x seems to be independent of isotope. The optimal values are tabulated below in Table 5.2.

Table 5.2: Optimal value of scaling factor as a function of element and basis set.

Element	STO-3G	DZP	TZ2P	cc-pVTZ	aug-cc-pVTZ
H	1.75	4.5	4.25	3.5	3
He	> 5	N/A	N/A	4.75	4.25
Li	> 5	4.25	N/A	3.25	N/A
Be	3	2.25	N/A	2.25	N/A
B	4.25	3	2.25	2.5	2.25
C	> 5	2.75	2.25	2.25	2.25
N	4.5	1.75	2.25	2.25	N/P
O	3	2.5	> 5	N/P	N/P
F	3.75	2.25	N/P	N/P	N/P

N/A: basis set not defined for atom
N/P: calculation not performed

From the above table it can be seen that there does not seem to be any discernible trend in the optimal scaling factors for the various basis sets as a function of atom. This suggests that atom-specific nuclear basis sets may need to be constructed.

5.4: Isotopologues of the Hydrogen Molecule

As an illustration of the modified ENMO method, the 'PES's of two isotopologues of the hydrogen molecule are presented. Isotopologues are defined to be molecules that differ from each other in only their isotopic constitution.[82] In contrast, isotopomers contain the same number of different types of isotopes, but differ in their positions.[82] As the concept of a PES strictly cannot be invoked in a non-Born-Oppenheimer method, it would be preferable to present mean geometries of the species studied. This would be possible if not for the fact that the problem of wavefunction instability needs to be addressed. Unless the molecular wavefunction is considered to be converged, one cannot compute the properties of the system with confidence. A true comparison can be carried out once this problematic situation is corrected.

The positions on the 'PES' in an ENMO calculation are the positions at which the basis functions are centred. This need not correspond to the mean position of the nuclei. Since the major contributor to the position of the nucleus tends to be the contracted function corresponding to the 1*s* (scaled) atomic function, it is a reasonable approximation that the nuclear position is near the centre of the basis functions. Due to the instability in the wavefunction, it is currently not possible to present a high quality PES for the full ENMO energy. The major features can, however be explained by means of the 00 term. The PES were computed for three isotopomers of hydrogen (H_2, HT, and T_2) using the TZ2P and cc-pVTZ basis sets with appropriate scaling factors taken from Table 5.2 and are presented in Figures 5.3 and 5.4 respectively.

Figure 5.3: PES of isotopologues of hydrogen computed using the TZ2P basis set.

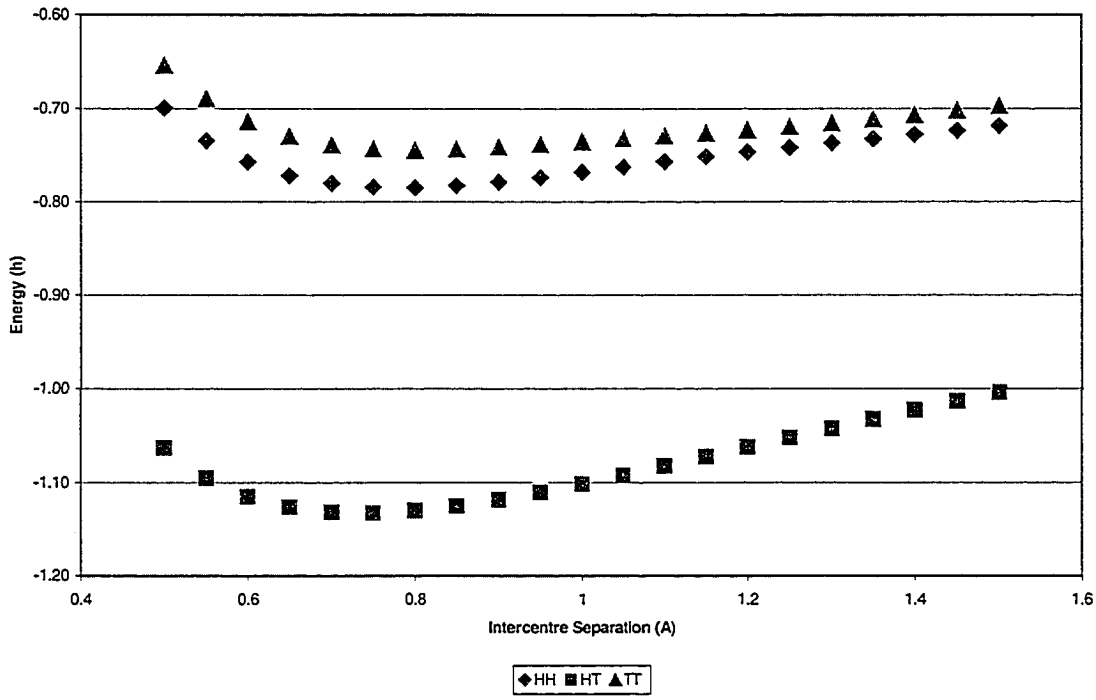

Figure 5.4: PES of isotopologues of hydrogen computed using the cc-pVTZ basis set.

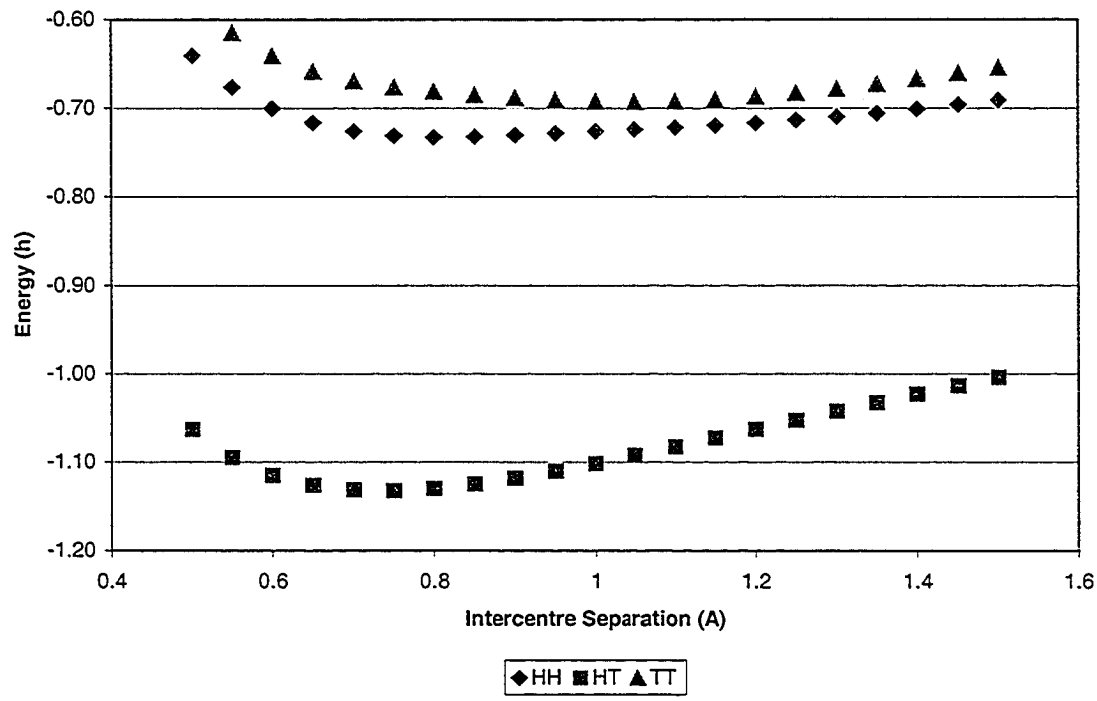

It can be seen from the above that the PES for the three isotopologues that there is a difference in the minima for the three curves, implying that the mean molecular geometry is a function of its isotopic composition. This result is expected, and contrary to the classical BO result.

5.5: Conclusions

An implementation of the modified ENMO method has been outlined and some salient features of the implementation have been outlined. The issues arising from the instability in the wavefunction and convergence difficulties have prevented a thorough examination of systems of interest. It is determined that nuclear basis sets must be optimised for the various atoms as per the atomic type. So doing would obviate the need for the scaling factor x. The computational expense of this method prevents it from being of general applicability. On the other hand, it has been possible to demonstrate that the effect of isotopic substitution can now be calculated using this method.

CHAPTER VI: SOLVATION OF SIMPLE IONS

6.1 Introduction

The process of solvation has been defined as "the sum of energetic and structural changes occurring in a system in the process of transferring gaseous ions (or atomic-molecular particles) into the liquid solvent, resulting in the formation of a homogeneous solution having a fixed chemical composition and structure".[83] The above definition fully encompasses the various physical changes that occur during the transfer of gaseous ions (from the point of view of the present work) into the solvated state. It is to be noted that the chemical effects of solvation are not considered as part of the primary process of solvation. Hence, under the above definition, electron donation from solvent to solute (or *vice versa*) is considered to be a secondary process (oxidation-reduction interaction) occurring after the solute has been solvated. Similar processes such as solvolysis, acid-base interactions, and the formation of aggregates have also been classified as secondary processes.[83] Hence, the mentioned definition of solvation only includes the physical rearrangement and reorientation of solvent molecules under the effect of the addition of solvent molecules (or ions) from the gas phase. It can thus be seen that there are differences between "real" and "ideal" solvation in most systems.

Ions in solution are understood to be solvated by means of short- and long-range interactions with the solvent molecules. The solvation region is divided into the *near* and *far* solvation zones. The *near* region refers to the molecules in the immediate

surroundings of the ion with a distinctly expressed geometrical arrangement, and the *far* region refers to those solvent molecules that solvate the ion while being beyond the range of the *near* zone.[83,84] The *near* zone may be understood to comprise the first and second solvation layers (shells). The *far* zone is not to be confused with the bulk as its structure is distorted with respect to the structure of the (isolated) bulk solvent. The *far* zone, though removed in space, is still bound to the ion. However, there is a greater amount of flexibility in the orientations available to solvent molecules in this region, as opposed to those in the *near* zone, which are tightly bound in (nearly) fixed orientations. The *near* and *far* zones may also be equivalently referred to as *primary* and *secondary* solvation zones.[83] Due to the strict definition of solvation, there has also been a suggestion to include a delineation of solvation into physical and chemical solvation, [85] where physical solvation includes the physical changes associated with a solute entering solution and chemical solvation involves the chemical interactions between the two. This however does not seem to be a popular distinction. Most chemists are comfortable referring to solvation in terms of 'solvation shells', 'solvation spheres', or 'coordination spheres'.

It is undeniable that the most accurate means of modelling solvated ions would be to perform *ab initio* molecular dynamics simulations invoking periodic boundary conditions. However, in light of the fact that the *near* region is believed to be rigid, and that this method is prohibitively expensive for most systems, it is advisable to propose methods that can be solved easily. The approach taken here is to model the *near* region separately so that the *far* region may be modelled separately as necessary. One method for modelling the rigid *near* region that has been applied successfully is the Boltzmann

weighting of various minima. In extreme cases, the *near* region has been approximated by the lowest energy structure.[73] It can be seen that this tends to yield unphysical results if not used with caution. The uncertainty in the coordination numbers of ions in solution may stem from the varying mean 'ground' geometry, especially since the experimental determinations seem to disagree as the counter-ion and concentration are varied.[84]

Understandably, the majority of theoretical studies into the solvation of ions deal with the hydration of the same. This is largely due to the fact that ion chemistry is most likely to be observed in aqueous systems, and since water is easier to calculate than most solvents owing to its smaller size. As one would expect, the theoretical studies conducted so far concentrate mainly on the solvation of Group I and II cations.[86-91] This is in addition to the studies dealing with the structures of water clusters of various sizes, aiming to understand the transition from small clusters to the bulk.[92,93] Water clusters also act as starting points for the understanding of the extended solvation environment around an ion. Solvated ion clusters, on the other hand, adequately approximate the local environments.

A good understanding of the first solvation shell of Group I and II metal cations is required to understand the coordination processes in solvation and biological processes. However, at present, only limited experimental data are available, for example the hydration of Group I metal cations, and their interaction with methanol.[94] The thermochemistry and geometries of metal cations with ammonia, formaldehyde, and

formamide are less well characterised. Theoretical methods afford an alternate method to obtaining information on these systems.

6.2 Calibration of Computational Scheme for Cation-Solvent Clusters

6.2.1 Goals

Gas-phase ion-solvent clusters are regarded as model systems for studying ions in solution.[95] A number of investigations, both experimental [96-99] and theoretical, [86-91,93,100] have explored the solvation of small ions and molecules in the gas phase and effects of the solvent on their chemistry. Previous theoretical studies on ion-solvent clusters include studies of water and ammonia with the Group I and Group II cations. Bauschlicher and co-workers [86] have studied the hydration of Na^+ with up to four water molecules and the solvation of positive and di-positive ions of magnesium, calcium and strontium in clusters containing up to three water or ammonia molecules.[87] Small ion-solvent clusters involving the heavier cation members of Groups I, II, and III in formal noble-gas configurations have been studied using quasi-relativistic pseudo-potentials by Kaupp and Schleyer.[101] The geometries were calculated at the Hartree-Fock level with single-point MP2 and MP4 energies computed thereafter. In a series of articles, Glendening and Feller explore the interactions of water clusters containing alkali and alkaline earth cations.[88-90,100]

A recent benchmarking study was conducted by Corral *et al.* [102] on the binding between a Ca^{2+} ion and an ammonia or formaldehyde molecule. Methods compared include a pair of density functional methods, CCSD(T), and the composite G3(CC), [103,104]

W1C, and W2C methods. [105,106] Zero-point vibrational energies and counterpoise correction for the BSSE were included in the binding energy calculations. B3LYP with a reasonably large basis set was found to provide good geometries, and to yield binding energies within 2 kcal mol^{-1} of the W2C results for both ammonia and formaldehyde complexes.

The most practical method to determine the properties of bulk-solvated ions with high accuracy is to select a computationally feasible method that can be extended to larger clusters but without sacrificing chemical accuracy. To this end, this study aims to determine the optimum DFT-based computational scheme for the calculation of large cation-solvent clusters such that the properties obtained are reliable. Properties are considered reliable herein if they contain negligible basis set superposition error and approach experimental accuracy, or appear converged based on comparison with other standard theoretical methods if experiment is unavailable. The solvents ammonia, formaldehyde, and water are used as model systems to simulate the bonding environments commonly encountered in biological systems. Additionally, these model systems are small enough that high-level coupled-cluster calculations are feasible. In order to perform a detailed calibration study of the methods, complexes of the Group I and II cations with single solvent molecules are considered. This will then enable one to extend the study of ion-solvent clusters by means of the methodology deemed most appropriate.

6.2.2 Computational Details

All calculations were performed using the Gaussian 98 suite of programs.[107] The B3LYP functional [108] was employed for DFT calculations. Additional geometry optimisations and frequencies were calculated using the G2 method [109-112] and CCSD(T)/6-311++G(3df,3pd). Counterpoise corrections [113,114] to estimate the basis set superposition error were determined for all levels of theory and are included in all energies reported herein unless otherwise stated. Structures were optimised with a series of Pople basis sets. Basis set convergence was studied by saturating the polarisation functions followed by diffuse functions. A frequency calculation was then performed at each optimised structure to determine the zero-point vibrational energy. For those systems where experimental data are available, thermal corrections were also computed at 298 K. The vibrational frequencies were calculated at the same level of theory as the optimisations.

Strictly from the point of view of electrostatics, one would expect the preferred geometries for the water and formaldehyde clusters to have C_{2v} symmetry and for the ammonia clusters to have C_{3v} symmetry. However, as other orientations are possible relaxed PES scans were performed to determine whether minima existed in these lower symmetry orientations. Angular scans were performed wherein the position of the cation was modified step-wise about the solvent molecule, which was allowed to relax in such a way as to compensate for the position of the cation. In the case of the ammonia molecule, it was necessary to fix the dihedral angles in the system, so as to prevent the ammonia molecule from 'following' the cation as its position was varied. It was observed in all

cases that the energy increased monotonically as the deformation was increased from the symmetric structures. Hence, only the (intuitive) high-symmetry orientations are true PES minima for clusters containing a metal cation and one solvent molecule of water, formaldehyde, or ammonia. These are the only structures included in this study.

6.2.3 Geometry Convergence

One of the goals of this study is to obtain the correct geometries of the metal ion-ligand clusters. It would be advantageous if one could find the lowest level at which the correct geometry can be obtained. Towards this end, the convergence of the cluster geometries with increasing basis set was studied. It was found that the only significant change in geometry with increasing basis set was in the M-O distance when the ligand is either water or formaldehyde, and in the M-N distance for ammonia. Figures 6.1 – 6.3 compare the distance between the metal centre and the binding atom on each ligand (M-L distance) to that obtained at the B3LYP/6-311++G(3df,3pd) level, the largest basis set in this study. The optimised geometries for each of the complexes at the B3LYP/6-311++G(3df,3pd) level are presented in tables 6.1 – 6.3.

Figure 6.1: Deviation in metal-oxygen distance of cation-water C_{2v} complex from the geometry calculated at the B3LYP/6-311++G(3df,3pd) level.

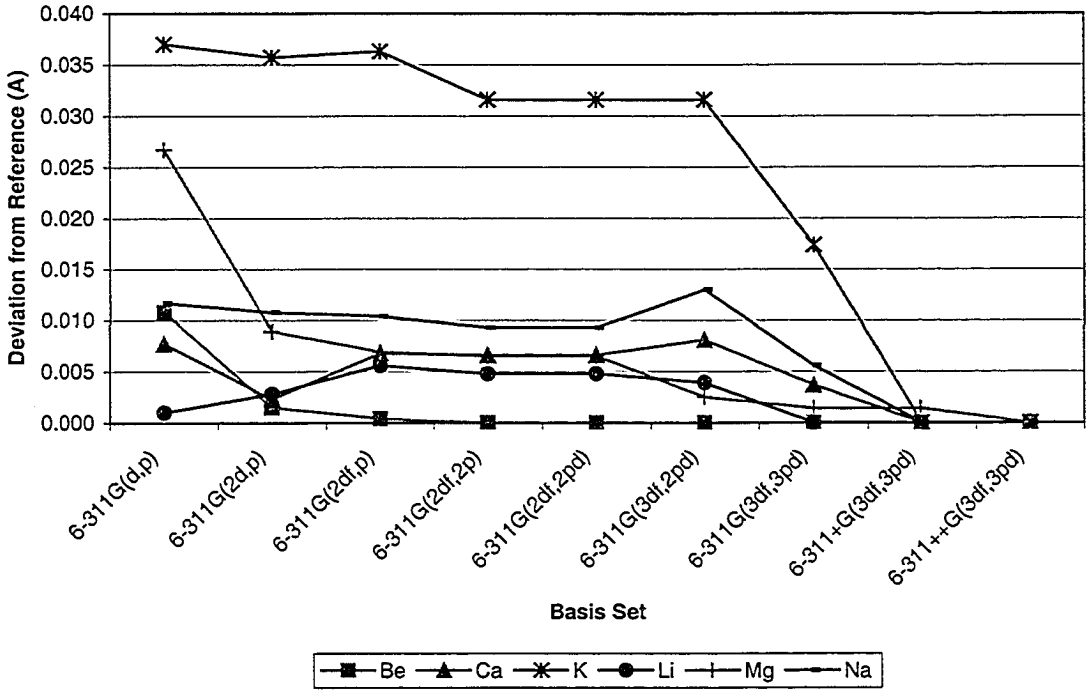

Table 6.1: Optimised geometries for metal cation-water C_{2v} clusters at the B3LYP/6-311++G(3df,3pd) level.

Cation	M-O Distance (Å)	O-H Distance (Å)	H-O-H Angle (°)
Li^+	1.8268	0.9657	105.69
Na^+	2.2126	0.9643	105.06
K^+	2.6184	0.9639	104.57
Be^{++}	1.4831	0.9936	107.85
Mg^{++}	1.9133	0.9780	105.74
Ca^{++}	2.2241	0.9747	104.47

Figure 6.2: Deviation in metal-oxygen distance of the cation-formaldehyde C_{2v} complex from the geometry calculated at the B3LYP/6-311++G(3df,3pd) level.

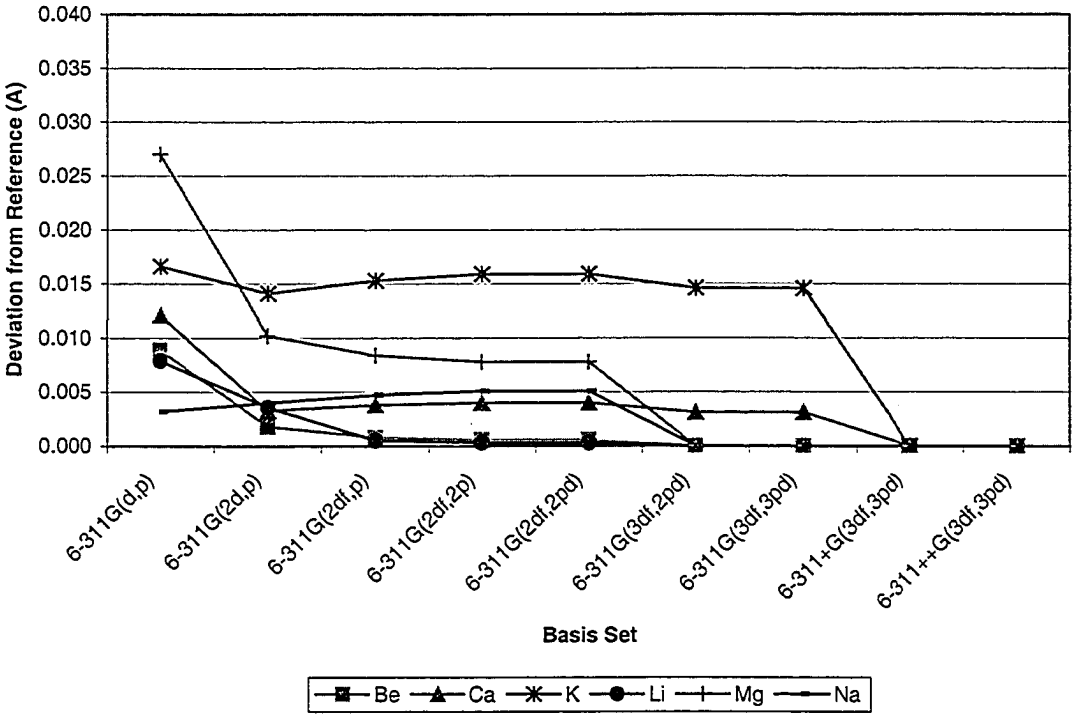

Table 6.2: Optimised geometries for metal cation-formaldehyde C_{3v} clusters at the B3LYP/6-311++G(3df,3pd) level.

Cation	M-O Distance (Å)	O-C Distance (Å)	C-H Distance (Å)	H-C-H Angle (°)
Li^+	1.7795	1.2146	1.0963	118.45
Na^+	2.1615	1.2113	1.0979	152.14
K^+	2.5597	1.2098	1.0990	117.44
Be^{++}	1.4154	1.2587	1.0962	122.71
Mg^{++}	1.8409	1.2383	1.0942	120.47
Ca^{++}	2.1355	1.2332	1.0947	119.73

Figure 6.3: Deviation in metal-nitrogen distance of the cation-ammonia C_{3v} complex from the geometry calculated at the B3LYP/6-311++G(3df,3pd) level.

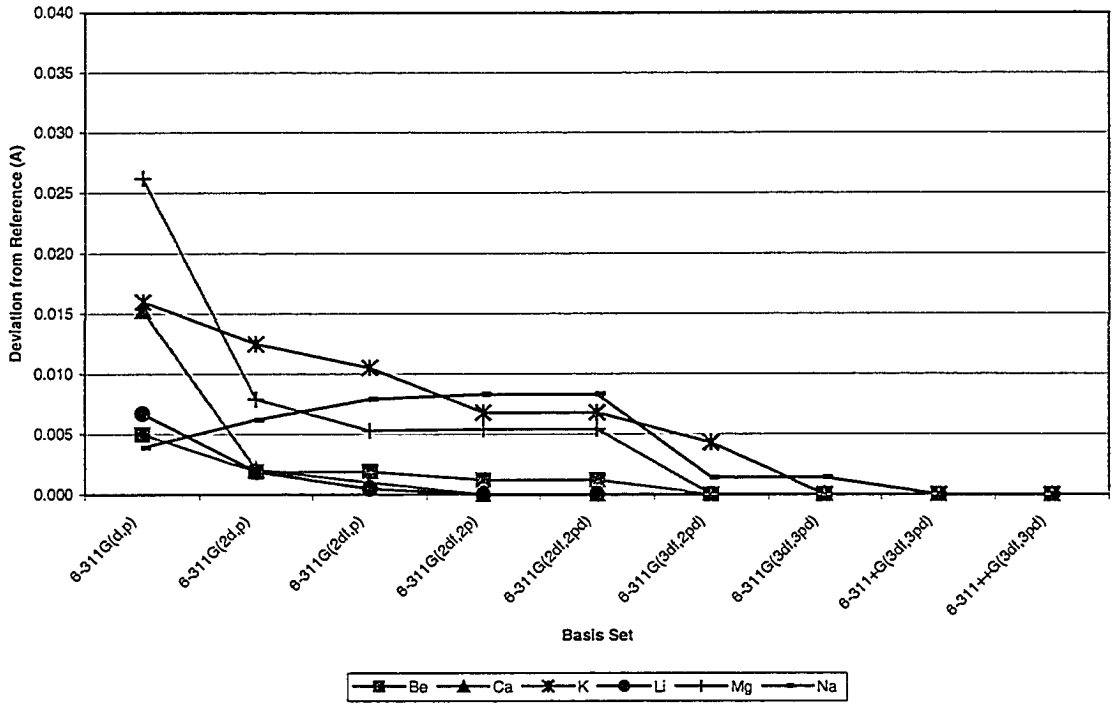

Table 6.3: Optimised geometries for metal cation-ammonia C_{3v} clusters at the B3LYP/6-311++G(3df,3pd) level.

Cation	M-N Distance (Å)	N-H Distance (Å)	M-N-H Angle (°)
Li^+	1.9617	1.0186	113.56
Na^+	2.3426	1.0176	113.42
K^+	2.7779	1.0170	113.51
Be^{++}	1.6072	1.0382	113.73
Mg^{++}	2.0424	1.0277	113.66
Ca^{++}	2.3693	1.0246	114.36

As expected, the M-L distance is seen to decrease as the basis set is expanded. The geometries for the Group II cation-ligand complexes appear to approach the basis set convergence limit faster (as a function of increasing basis set) than the corresponding Group I clusters. The geometries obtained at the B3LYP/6-311+G(3df,3pd) level are identical to the reference geometry in nearly all cases. Convergence may therefore be taken as essentially complete at the 6-311+G(3df,3pd) level. Loose convergence to within 0.01 Å occurs quickly for all species (except potassium), reaching a consensus at the 6-311G(2df,2p) level. Hence, the 6-311G(2df,2p) basis set is a good medium-level estimate of geometry and a logical starting point for higher quality calculations.

6.2.4 Binding Energy

Unfortunately, experimental binding energies are not available for a majority of the systems studied here. Hence, it was necessary to perform parallel calculations using established methods in order to test the veracity of our results. One such method is the G2 method of Pople and co-workers, [109-111] which is a well-established composite method capable of reproducing accurate binding energies for small molecules. As the G2 method was not calibrated on weakly bound complexes, it was decided to also perform additional calculations at the CCSD(T)/6-311++G(3df,3pd) level.

Dzidic and Kebarle [98] have determined the experimental enthalpies of association at 298 K and have shown that $\Delta_f H^{298} = \Delta_f E^{298}$ for the systems studied. The values compared in Figure 6.4 are the binding energies for the system with the appropriate thermal correction. Figure 6.4 shows that the B3LYP series tends towards under-binding

the complexes as the size of the basis set is increased. Taking BSSE into account, the best correspondence with experiment in the B3LYP series is observed when using the 6-311G(2df,2p) basis, where the deviation from experimental binding energies is lower than 5 kJ mol^{-1} (chemical accuracy). However, this is due most likely to a fortuitous cancellation of errors as there is still a significant BSSE at this level (see section 5.2.5), suggesting incomplete recovery of correlation energy. The basis set convergence limit is achieved at the 6-311+G(3df,3pd) level.

Figure 6.4: Deviation of B3LYP-calculated binding enthalpies from available experimental data.

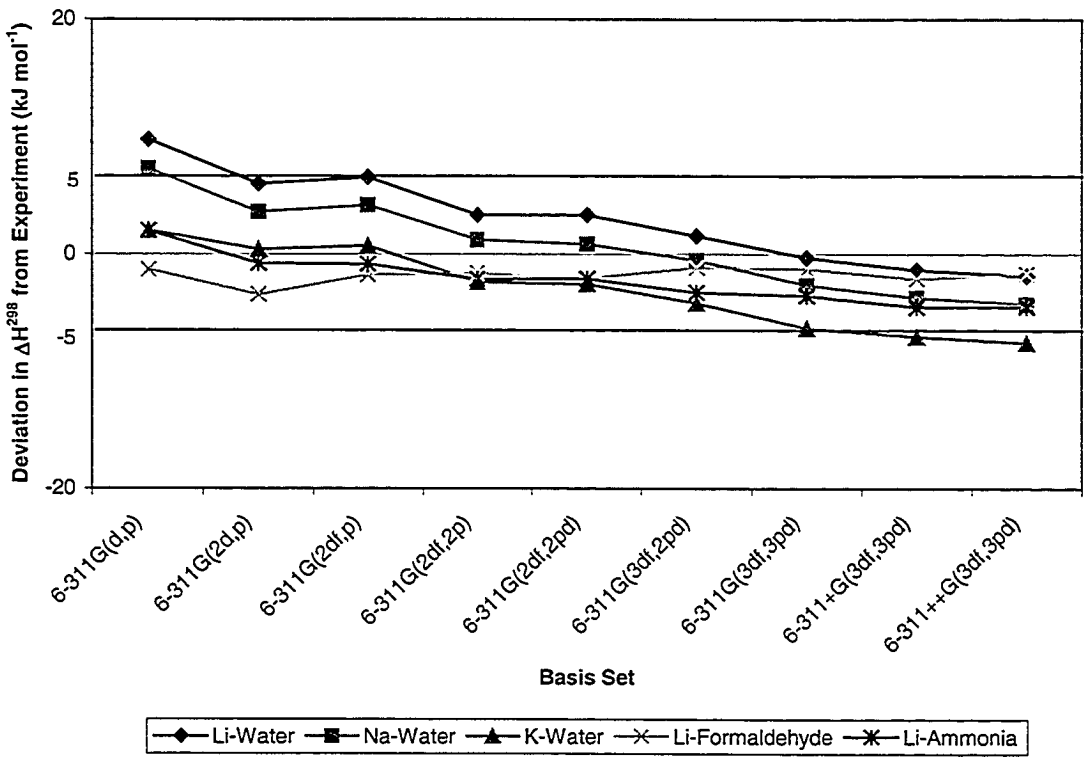

The B3LYP/6-311+G(3df,3pd) results compare well with the available experimental data in all cases and are qualitatively in agreement with other theoretical methods (see tables 6.4 – 6.6). The $[K-H_2O]^+$ system is the only system in which the deviation from the experimental binding energy exceeds 5 kJ mol^{-1} (7.1 kJ mol^{-1}). In particular, the lithium systems all agree with experiment to within 2 kJ mol^{-1}. There are previously reported W2C results [102] for $[Ca-H_2CO]^{2+}$ and $[Ca-NH_3]^{2+}$, with which the current results match well. However, further comment cannot be made, as those results were not thermally corrected. Rough comparison with the current 0 K results suggests a widening in the gap from the reported W2C results by ~2-3 kJ mol^{-1}.

Table 6.4: Absolute ΔH^{298} (kJ mol^{-1}) of metal-water (C_{2v}) clusters.

Cation	B3LYP/ 6-311+G(3df,3pd)	Experiment [a]	MP2 [b]	CCSD(T)	G2
Li^+	141.6	142.2 (est.)	139.8	130.8	145.5
Na^+	97.6	100.4	98.4	87.6	100.9
K^+	67.8	74.9	76.2	66.5	79.0
Be^{++}	617.4			582.1	601.3
Mg^{++}	343.8			317.6	333.8
Ca^{++}	238.1			221.4	232.8

[a] Dzidic and Kebarle, 1970

[b] Glendening and Feller, 1995, converted from kcal mol^{-1}

Table 6.5: Absolute ΔH^{298} (kJ mol^{-1}) of metal-formaldehyde (C_{2v}) clusters.

Cation	B3LYP/ 6-311+G(3df,3pd)	Experiment [a]	W2C [b]	CCSD(T)	G2
Li^+	150.4	151		136.8	143.9
Na^+	104.9			93.0	99.4
K^+	74.7			72.6	78.5
Be^{++}	704.9			659.5	670.9
Mg^{++}	392.7			361.5	370.6
Ca^{++}	283.3		274.7	259.9	264.8

[a] Krestov *et al.*, 1994

[b] Corral *et al.*, 2003, thermal corrections unavailable

Table 6.6: Absolute ΔH^{298} (kJ mol^{-1}) of metal-ammonia (C_{3v}) clusters.

Cation	B3LYP/ 6-311+G(3df,3pd)	Experiment [a]	W2C [b]	CCSD(T)	G2
Li^+	161.3	163		151.3	157.6
Na^+	112.3			101.3	107.3
K^+	74.4			73.5	78.2
Be^{++}	712.8			681.0	691.1
Mg^{++}	413.4			381.5	389.9
Ca^{++}	272.0		274.7	254.4	257.9

[a] Krestov *et al.*, 1994

[b] Corral *et al.*, 2003, thermal corrections unavailable

From the tables, it can also be seen that the G2 method provides a reasonable estimate (<10 kJ mol^{-1}) of the experimental binding enthalpies. The correspondence between the G2 method and experimental binding energy is better than 5 kJ mol^{-1} for the mono-hydrated systems, and better than 7 kJ mol^{-1} for the interaction of a lithium ion with one molecule of formaldehyde or ammonia. G2 is therefore a reasonable method for predicting the energies of weakly bound systems, giving results comparable to experiment in a computationally inexpensive fashion. However, the same cannot be said for the coupled-cluster method. The systems studied here are under-bound by the coupled-cluster method by ~10-20 kJ mol^{-1} relative to experiment. This suggests that the CCSD(T) calculations carried out are not basis set converged even at the 6-311++G(3df,3pd) level. Further computations were performed up to the cc-pCVTZ level for selected systems, at which point the energies and geometries had still not attained basis set convergence. Since convergence can only be attained at a higher level than that employed, this line of inquiry was discontinued, as it is unlikely that the resulting method would be practical for the study of larger clusters.

6.2.5 Basis Set Superposition Error (BSSE)

The BSSE was calculated for each of the complexes (and at each level of theory) by the counterpoise method.[113,114] Figure 6.5 shows the deviation of the calculated energies from experiment where the BSSE is not taken into account. As expected, the resultant curve shows significant over-binding at most levels. The BSSE correction for each of the systems is seen to remain fairly constant until the 6-311G(3df,3pd) level, at which point there is a sharp decrease. Addition of a diffuse function to the heavy atoms

further reduces the counterpoise energy considerably. At the 6-311+G(3df,3pd) level, the BSSE is observed to be almost uniformly and significantly smaller than 5 kJ mol^{-1} and there is seen to be little change when a set of diffuse functions is added to the hydrogen atoms. The BSSE at this level is negligible as compared to the limit of chemical accuracy (5 kJ mol^{-1}).[73] Hence, it is deduced that the structures obtained at the 6-311+G(3df,3pd) level and higher are counterpoise-correct structures.

Figure 6.5: Deviation of B3LYP-calculated binding enthalpies from available experimental data when BSSE is not included.

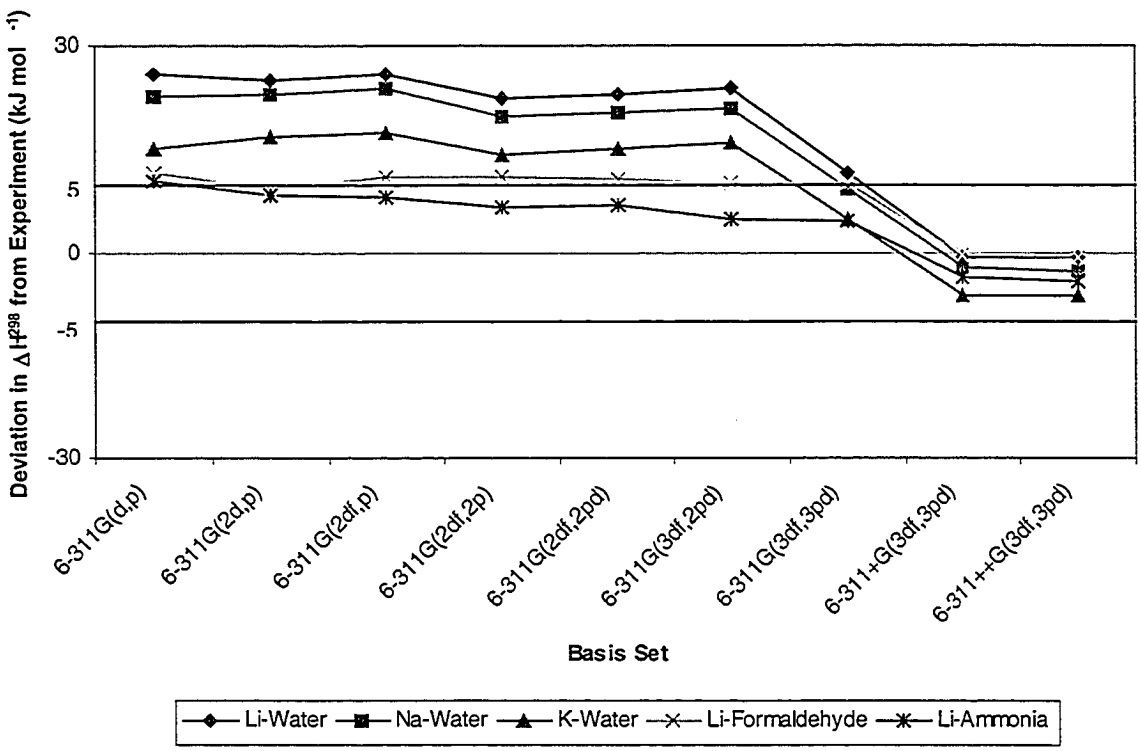

Comparing results with those reported in section 6.2.3, it is recalled that the geometry convergence was achieved at the 6-311+G(3df,3pd) level. As this is also the level at which the BSSE becomes negligible, one can be assured that the geometry

therefore recommended for the study of larger clusters, as counterpoise corrections become intractable with increasing cluster size.[115]

6.3: Calibration of Computational Scheme for Halide-Water Clusters

6.3.1: Goals and Computational Method

The requirements of electro-neutrality require an electrolyte to contain negative ions in direct proportion to the concentration of cations. It is hence equally important to be able to model the interactions of anions in solution. This enables one to generate a method by which electrolytic systems can be modelled. However, the experimental estimation of the binding of simple anions with solvent molecules is in very short supply.[84,116,117] The scarceness is only matched by the number of studies attempting to tackle the issue by theoretical methods.[118-120] However, it is seen that all previous attempts have approached the issue of cluster formation using very detailed methods and small basis sets. There also seems to be some inconsistency in the inclusion of the BSSE correction as when only 50 % BSSE is included.[119] In the absence of any strict calibration studies, it is not possible to know with any degree of confidence whether the choice of method is appropriate for the system being studied. The calibration of anion clusters was carried out similar to the method outlined above for the cation clusters (section 6.2.2) except that the calculations were performed using the Gaussian 03 suite of programs.[121]

6.3.2: Geometry Convergence

It was noticed that there is only one pair of equivalent minima on the PES for the halide ion-water system, corresponding to the in-plane C_s geometry. The four atoms in

obtained at the 6-311+G(3df,3pd) level is both basis-set converged and BSSE-corrected. This implies that one need not perform a counterpoise-corrected geometry optimisation to obtain the optimal geometry.

Computations of clusters containing multiple ligands are potentially problematic as the partitioning scheme to be used is not unique. Hence, it is undesirable to have a significant residual BSSE in the final energy.

6.2.6 Conclusions

The formation of mono-solvated complexes of Group I and II cations with water, formaldehyde, and ammonia was studied with the aim of developing a computational scheme to be employed with larger clusters. It has been shown that the B3LYP geometry convergence limit for the Pople series of basis sets is attained at 6-311+G(3df,3pd). This is also the level at which the BSSE becomes essentially insignificant. Hence, the geometries calculated at this level are BSSE-correct geometries. For most systems, a reasonable, though still BSSE-laden, starting geometry can be obtained at the 6-311G(2df,2p) level and the geometry can be further refined from that point. For binding energies, DFT agrees with available experiment and high-level W2C results to within 5 kJ mol^{-1}, which is comparable to G2's performance and superior to CCSD(T) at this basis set level. The best agreement with experiment is observed at the 6-311G(2df,2p) level when BSSE has been taken into account, and at the 6-311+G(3df,3pd) level when counterpoise calculations have become unnecessary. The use of the 6-311+G(3df,3pd) basis set is

the system are coplanar and the halide ion is off the axis of the water molecule. The C_{2v} structure is found to be a saddle point connecting the two minima. It can be trivially shown that the halide-water clusters are incompletely represented in the absence of diffuse functions on both the heavy atoms and hydrogen atoms. Hence, only those results including diffuse functions on hydrogen atoms as well as heavy atoms are included. Unlike the case of the cation-solvent clusters, the halide-water cluster geometries cannot be shown to depend predominantly on one parameter (distance or angle). Therefore, the root-mean-square-deviation in positions was compared in order to determine the level at which geometry convergence is achieved. As the geometries of the complexes are sensitive to the inclusion of counterpoise corrections, the reference geometry is taken to be the counterpoise-corrected geometry at the largest available correlation consistent basis set [122-124] for the elements (aug-cc-pV5Z) present in this study. The reference geometry for each complex is given in Table 6.7 below, and the overall convergence behaviour is portrayed in Figure 6.6.

Table 6.7: Counterpoise optimised geometries for halide ion-water complexes at B3LYP/aug-cc-pV5Z level.

	F^-	Cl^-	Br^-
O-X Distance (Å)	2.4506	3.1339	3.3407
H1-O Distance (Å)	0.9587	0.9594	0.9598
H2-O Distance (Å)	1.0599	0.9900	0.9835
H1-O-H2 Angle (°)	102.86	93.96	91.07
X-H2-O Angle (°)	178.30	172.19	169.44

Figure 6.6: Convergence of geometry for halide-water clusters as a function of basis set, at the B3LYP level.

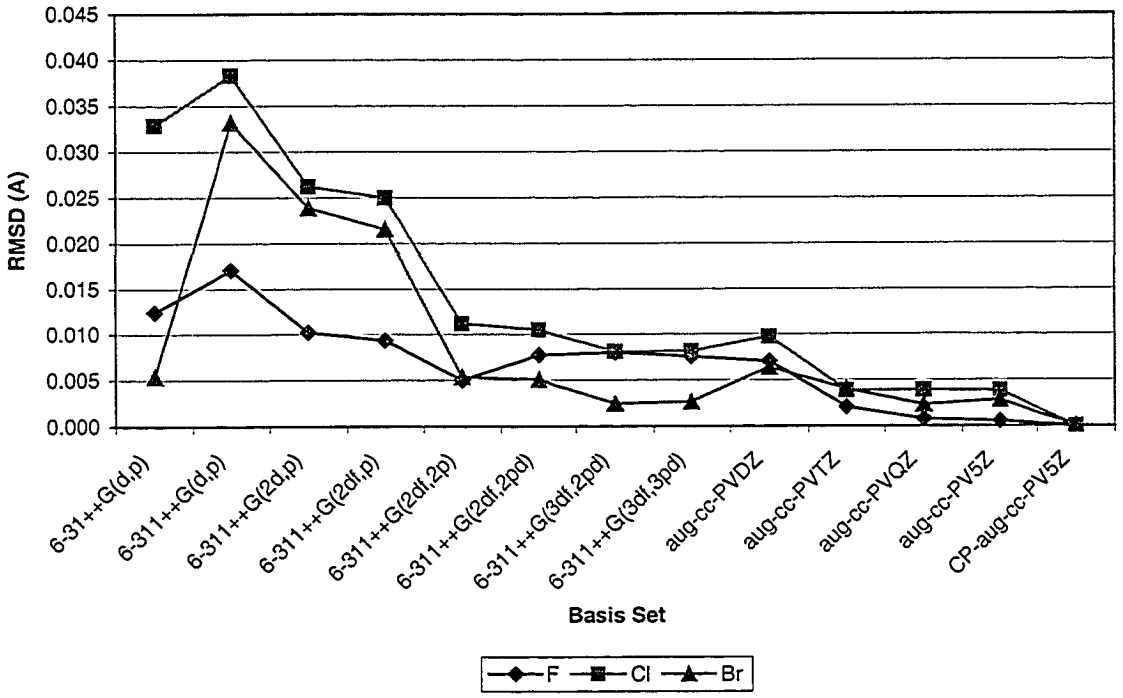

As can be seen from the above figure, the complex geometry is convergent with respect to basis set, with mean atomic convergence to within 5 mÅ attained for all three halide complexes only when augmented Dunning basis sets are used (from the augmented triple-zeta level onward). Convergence to within 10 mÅ can be attained at the 6-311++G(3df,2pd) level. Absolute convergence is only achieved at the reference level. This being the largest basis available to encompass the elements involved in this study, it can be safely assumed that this represents a nearly converged geometry. It is however very likely that the implementation of a more extended basis set may lead toward absolute convergence. Due to the lack of basis set convergence in geometry, there is a reduced

confidence in the nature of the results that may be obtained if this method were applied to the study of clusters involving multiple water molecules. Counterpoise corrected optimisations at other levels also show similar behaviour to the figure above, and hence there is little improvement from performing counterpoise corrected optimisations except when very high levels of accuracy are desired involving the use of very large basis sets.

6.3.3: Binding Energy and Basis Set Superposition Correction

Limited experimental data exist for the binding of halide ions with water molecules. The available data are due to Kebarle, [117] and Weis and co-workers.[116] These authors report binding enthalpies, while Kebarle also presents binding energies. It is observed that the BSSE-corrected binding energy computed at all levels is nearly identical when diffuse functions on hydrogen and heavy atoms are included, and that these values yield the best agreement with the available experimental data. The interaction is significantly under-bound when diffuse functions are not included in the calculation. Similar values to the above are obtained when diffuse functions are omitted for the hydrogen atoms. Hence, the inclusion of diffuse functions on the heavy atoms is very important to the energetics of the halide-water system. In fact, the inclusion of diffuse functions is the most important determining factor on the accuracy with which the energetics of the system can be estimated. The variations of the formation enthalpies with basis set for the systems are shown in Figure 6.7. All energies are zero-point and BSSE corrected at the geometry optimised at the same level of theory.

Figure 6.7: Variation of B3LYP binding enthalpy for halide ion-water complexes relative to experimental values as a function of basis set.

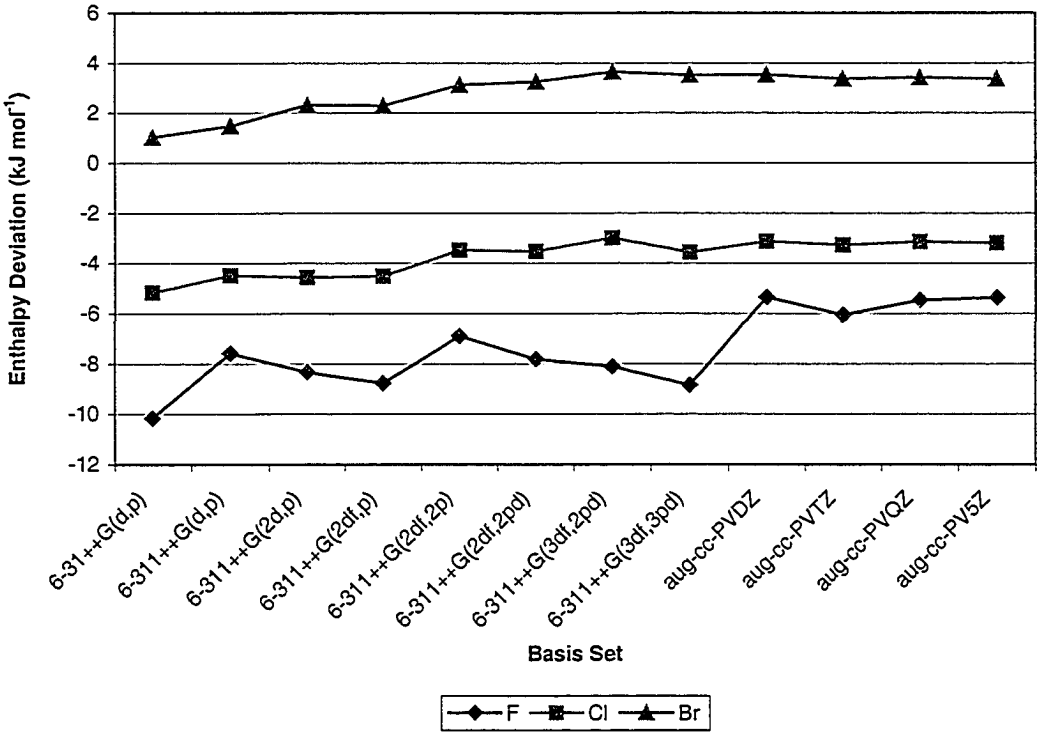

It can be seen from the above that the binding enthalpy migrates upward (less negative) as the basis set is increased. In the case of the fluoride and chloride ions, this represents an improvement in the reported binding enthalpy relative to experiment, whereas the bromide enthalpy migrates away from the experimentally reported value. However, it seems that increasing the basis set in all cases seems to stabilise the reactants more than the complex (when BSSE corrected) and this leads to the observed trend. A similar behaviour is observed in the case of the binding energy at 298 K, except that in this case the binding energy is significantly overestimated for the fluoride complex. The remaining two complexes show very little difference in behaviour between when the

binding energies and binding enthalpies are compared. The variation of the binding energy as a function of basis set is presented in Figure 6.8.

Figure 6.8: Variation of B3LYP binding energy for halide ion-water complexes as a function of basis set.

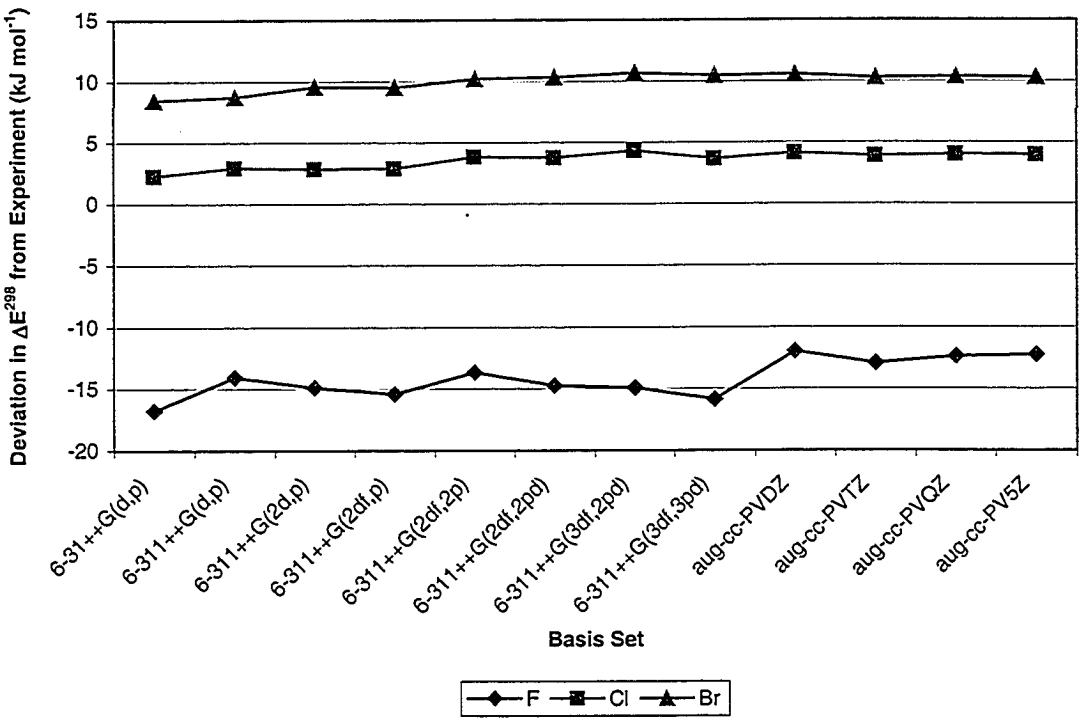

Similar results to those presented earlier in this section were obtained when the PBE functional [125] was employed. It can be seen from Figure 6.9 that the data produced using this method is similar to those obtained at the B3LYP level. The deviation in this case tends towards over-binding of the complex relative to the experimental determination, as compared to the B3LYP situation, wherein only the binding enthalpy of the fluoride complex was overestimated. Hence, it can be seen that the use of density functional methods is inadequate to the study of halide ion-water clusters. In order to

determine whether the deviant behaviour is a result of the incomplete recovery of correlation energy, reference calculations were carried out using higher-level correlated methods and composite reference methods, these results being reported in Figure 6.10.

Figure 6.9: Variation of PBE binding enthalpy for halide ion-water complexes as a function of basis set.

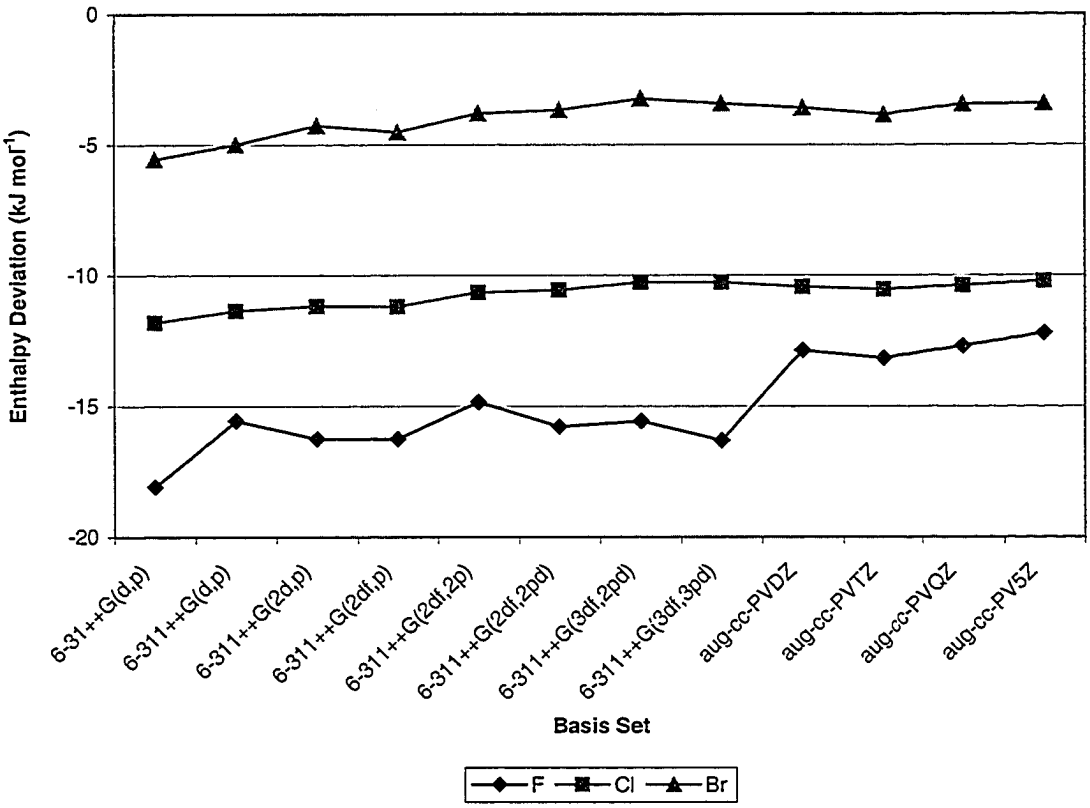

Figure 6.10: Variation of binding enthalpy for halide ion-water complexes as a function of method using the 6-311++G(3df,3pd) basis set, unless mentioned otherwise.

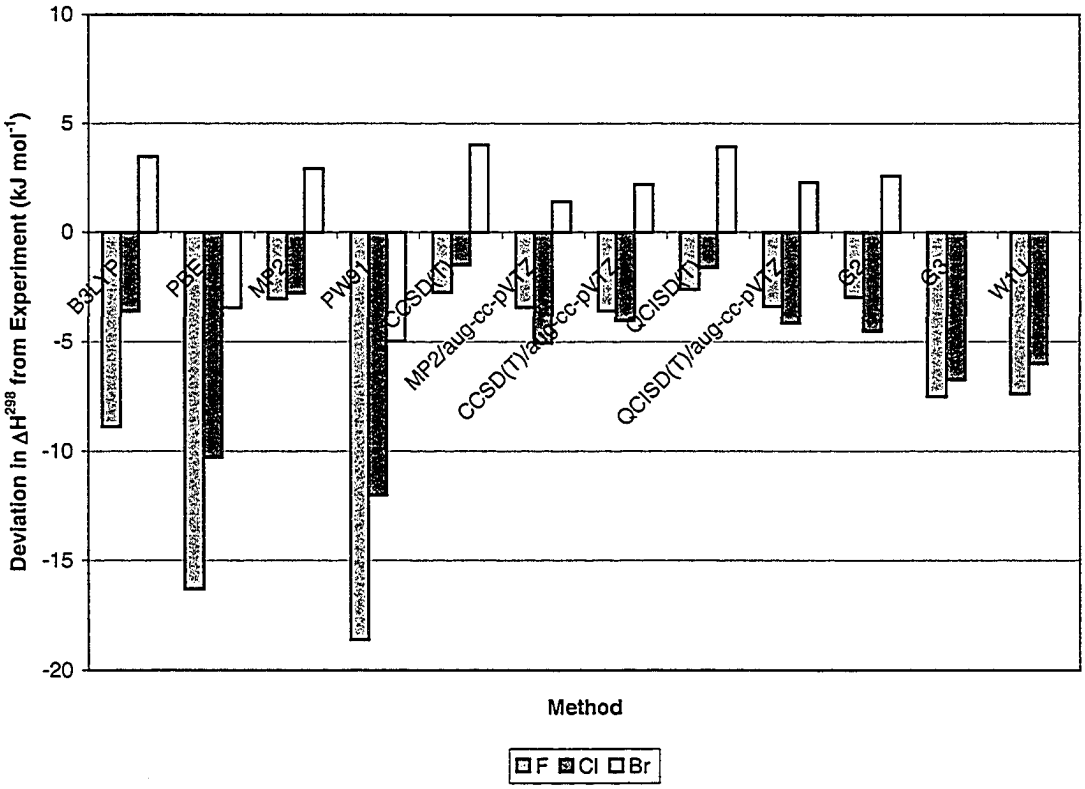

In the above figure, there are no data for the bromide ion complex under the G3 and W1U methods, as the basis sets required for these computations are not defined for the bromine atom. It can be seen that of the methods used, the density functional methods display the greatest deviation from experiment. Comparing the results of the post-Hartree-Fock methods computed at the 6-311++G(3df,3pd) and aug-cc-pVTZ bases, one can see that the deviations are shifted downwards at the larger basis set. This implies that the complex tends to be stabilised more than the reactants as the basis set is increased when used in conjunction with higher correlated methods. This is the opposite of the trend observed with density functional methods. It can be deduced therefore that density functional methods under-perform compared to post-Hartree-Fock methods for these

systems. The counterpoise corrected energies obtained from these higher-level methods display a good correspondence with experimentally available data, and suggest that these methods can be used in further studies. Unfortunately, these methods are computationally expensive (at the basis set levels required) making further studies prohibitive. This improvement comes at the expense of the confidence one can place in the calculations. The BSSE is found to be extremely large in all cases studied, especially when the post-Hartree-Fock methods are used with Pople basis sets. There is some improvement when these methods are used with Dunning sets, as noted in Figure 6.11.

Figure 6.11: Basis set superposition energy of halide ion-water complexes at different levels of theory, employing the 6-311++G(3df,3pd) basis set, unless noted otherwise.

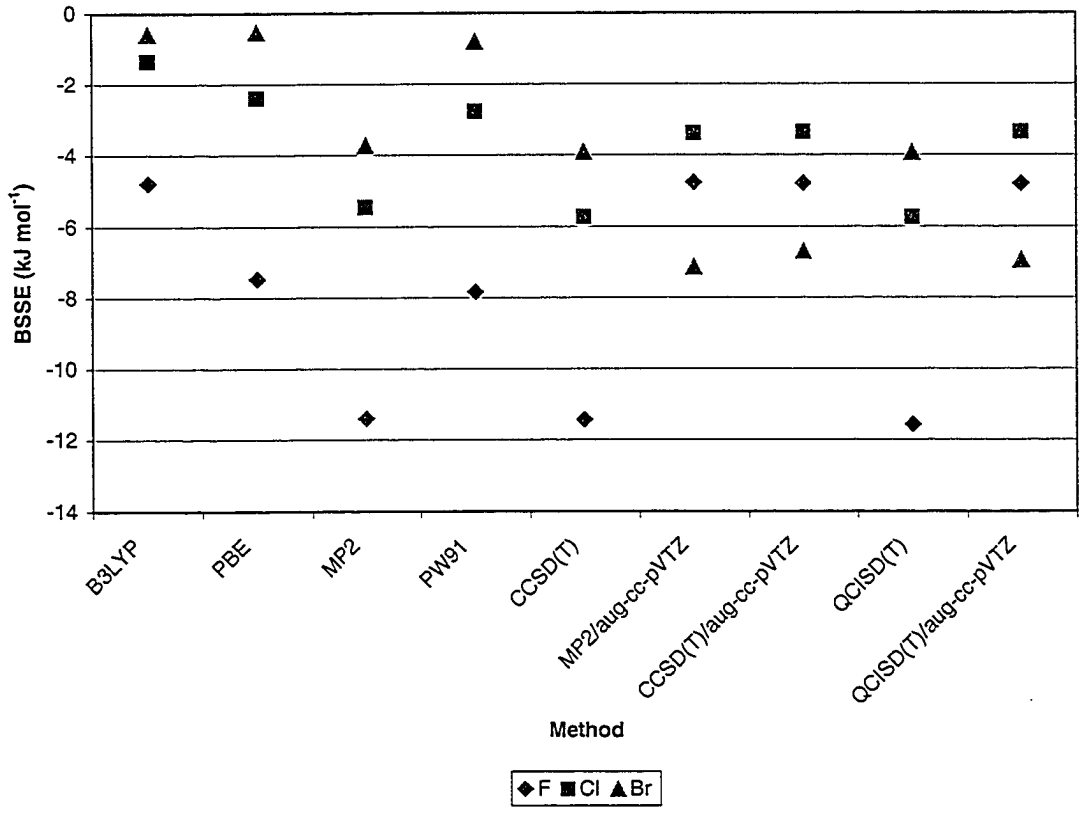

It is interesting that the BSSE in most cases exceeds the deviation observed and is in no case negligible within the Pople series of basis sets. It is also to be noted that the greatest improvement in the BSSE occurs in the case of the fluoride complex when the basis set is enlarged. However, this is accompanied by a marked worsening of the BSSE for the bromide complex. This seems to imply that improvement in the quality of the basis set does not necessarily lead to improvement in the description of the system. This suggests that it may be necessary to perform counterpoise-corrected optimisations for systems of this type, as the deformation of the cluster geometry due to BSSE appears to be significant. This is not a practical method for routine calculations, as analytic derivatives are not currently implemented for the methods beyond MP2.

The extent of improvement along the augmented Dunning series was studied by comparing results obtained using the B3LYP and MP2 methods; the former due to its superior results from among the density functional methods and the latter due to the resource constraints that would not permit the use of more extensive (and also expensive) methods. The zero point correction for the MP2/aug-cc-pV5Z geometry is calculated at the MP2/aug-cc-pVQZ level, as it was not possible to perform this computation. Figure 6.12 shows that the application of the MP2 method to the Dunning series leads to a progressive increase in the binding enthalpy with increasing basis set size. This is to be contrasted with Figure 6.13 wherein the BSSE for the same series is shown to decrease consistently. This reduction in the BSSE nearly completely accounts for the change in the binding energy (and enthalpy) of the complex. The absolute (0 K) binding energies

for the complexes are virtually unchanged when the BSSE is ignored. This is in contrast to the B3LYP situation, which appears to have achieved convergence and the changes in binding energy and BSSE are negligible with respect to the increase in basis set size.

Figure 6.12: Comparison between B3LYP and MP2 binding enthalpies relative to experiment as a function of augmented Dunning basis set.

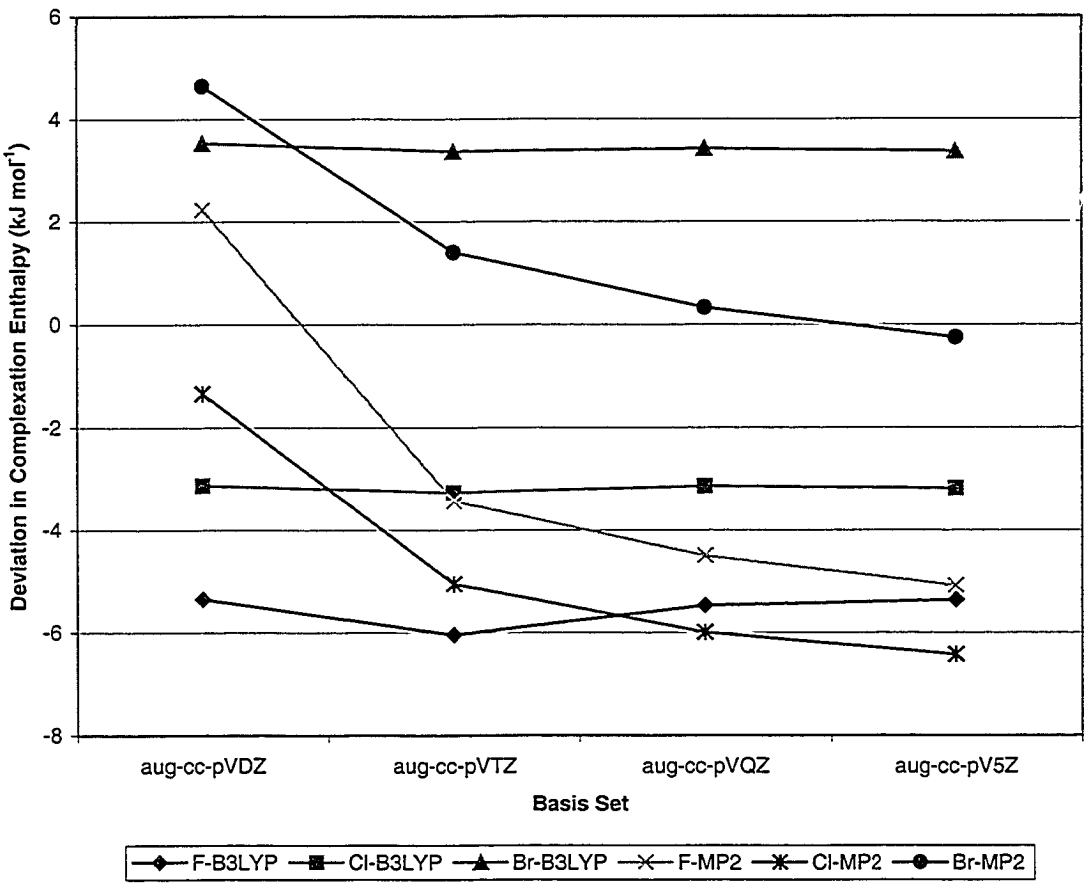

Figure 6.13: Variation BSSE corrections for B3LYP and MP2 methods with augmented Dunning basis sets for halide ion-water complexes.

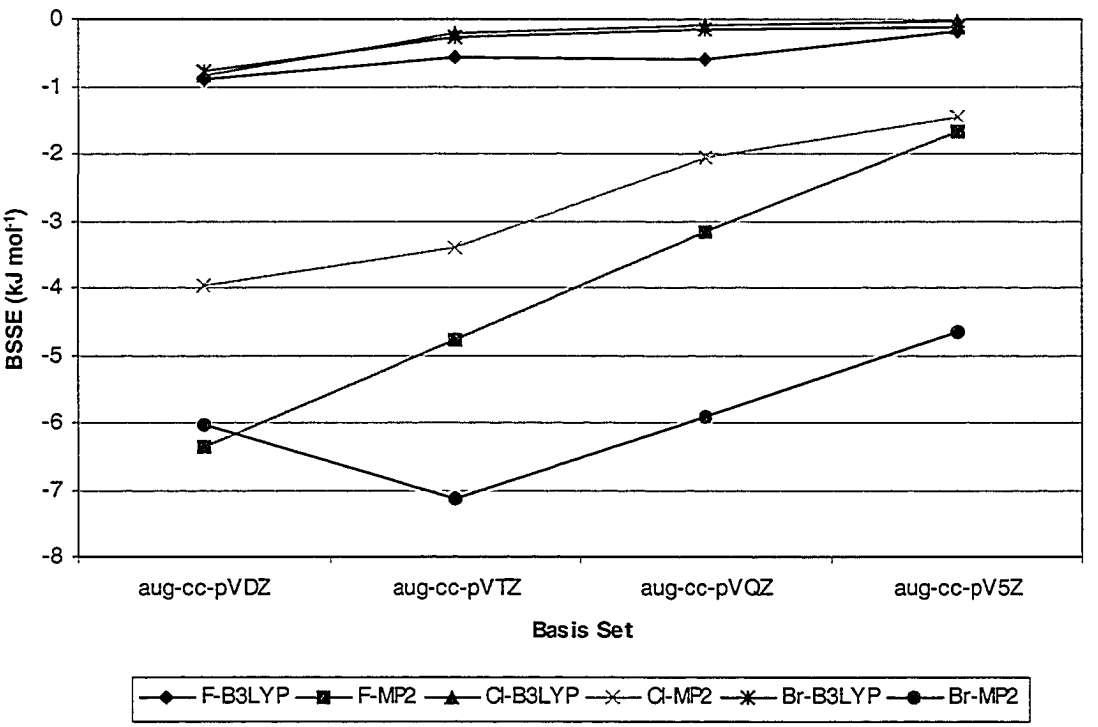

6.3.4: Conclusions

It is seen that the properties of halide ion-water clusters are slowly convergent with respect to basis set. The basis set converged complex geometry is not attained in either the DFT or MP2 series. It is also observed that the BSSE is non-vanishing even at the largest basis levels available, thus casting doubt on the results of any calculations on these systems. This especially true of water clusters containing a halide ion and multiple water molecules, as the BSSE cannot be estimated in a non-unique manner for a system containing more than two fragments (molecules). Since the BSSE in these systems is

comparable to the binding energy of the complex, the complexation energy can also not be reported with much confidence. The BSSE corrected complexation energies for all the systems studied are within chemical accuracy (5 kJ mol^{-1}) of the experimental values when the B3LYP functional is used. Other density functional methods yield slightly inferior complexation energies as compared to experiment.

The density functional methods are (expectedly) out-performed by post-Hartree-Fock methods with correlation consistent basis sets. These latter methods suffer from the large residual BSSE present even at the largest basis currently available for these systems. This implies the necessity for counterpoise-corrected geometry optimisations. This is not practical for a few reasons. There are currently no analytic gradients available for these methods and so the Hessian would have to be computed using the energy-points algorithm. This algorithm computes the energy at each 'point' on the potential energy surface. The Gaussian package currently does not perform counterpoise-corrected optimisations for methods that do not have analytic derivatives. However, this can be implemented easily, albeit at great computational expense as the counterpoise correction would have to be performed for every 'point' that is calculated on the PES. The curvature around each point is computed by either a five- or seven- point algorithm, so it can be seen how impractical such a method would be. In conclusion, it is possible to see that no method/basis combination currently exists that would enable the study of halide ion-water clusters with any degree of confidence. There arises confidence in a scheme when one can obtain accurate results with a good geometry and devoid of BSSE, which unfortunately is not possible as of yet.

CHAPTER VII: FUTURE DIRECTIONS

The results contained herein are but a humble contribution to the vast body of knowledge that lies unexplored. As such, it is highly presumptuous to believe that what has been achieved is anything more than a small step on the path to improving the understanding of the physico-chemical world. That the method developed and implemented in previous chapters is incomplete is known and readily acknowledged. Given this backdrop, this chapter deals with some of the possible directions toward improvement of the previously detailed method.

7.1 Magnetic and Spin Effects

A significantly important improvement would be the inclusion of magnetic effects, which are presently being ignored. Though the energetic effect is expected to be small, they are not non-existent and hence any complete treatment would require the inclusion of these effects. It is known that moving charges generate magnetic fields, and that most (except for a rare few) sub-molecular particles have intrinsic spin. It is therefore not inconceivable that there would be interactions between particle spin and the magnetic currents generated by particle motion within the molecule. The intrinsic spins of the particles interact with each other and with any external field. It has been shown that the interactions involving the spin are independent of the spatial parameters and hence the total Hamiltonian can be separated into spatial and spin contributions.[126,127] The spin Hamiltonian is given by

$$\hat{H}_{spin} = \hat{H}_{mag} + \hat{H}_Z + \hat{H}_{SO} + \hat{H}_{S-S}$$

The terms making up the spin Hamiltonian can be enumerated as being the magnetic interaction (with an external field), the Zeeman interaction, spin-orbit coupling, and the spin-spin coupling (relating to the NMR, ESR, and hyperfine interactions) terms respectively. The various contributions are given by

$$\hat{H}_{mag} = \sum_a \beta_a \mathbf{B} \cdot (\mathbf{r}(a) \times \mathbf{p}(a)) + \frac{Z_a^2 e^2}{8 m_a c^2} (\mathbf{B} \times \mathbf{r}(a))^2$$

$$\hat{H}_Z = \sum_a g_a \beta_a \mathbf{B} \cdot \mathbf{I}(a)$$

$$\hat{H}_{SO} = \sum_{a \neq b} g_a \beta_a \beta_b \left[\frac{|Z_b| \mathbf{I}(a) \cdot \mathbf{M}^b(a)}{r_{ab}^3} - \frac{2\mathbf{I}(a)\mathbf{M}^a(b) + \mathbf{I}(a)\mathbf{M}^b(a)}{r_{ab}^3} \right]$$

$$\hat{H}_{S-S} = \frac{1}{2} \sum_{a \neq b} \left[g_a \beta_a g_b \beta_b \left\{ \frac{(\mathbf{I}(a) \cdot \mathbf{r}(ab))(\mathbf{I}(b) \cdot \mathbf{r}(ab)) - r_{ab}^2 \mathbf{I}(a) \cdot \mathbf{I}(b)}{r_{ab}^5} \right\} + \frac{8\pi}{3} \delta(\mathbf{r}_{ab}) \mathbf{I}(a) \cdot \mathbf{I}(b) \right]$$

It is obvious that in a molecule in the absence of an external magnetic field $\mathbf{B}$, the magnetic and Zeeman interactions vanish. The spin-orbit contribution is seen to be dependent on the spin vectors $\mathbf{I}$ of the various particles a,b and their mutual field-corrected angular momentum ($\mathbf{M}^b(a) = \frac{1}{\hbar} \mathbf{r}(ba) \times \left\{ \mathbf{p}(a) + \frac{e}{c} \mathbf{A} \right\}$). It may be recalled that $\mathbf{A}$ is a general applied electromagnetic field and that $\nabla \times \mathbf{A} = \mathbf{B}$ and $\frac{\partial \mathbf{A}}{\partial t} = -\mathbf{E}$. [71] It is only in the spin-spin Hamiltonian that explicit interactions of the form $\mathbf{I}(a) \cdot \mathbf{I}(b)$ appear. The contact term in the spin coupling Hamiltonian is said to be vanishingly small and ignored in most applications.[126]

It is expected that implementation of the above operators into the modified ENMO method will enable a better representation of molecular systems. It is preferable to develop a method by which these interactions can be included during the SCF procedure. This should generate true spin-state dependent results.

7.2 Relativistic Corrections

For the sake of completeness, one would include the effects of special relativity as this is known to be significant in molecules containing high atomic number nuclei.[128] However, high atomic number nuclei tend to be even more massive, and it is expected that their deviation from the Born-Oppenheimer results will be minimal. It is also noteworthy that a complete relativistic treatment would also solve for the spin (and magnetic) properties simultaneously.[13,127] The use of relativistic Hamiltonian and wavefunctions would necessarily redefine the method proposed, as space and spin are no longer separable under relativistic quantum theory. One would also require using a four-vector representation for the wavefunctions, and the shapes of the operators would also need to be modified to include the extra dimension. As this is necessarily a subject that will have to be dealt with *de novo*, further improvement in this direction is not possible in this current work. In addition, a complete relativistic treatment would include all magnetic effects that may arise due to interactions between all pairs of particles bearing non-zero spin.

REFERENCES

(1) Born, M.; Oppenheimer, R. *Ann. Physik* **1927**, *84*, 457-84.

(2) Born, M.; Oppenheimer, R. In *Quantum Chemistry: Classic Scientific Papers*; Hettema, H., Ed.; World Scientific: Singapore, 2000; Vol. 8.

(3) Pople, J. A.; Beveridge, D. L. *Approximate Molecular Orbital Theory*; McGraw-Hill Book Company, 1970.

(4) Koch, W.; Holthausen, M. C. *A Chemist's Guide to Density Functional Theory*; 2 ed.; Wiley-VCH, 2001.

(5) Pilar, F. L. *Elementary Quantum Chemistry*; 2 ed.; McGraw-Hill Publishing Company: Highstown, NJ, 1990.

(6) Hartree, D. R. *Proc. Cambridge Phil. Soc.* **1928**, *24*, 89-110.

(7) Fock, V. *Z. Physik* **1930**, *61*, 126.

(8) Slater, J. C. *Phys. Rev.* **1930**, *35*, 210-11.

(9) Slater, J. C. *Phys. Rev.* **1929**, *34*, 1293-1322.

(10) Koopmans, T. *Physica* **1933**, *1*, 104-13.

(11) Roothaan, C. C. J. *Revs. Modern Phys.* **1951**, *23*, 69-89.

(12) Roothaan, C. C. J. *Revs. Modern Phys.* **1960**, *31*, 179-85.

(13) Jensen, F. *Introduction to Computational Chemistry*; John Wiley & Sons, 2001.

(14) Atkins, P. W.; Friedman, R. S. *Molecular Quantum Mechanics*; 3 ed.; Oxford University Press: Oxford, 1997.

(30) Wardlaw, D. M.; Marcus, R. A. *Chem. Phys. Lett.* **1984**, *110*, 230-4.

(31) Marcus, R. A. *J. Chem. Phys.* **1964**, 2624-33.

(32) Marcus, R. A. *J. Chem. Phys.* **1964**, *41*, 2614-23.

(33) Marcus, R. A. *J. Chem. Phys.* **1965**, *43*, 1598-605.

(34) Coxon, J. A.; Colin, R. *J. Mol. Spect.* **1997**, *181*, 215-23.

(35) Shigeta, Y.; Nagao, H.; Nishikawa, K.; Yamaguchi, K. *Int. J. Quant. Chem.* **1999**, *75*, 875-883.

(36) Handy, N. C.; Yamaguchi, Y.; Schaefer, H. F., III *J. Chem. Phys.* **1986**, *84*, 4481-4.

(37) Sellers, H.; Pulay, P. *Chem. Phys. Lett.* **1984**, *103*, 463-5.

(38) Kolos, W.; Wolniewicz, L. *Phys. Lett.* **1962**, *2*, 222-3.

(39) Kolos, W.; Wolniewicz, L. *Rev. Mod. Phys.* **1963**, *35*, 473-83.

(40) Byron, F. W. J.; Fuller, R. W. *Mathematics of Classical and Quantum Physics*; Dover Publications, Inc.: New York, New York, 1992.

(41) Pettitt, B. A. Ph.D. Thesis, Dalhousie University, 1985.

(42) Pettitt, B. A. *Chem. Phys. Lett.* **1986**, *130*, 399-402.

(43) Bubin, S.; Adamowicz, L. *J. Chem. Phys.* **2003**, *118*, 3079-3082.

(44) Bubin, S.; Adamowicz, L. *J. Chem. Phys.* **2004**, *121*, 6249-6253.

(45) Bubin, S.; Adamowicz, L. *J. Chem. Phys.* **2004**, *120*, 6051-6055.

(46) Bubin, S.; Adamowicz, L. *Chem. Phys. Lett.* **2005**, *403*, 185-191.

(47) Bubin, S.; Bednarz, E.; Adamowicz, L. *J. Chem. Phys.* **2005**, *122*, 041102/1-041102/4.

(48) Cafiero, M.; Adamowicz, L. *Phys. Rev. Lett.* **2002**, *89*, 073001/1-073001/4.

(15) Dykstra, C. E. *Ab Initio Calculation of the Structures and Properties of Molecules*; Elsevier Science Publishers BV: Amsterdam, 1988.

(16) Baerends, E. J.; Gritsenko, O. V.; van Leeuwen, R. In *Chemical Applications of Density Functional Theory*; Laird, B. B., Ross, R. B., Ziegler, T., Eds.; American Chemical Society, **1995**.

(17) Slater, J. C. *Physical Reviews* **1951**, *81*, 385-90.

(18) Wigner, E.; Seitz, F. *Phys. Rev.* **1933**, *43*, 804-10.

(19) Wigner, E.; Seitz, F. *Phys. Rev.* **1934**, *46*, 509-24.

(20) Hohenberg, P.; Kohn, W. *Phys. Rev.* **1964**, ***136***, B 864-B 871.

(21) Laird, B. B.; Ross, R. B.; Ziegler, T. In *Chemical Applications of Density Functional Theory*; Laird, B. B., Ross, R. B., Ziegler, T., Eds.; American Chemical Society, **1995**.

(22) Kohn, W.; Sham, I. J. *Phys. Rev.* **1965**, ***140***, A 1133.

(23) Szabo, A.; Ostlund, N. S. *Modern Quantum Chemistry: Introduction to Advanced Electronic Structure Theory*; First ed.; Dover Publications, Inc.: Mineola, New York, 1982.

(24) Pople, J. A.; Nesbet, R. K. *J. Chem. Phys.* **1954**, *22*, 571-2.

(25) Pechukas, P. *Ber. Bunsenges. Phys. Che.* **1982**, *86*, 372-8.

(26) Truhlar, D. G.; Garrett, B. C.; Klippenstein, S. J. *J. Phys. Chem.* **1996**, *100*, 12771-800.

(27) Marcus, R. A. *J. Chem. Phys.* **1986**, *85*, 5035-40.

(28) Klippenstein, S. J.; Marcus, R. A. *J. Chem. Phys.* **1989**, *91*, 2280-92.

(29) Klippenstein, S. J.; Marcus, R. A. *J. Chem. Phys.* **1990**, *93*, 2418-24.

(49) Cafiero, M.; Adamowicz, L. *Phys. Rev. Lett.* **2002**, *88*, 033002/1-033002/4.

(50) Cafiero, M.; Adamowicz, L. *J. Chem. Phys.* **2002**, *116*, 5557-5564.

(51) Cafiero, M.; Adamowicz, L.; Duran, M.; Luis, J. M. *Theochem* **2003**, *633*, 113-122.

(52) Cafiero, M.; Bubin, S.; Adamowicz, L. *PCCP* **2003**, *5*, 1491-1501.

(53) Cafiero, M.; Adamowicz, L. *Chem. Phys. Lett.* **2004**, *387*, 136-141.

(54) Scheu, C. E.; Kinghorn, D. B.; Adamowicz, L. *J. Chem. Phys.* **2001**, *114*, 3393-3397.

(55) Kinghorn, D. B.; Adamowicz, L. *J. Chem. Phys.* **1997**, *106*, 8760-8768.

(56) Kinghorn, D. B.; Adamowicz, L. *J. Chem. Phys.* **2000**, *113*, 4203-4205.

(57) Bednarz, E.; Bubin, S.; Adamowicz, L. *Mol. Phys.* **2005**, *103*, 1169-1182.

(58) Margenau, H.; Murphy, G. M. *The Mathematics of Physics and Chemistry*; 2 ed.; Robert E. Krieger Publishing Co.: Huntington, New York, 1956.

(59) Thomas, I. L. *Phys. Rev.* **1969**, *185*, 90-94.

(60) Thomas, I. L. *Phys. Rev. A* **1970**, *2*, 728-33.

(61) Thomas, I. L.; Joy, H. W. *Phys. Rev. A* **1970**, *2*, 1200-08.

(62) Thomas, I. L. *Phys. Rev. A* **1970**, *2*, 1675-77.

(63) Thomas, I. L. *Phys. Rev. A* **1971**, *3*, 565-7.

(64) Thomas, I. L. *Phys. Rev. A* **1971**, *3*, 1022-26.

(65) Thomas, I. L. *Phys. Rev. A* **1971**, *4*, 457-59.

(66) Thomas, I. L. *Phys. Rev. A* **1972**, *5*, 1104-10.

(67) Bochevarov, A. D.; Valeev, E. F.; Sherrill, C. D. *Molecular Physics* **2004**, *102*, 111-123.

(68) Tachikawa, M.; Mori, K.; Nakai, H.; Iguchi, K. *Chemical Physics Letters* **1998**, *290*, 437-42.

(69) Pauli, W. *Phys. Rev.* **1940**, *58*, 716-722.

(70) Shankar, R. *Principles of Quantum Mechanics*; 2nd ed.; Kluwer Academic: New York, New York, 1994.

(71) Dirac, P. A. M. *The Principles of Quantum Mechanics*; Oxford University Press: Oxford, 1958.

(72) Casida, M. E. In *Recent Advances in Density Functional Methods, Part I*; Chong, D. P., Ed.; World Scientific, 1995.

(73) Young, D. C. *Computational Chemistry: A Practical Guide for Applying Techniques to Real World Problems*; John Wiley and Sons: New York, 2001.

(74) Bunker, P. R. *Molecular Symmetry and Spectroscopy*; Academic Press: New York, 1979.

(75) Bunker, P. R.; Jensen, P. *Molecular Symmetry and Spectroscopy*; 2 ed.; NRC Research Press: Ottawa, 1998.

(76) Li, H.; Jensen, J. H. *Theor. Chem. Acc.* **2002**, *107*, 211-219.

(77) Crawford, T. D.; Sherrill, C. D.; Valeev, E. F.; Fermann, J. T.; King, R. A.; Leininger, M. L.; Brown, S. T.; Janssen, C. L.; Seidl, E. T.; Kenny, J. P.; Allen, W. D.; 3.2 ed., 2003.

(78) Tachikawa, M.; Osamura, Y. *Theor. Chem. Acc.* **2000**, *104*, 29-39.

(79) Lima, J. A. S.; Plastino, A. R. *Braz. J. Phys.* **2000**, *30*, 176-180.

(80) Yamaguchi, Y.; Schaefer, H. F., III *J. Chem. Phys.* **1980**, *73*, 2310-18.

(81) Thomas, J. R.; DeLeeuw, B. J.; Vacek, G.; Crawford, T. D.; Yamaguchi, Y.; Schaefer, H. F., III *J. Chem. Phys.* **1993**, *99*, 403-16.

(82) McNaught, A. D.; Wilkinson, A. *IUPAC Compendium of Chemical Terminology: The Gold Book*; 2nd ed.; Blackwell Science, 1997.

(83) Krestov, G. A. *Thermodynamics of Solvation: Solution and Dissolution, Ions and Solvent, Structure and Energetics*; Ellis Horwood, 1991.

(84) Krestov, G. A.; Novosyolov, N. P.; Perelygin, I. S.; Kolker, A. M.; Safanova, L. P.; Ovchinnikova, V. D.; Trostin, V. N. *Ionic Solvation*; Ellis Horwood Ltd: Chichester, West Sussex, UK, 1994.

(85) Khumotov, N. E. *Russ. J. Phys. Chem.* **1956**, *30*, 2160.

(86) Bauschlicher, C. W. J.; Langhoff, S. R.; Partridge, H. *J. Chem. Phys.* **1991**, *95*, 5142-8.

(87) Bauschlicher, C. W. J.; Sodupe, M.; Partridge, H. *J. Chem. Phys.* **1992**, *96*, 4453-63.

(88) Feller, D.; Glendening, E. D.; Woon, D. E.; Feyereisen, M. W. *J. Chem. Phys.* **1995**, *103*, 3526-42.

(89) Glendening, E. D.; Feller, D. *J. Phys. Chem.* **1995**, *99*, 3060-7.

(90) Glendening, E. D.; Feller, D. *J. Phys. Chem.* **1996**, *100*, 4790-7.

(91) Merrill, G. N.; Webb, S. P.; Bivin, D. B. *J. Phys. Chem. A* **2003**, *107*, 386-396.

(92) Maheshwary, S.; Patel, N.; Sathyamurthy, N.; Kulkarni, A. D.; Gadre, S. R. *J. Phys. Chem. A* **2001**, *105*, 10525-37.

(93) Upadhyay, D. M.; Shukla, M. K.; Mishra, P. C. *Int. J. Quant. Chem.* **2001**, *81*, 90-104.

(94) Weinheimer, C. J., Univ. of Illinois, 1998.

(95) Hartke, B.; Charvat, A.; Reich, M.; Abel, B. *J. Chem. Phys.* **2002**, *116*, 3588-3600.

(96) Armentrout, P. B.; Baer, T. *J. Phys. Chem.* **1996**, *100*, 12866-12877.

(97) Meot-Ner, M.; Speller, C. V. *J. Phys. Chem.* **1986**, *90*, 6616 - 6624.

(98) Dzidic, I.; Kebarle, P. *J. Phys. Chem.* **1970**, *74*, 1466-74.

(99) Rudolph, W.; Brooker, M. H.; Pye, C. C. *J. Phys. Chem.* **1995**, *99*, 3793-7.

(100) Feller, D.; Glendening, E. D.; Kendall, R. A.; Peterson, K. A. *J. Chem. Phys.* **1994**, *100*, 4981-97.

(101) Kaupp, M.; Schleyer, P. v. R. *J. Phys. Chem.* **1992**, *96*, 7316-23.

(102) Corral, I.; Mo, O.; Yanez, M.; Scott, A. P.; Radom, L. *J. Phys. Chem. A* **2003**, *107*, 10456-61.

(103) Curtiss, L. A.; Raghavachari, K.; Redfern, P. C.; Rassolov, V.; Pople, J. A. *J. Chem. Phys.* **1998**, *109*, 7764-7776.

(104) Curtiss, L. A.; Raghavachari, K.; Redfern, P. C.; Baboul, A. G.; Pople, J. A. *Chem. Phys. Lett.* **1999**, *314*, 101-107.

(105) Iron, M. A. O. M.; Martin, J. M. L. *Mol. Phys.* **2003**, *101*, 1345-61.

(106) Sullivan, M. B.; Iron, M. A. O. M.; Redfern, P. C.; Curtiss, L. A.; Martin, J. M. L.; Radom, L. *J. Phys. Chem. A* **2003**, *107*, 5617-30.

(107) Frisch, M. J.; Trucks, G. W.; Schlegel, H. B.; Scuseria, G. E.; Robb, M. A.; Cheeseman, J. R.; Zakrzewski, V. G.; Montgomery, J., J. A. ; Stratmann, R. E.; Burant, J. C.; Dapprich, S.; Millam, J. M.; Daniels, A. D.; Kudin, K. N.; Strain, M. C.; Farkas, O.; Tomasi, J.; Barone, V.; Cossi, M.; Cammi, R.; Mennucci, B.;

Pomelli, C.; Adamo, C.; Clifford, S.; Ochterski, J.; Petersson, G. A.; Ayala, P. Y.; Cui, Q.; Morokuma, K.; Malick, D. K.; Rabuck, A. D.; Raghavachari, K.; Foresman, J. B.; Cioslowski, J.; Ortiz, J. V.; Baboul, A. G.; Stefanov, B. B.; Liu, G.; Liashenko, A.; Piskorz, P.; Komaromi, I.; Gomperts, R.; Martin, R. L.; Fox, D. J.; Keith, T.; Al-Laham, M. A.; Peng, C. Y.; Nanayakkara, A.; Gonzalez, C.; Challacombe, M.; Gill, P. M. W.; Johnson, B.; Chen, W.; Wong, M. W.; Andres, J. L.; Gonzalez, C.; Head-Gordon, M.; Replogle, E. S.; Pople, J. A.; Gaussian, Inc.: Pittsburgh PA,, 1998.

(108) Becke, A. D. *J. Chem. Phys.* **1993**, *98*, 5648-5652.

(109) Curtiss, L. A.; Raghavachari, K.; Trucks, G. W.; Pople, J. A. *J. Chem. Phys.* **1991**, *94*, 7221-30.

(110) Curtiss, L. A.; Raghavachari, K.; Pople, J. A. *J. Chem. Phys.* **1993**, *98*, 1293-8.

(111) Curtiss, L. A.; Raghavachari, K.; Pople, J. A. *J. Chem. Phys.* **1995**, *103*, 4192-200.

(112) Curtiss, L. A.; Raghavachari, K.; Redfern, P. C.; Pople, J. A. *J. Chem. Phys.* **1997**, *106*, 1063-1079.

(113) Boys, S. F.; Bernardi, F. *Mol. Phys.* **1970**, *19*, 553.

(114) van Duijneveldt, F. B.; van Duijneveldt-van de Rijdt, J. G. C. M.; van Lenthe, J. H. *Chem. Rev.* **1994**, *94*, 1873-85.

(115) Viswanathan, B.; Barden, C. J.; Ban, F.; Boyd, R. J. *Mol. Phys.* **2005**, *103*, 337-344.

(116) Weis, P.; Kemper, P. R.; Bowers, M. T. *JACS* **1999**, *121*, 3531-2.

(117) Kebarle, P. *Mod. Asp. Electrochem.* **1974**, *9*, 1-16.

(118) Combariza, J. E.; Kestner, N. R.; Jortner, J. *J. Chem. Phys.* **1994**, *100*, 2851-64.

(119) Lee, H. M.; Kim, D.; Kim, K. S. *J. Chem. Phys.* **2002**, *116*, 5509-20.

(120) Sheu, W.-S.; Liu, Y.-T. *Chem. Phys. Lett.* **2003**, *374*, 620-625.

(121) Frisch, M. J.; Trucks, G. W.; Schlegel, H. B.; Scuseria, G. E.; Robb, M. A.; Cheeseman, J. R.; J. A. Montgomery, J.; Vreven, T.; Kudin, K. N.; Burant, J. C.; Millam, J. M.; Iyengar, S. S.; Tomasi, J.; Barone, V.; Mennucci, B.; Cossi, M.; Scalmani, G.; Rega, N.; Petersson, G. A.; Nakatsuji, H.; Hada, M.; Ehara, M.; Toyota, K.; Fukuda, R.; Hasegawa, J.; Ishida, M.; Nakajima, T.; Honda, Y.; Kitao, O.; Nakai, H.; Klene, M.; Li, X.; Knox, J. E.; Hratchian, H. P.; Cross, J. B.; Adamo, C.; Jaramillo, J.; Gomperts, R.; Stratmann, R. E.; Yazyev, O.; Austin, A. J.; Cammi, R.; Pomelli, C.; Ochterski, J. W.; Ayala, P. Y.; Morokuma, K.; Voth, G. A.; Salvador, P.; Dannenberg, J. J.; Zakrzewski, V. G.; Dapprich, S.; Daniels, A. D.; Strain, M. C.; Farkas, O.; Malick, D. K.; Rabuck, A. D.; Raghavachari, K.; Foresman, J. B.; Ortiz, J. V.; Cui, Q.; Baboul, A. G.; Clifford, S.; Cioslowski, J.; Stefanov, B. B.; Liu, G.; Liashenko, A.; Piskorz, P.; Komaromi, I.; Martin, R. L.; Fox, D. J.; Keith, T.; Al-Laham, M. A.; Peng, C. Y.; Nanayakkara, A.; Challacombe, M.; Gill, P. M. W.; Johnson, B.; Chen, W.; Wong, M. W.; Gonzalez, C.; Pople, J. A.; Gaussian, Inc.: Pittsburgh PA, 2003, 2003.

(122) Woon, D. E.; Dunning, T. H., Jr. *J. Chem. Phys.* **1993**, *98*, 1358-71.

(123) Woon, D. E.; Dunning, T. H., Jr. *J. Chem. Phys.* **1994**, *100*, 2975-88.

(124) Woon, D. E.; Dunning, T. H., Jr. *J. Chem. Phys.* **1995**, *103*, 4572-85.

(125) Perdew, J. P.; Burke, K.; Ernzerhof, M. *Phys. Rev. Lett.* **1996**, *77*, 3865-68.

(126) McWeeny, R. *Spins in Chemistry*; Academic Press: London, 1970.

(127) Breit, G. *Phys. Rev.* **1930**, *35*, 1447-51.

(128) Balasubramanian, K. *Relativistic Effects in Chemistry; Part A: Theory and Techniques*; John Wiley & Sons, Inc.: New York, 1997.